GRADUATE PROGRAM

ADDIS ABABA SCIENCE AND TECHNOLOGY UNIVERSITY

Impact of Climate Change on the Hydrology of Upper Blue Nile Basin
(Case study on Megech Watershed)

M.Sc Thesis by Teferi Demissie

School:	**Civil Engineering and Construction Technology**
Department:	**Civil Engineering**
Program:	**Hydraulic Engineering**
Major Advisor:	**Habtamu Itefa (Dr.Ing)**

June 1, 2016

Addis Ababa

APROVAL PAGE
GRADUATE PROGRAM

ADDIS ABABA SCIENCE AND TECHNOLOGY UNIVERSITY

Submitted by:

_____	_____	_____
Name of the student	Signature	Date

Approved by:

1. _____	_____	_____
Name of Major Advisor	Signature	Date
2._____	_____	_____
Name of Co-Advisor	Signature	Date
3._____	_____	_____
Name of Chairman, DGC[1]	Signature	Date
4._____	_____	_____
Name of Dean, Graduate Program	Signature	Date
5._____	_____	_____
Name of Chairman, CGP[2]	Signature	Date

[1]Departmental Graduate Council

[2] Council of Graduate Programme

ACKNOWLEDGEMENT

Before all my gratitude is to the architect and superintendent of this gigantic world, Jesus Christ with his mother Saint Marry, all his Angels and Saints for his incredible and marvel contributions for me to be here.

Next I would like to put-across my frank gratitude to my advisor Dr.-Ing Habtamu Itefa for his precious, decent and professional advices and constructive comments starting from the proposal development to the execution of this thesis.

My recognition also extended to the staff of the Ministry of Water, Irrigation and Electricty (MOWIE), National Meteorological Service Agency (NMA), International Water Management Institute (IWMI), Water Works Design and Supervision Enterprise (WWDSE) and Ministry of Agriculture and Natural Resource for their all rounded support and cooperation in availing the necessary data.

Finally I thank all my classmates for all challenges, knowledge sharing and cheerful time we spent together at Addis Ababa Science and Technology University.

DECLARATION

I, Teferi Demissie, declare that this thesis is my original work and it has not been presented and will not be presented by me to any other university for similar or any other degree award.

Signature: _____

Date: _____

ABSTRACT

Climate change refers to a change in the state of the climate that can be identified by changes in the mean and/or the variability of its properties and that persists for an extended period, typically decades or longer. A major effect of climate change is likely to be alteration in hydrological cycle and change in water availability. Globally, climate change has an overall net negative impact on water resources. Lake Tana sub-basin is located in Blue Nile Basins, which is one of 12 basins in Ethiopia and contain more agricultural land. Gilgel Abay, Ribb, Gumera and Megech are the main rivers feeding 90% inflow of Lake Tana. The analysis made at Bahirdar station shows great fluctuation in annual mean water level of 1.9m to 3.2m from 1981 to 2006. Megech watershed have an effect on the Lake Tana water level as it is a major tributary to the lake with a significant amount of inflow.

The SDSM result indicated Megech watershed is vulnerable to climate change. The annual average temperature increased from 0.61 ^{0}c to 2.94 ^{0}c and 0.52 ^{0}c to 2.03 ^{0}c for medium-higher emission and medium-lower emission for 2020s, 2050s and 2080s. Although annual average minimum temperature increased from 0.97 ^{0}c to 3.12 ^{0}c and 0.86 ^{0}c to 2.53 ^{0}c for A2a and B2a scenarios of the same time period. Downscaled precipitation of Megech watershed indicates less annual average precipitation change from - 2.03 % to - 7.60 % and - 0.99 % to - 5.96 % for A2a and B2a scenarios in 2020s(2011-2040), 2050s(2041-2070) and 2080s(2071-2099).

The SWAT model result shows decreasing flow of Megech due to climate change from near to end of the century. It used 2008 land use/ land cover and soil property data to generate the impact of climate change on the flow. From the analysis there will be a reduction of Megech River annual flow in - 5.19 %, - 19.71 %, - 12.57 % and - 4.54 %,- 7.90 %,- 11.06 % for 2020s, 2050s and 2080s for A2 and B2 emission scenarios. Hence there is an indication for impact of climate change on the stream of the river and water resource utilization in basin shall be planned in due consideration to such fluctuation in stream flow, rainfall and temperature.

Dedicated

To

My Dad and Mom

TABLE OF CONTENTS

LIST OF FIGURES

LIST OF TABLES

ACRONYMS and ABBREVIATIONS

AGCM	Atmospheric General Circulation Models
AOGCM	Atmospheric Ocean Global Circulation Model
AR4	Fourth Assessment Report Intergovernmental panel on climate change
CN	Curve Number
CO_2	Carbon Dioxide
DEM	Digital Elevation Model
ENSO	El-Nino-Southern Oscillation
FAO	Food and Agricultural Organization
FDRE	Federal Democratic Republic of Ethiopia
GCMs	Global Climate Models
GHG	Green House gas
GIS	Geographical Information System
Gt	Giga tons
GCCIUS	Global Climate Change Impact on United State
HRU	Hydrologic Response Unit
IPCC	Intergovernmental Panel on Climate Change
ITCZ	Inter-Tropical Convergence Zone
LARS-WG	Long Ashton Research Station Weather
NWP	Numerical weather prediction
NSE	Nashi-Sutcliffe model efficiency

NMA	National Metrological Agency
OGCM	Ocean General Circulation Model
PBIAS	Percentage of Bias
PET	Potential Evapotranspiration
R^2	Coefficient of Determination
RCMs	Regional Climate Models
SDSM	Statistical Downscaling Model
SWAT	Soil and Water Assessment Tool
SRES	Special Report on Emission Scenarios
SCS	Soil Conservation Service
SPAW	Soil-plant-Atmosphere-Water field and pond hydrology
TGICA	Scenario Support for Impact and Climate Assessment
TAR's	Third Assessment Reports
UNESCO	United Nations Educational, Social and Cultural Organization
UNEP	United Nations Environmental Protection
UTM	Universal Transverse Mercator
WMO	World Meteorological Organization
WWDSE	Water Works Design and Supervision
MOWR	Ministry of Water Resource

CHAPTER ONE

1 INTRODUCTION

1.1 Background

Climate change refers to a change in the state of the climate that can be identified (e.g. using statistical tests) by changes in the mean and/or the variability of its properties and that persists for an extended period, typically decades or longer. It refers to any change in climate over time, whether due to natural variability or as a result of human activity (IPCC, 2013).

Changes in climate occur as a result of both internal variability within the climate system, and external factors (both natural and anthropogenic). The influence of external factors on climate can be broadly compared using the concept of radiative forcing. A positive radiative forcing, such as that produced by increasing concentrations of greenhouse gases, tends to warm the surface. A negative radiative forcing, which can arise from an increase in some types of aerosols (microscopic airborne particles) tends to cool the surface. Natural factors, such as changes in solar output or explosive volcanic activity, can also cause radiative forcing. Most of the observed increase in global average temperatures since the mid-20th century is very likely due to the observed increase in anthropogenic greenhouse gas concentrations. This is an advance since the intergovernmental panel on climate change third assessment reports conclusion that "most of the observed warming over the last 50 years is likely to have been due to the increase in greenhouse gas concentrations (IPCC, 2007).Variability is reflected not only in temperature – variability in the hydrological cycle, which is often of much greater importance to human populations, has been quite extreme on all timescales in the past (Steffen, 2004).

A major effect of climate change is likely to be alteration in hydrological cycle and change in water availability. Increasing evaporation with change in precipitation has the potential to affect runoff, the frequency and intensity of floods and drought, soil moisture and water availability for irrigation and hydroelectric generation (Shimelis *et al.*, 2011).

According to the intergovernmental panel on climate change fourth assessment report, globally, climate change has an overall net negative impact on water resources. New results from fourth assessment report findings that more people experience water scarcity under climate change

than experience of its increase. However, most post-fourth assessment report research focuses on increased water scarcity. The world temperature increase approximately by 2°C and around 59% of the world's population exposed to blue water shortage (i.e. irrigation water shortage) on single climate model projection (Simon *et al.*, 2011).

The climate of Africa is both varied and varying. Varied, because climate ranges from humid equatorial to seasonally arid and sub-tropical Mediterranean and varying because all these climates exhibit differing degrees of temporal and spatial variability. At the sub regional scale, Africa is vulnerable to El Nino-Southern Oscillation(which consists affects regional variations of precipitation and temperature over much of the tropics, sub-tropics and some mid-latitude areas) and related extreme events (drought, floods, and changes in hydrologic patterns). The portion of sub-Saharan Africa that depends entirely on the Nile River for its water supply is particularly susceptible to hydrologic changes that might be associated with a warmer climate. Flooding and droughts will be increasingly difficult to cope with in the face of increasing pressures on water supplies due to rapid population growth and dwindling resources (Tazebe *et al.*, 2009).

Scaling climatic impact on Africa by 2020, between 75 and 250 million of people are projected to be exposed to increased water stress due to climate change. In some countries, yields from rain-feed agriculture could be reduced by up to 50%. Agricultural production, including access to food, in many African countries is projected to be severely compromised. This would further adversely affect food security. By 2080, an increase of 5 to 8% of arid and semi-arid land in Africa is projected under a range of climate scenarios (high confidence) (IPCC, 2007).

Ethiopia's economy and ecological system is vulnerable to climate change. Ethiopian economy is highly dependent on rain-feed agriculture. According to Ethiopian demographic report in 2013 around 96 million peoples live in Ethiopia, and over 82% are living in rural areas also have Population growth of 2.9%. Environmental challenges in Ethiopia include climate change, soil degradation, deforestation, loss of biodiversity and ecosystem services, and pollution of land, air and water (Emelie *et al.*, 2013).

Lake Tana sub-basin is located in Blue Nile Basins, which is one of 12 basins in Ethiopia and contain more agricultural land. It is located in North West highland of the country. This basin

is of critical national significance as it has great potential for irrigation, hydropower, high value crops and livestock production, ecotourism and more. Gilgel Abay, Ribb, Gumera and Megech are the main rivers feeding Lake Tana and contribute more than 90% of the flow.

Assessing the impact of climate change on stream flows, soil moisture, groundwater and other hydrological parameters essentially involves taking projections of climatic variables (e.g., precipitation, temperature, humidity, mean sea level pressure etc.) at a global scale, downscaling these global-scale climatic variables to local-scale hydrologic variables, and computing hydrological components for water resources variability and risks of hydrologic extremes in the future. Projections of climatic variables globally performed with General Circulations Models (GCMs), which provide projections at large spatial scales. Such large-scale climate projections must then be downscaled to obtain smaller-scale hydrologic projections using appropriate linkages between the local climates (Shimelis *et al.*, 2011).

This study reports on the investigation result of impact of climate change on water resources in a Megech Watershed located in Lake Tana sub-basin for the near (2011-2041) and far (2070-2099) future. Soil and Water Assessment Tool Model (SWAT 2005) was used to study the effect of climate change at sub-basin level. In this study focuses has been made on analyzing the water balance including precipitation and river discharge.

1.2 Statement of the problem

Climate change in regions influence natural processes of a watershed ecosystem and have long-term implications on economic and ecological processes (Abouabdillah *et al.,* 2010). Ethiopia follows agricultural led industrialization that is strongly connected to climate change. Large part of the country is arid and semi-arid. High change of climatic variability, complex topography, poor agricultural practice, poor watershed management, high population pressure, low economic development, low adaptive capacity, inadequate infrastructure, weak institutional (governmental) capacities are among many reasons for high climate change vulnerability of the country and the Upper Blue Nile river basin (Cherie, 2013).

Gilgel Abay, Ribb, Gumera and Megech are the main rivers feeding 90% inflow of Lake Tana (Shimelis *et al.,* 2011). Megech watershed is endowed with rich and unique terrestrial and aquatic biodiversity, ranging from forests, wildlife and fisheries. Due to increase in population, poor agricultural practices, unsustainable fishing, deforestation, high soil erosion and the search for more agricultural land, people settlement on cultivate forested areas, and marginally unproductive land are the reasons that may cause climate change on the watershed. This watershed is used for various purposes like, water supply and irrigation. Recently, there is development of irrigation project located in the northern part of the Lake Tana sub-basin, west of Megech River in the area of 5,254 ha. The Government of Federal Democratic Republic of Ethiopia (FDRE) gives greater attention for the development of irrigation projects on the watershed, although report indicates the climatic change is resulting in the Lake Tana water level drop and observed frequent flooding. The analysis made at Bahirdar station shows great fluctuation in annual mean water level of 1.9m to 3.2m from 1981 to 2006 (WWDSE, 2008).

The Megech watershed have an effect on the Lake Tana water level as it is a major tributary to the lake with a significant amount of water inflow. On the other hand, operational researches of similar nature on the Megech watershed area are limited. This study, therefore, focuses to address the impact of climate change on Megech watershed. It will have a paramount importance in giving an insight on the vulnerability of Megech watershed to climate change and tries to suggest practical recommendations.

1.3 Objective

General objective

To assess the climate change impacts on the hydrology of Megech Watershed for sustainable water resource utilization.

Specific objective

- ✓ To develop climatic scenario for maximum temperature, minimum temperature and precipitation based on General Circulation Modeling (GCM) and Statically Downscaling Model (SDSM) for Megech watershed.
- ✓ To assess the effect of climatic change on surface hydrology of Megech watershed by using the climate scenario data and hydrological model.

1.4 Thesis layout

The thesis is organized in five chapters: Chapter one provides brief introduction about climate change, cause of climate change and its effect on climatic variables , about the problem that initialize this study, the objective of the study , the outline of the thesis and the overall frame work of the research.

Chapter two describes the reviewed literature related to the study on the concept of climatic change, Global Circular Model (GCM), downscaling concept and Statistical Downscaling Model (SDSM) overview of the SWAT model.

Chapter three deals with the methodology adopted for the study. In Chapter four the main part of research study, data analysis and model simulations, model calibration and validation and results are presented. Finally, Chapter five presents conclusion and recommendations based on the results of the models and the data used for this study. In addition References and Appendixes are attached at the end.

CHAPTER TWO

2 LITERATURE REVIEW

2.1 Previous studies in upper Blue Nile Basin

Climatic impact assessment in upper Blue Nile basin has been studied. The most relevant are presented as follows;

The study of Tazebe *et al.* (2009) on potentail impact of climate change on the hydrology and water resource of the Nile River basin using macroscale hydrological model driven by 21 century simulation of temeprature and precipitation downscaled from 11 Global Circulation Model(GCMs) and two emisssion of senarios A2 and B2. The result from average of multimodels showed the entire Nile basin experience increasing in precipitation in early century (2010-2039) and decrease in (2040-2069) and (2070-2099) also minimum and maximum tempearture increases in all periods. In addition, the Nile River basin stream flow increased in near (2010-2039) and decreases in (2040-2069) and (2070-2099) following precipitation.

Shimelis *et al.* (2011) has carried out climatic change impact on the agricultural water resouce variability in the northen highlands of Ethiopia in their study using 15 GCM downscaled result on SWAT model for B1, A1b and A2 emission senarios. They conclued GCM don't project significant change in rainfall in the region because of half of the models indicating increasing and half suggest decreasing and all models show regional warming in all periods the smallest change indicated in lower emission B1 and the largest change are in higher emission A2. Their output of SWAT model from the downscaled result of GCMs the stream flow shows reduction in all future periods only one from GCM result indicates increasing of stream flow in future periods for all emission senarios.

Cherie (2013) also study downscaling and modelling the effects of climate change on hydrology and water resouces in Upper Blue Nile River basins, Ethiopia performed by three GCMs and two types of downscaling model that used as input for SWAT model. He concluded that maximum tempearure indicates rise for 0.6 ^{0}c to 2.7 ^{0}c for 2050 (2045-2065) silmilarly, 2090 (2081-2100) indicates 0.9 ^{0}c to 4.63 ^{0}c and minimum temperature 1^{0}c to 4.6 ^{0}c for A1B and A2 emission senarios. The precipitation also indicates decreasing in all future time periods for both

senarios. In his finding the future simulated stream flow of Upper Blue Nile basin from Stastical Downscaling Model (SDSM) and Long Ashton Research Station Weather Generator (LARS-WG) indicates there is declination of flow from 10% to 61% for future Blue Nile stream flow.

Elshamy *et al*. (2009) in his study on the impact of climate change on water resouces of Upper Blue Nile River basin using 17 GCMs and one emission scenarios. He concludes that annual precipitation change shows decreasing and increasing within the range of - 15 % and + 14 % for all different 17 GCMs. Although maximum and minimum temperature shows incerement for most of the GCMs. Finally, he conclude that almost there is no change in the annual total rainfall for 2020s, 2050s and 2080s.

This above mention studies are not the only conducted research on Upper Blue Nile basin but the most relevant to this case study. They all shows different result according to the statement of Cherie (2013) inconsistancy of the result on the prediction of future impact of climate change arise due to the number and type of GCM, type of emission scenarios , length of both predictand and predictor data set, period of analysis (time slices), type of observation data, spatail and temporal resolution for observed and predictor data set, different modelling approches both climate and hydrology prediction study and scale of study.

2.2 Climate change

IPCC (2013) definition climate change is long term shift in statics of the weather (including average). Those change occurs due to direct or indirect attribution human activities that alters the composition of global atmosphere or natural variability observed over comparable time periods.

Human activities since the beginning of the industrial revolution changes in the chemical composition of the earth's atmosphere (kumar, 2006). Earth's climate depends on the function of natural greenhouse effect. This effect is caused by heat-trapping gases (also known as greenhouse gases) like water vapor, carbon dioxide, ozone, methane, and nitrous oxide, which absorb heat radiated from the Earth's surface and lower atmosphere and then radiate the energy back to surface (karl, 2009). Changes of atmospheric concentarion of GHGs, land cover and solar radiation changes the energy balance of climate system this is cause for climatic change

that resulted positive or negative changes in energy balance due to these factors are expressed as radiative forcing, that used to compare warming or cooling influences on global climate (IPCC, 2001).

2.3 Cause of climate change

GCCIUS (2009) described climate is influenced both by human induced and natural process. Increasing of carbon dioxide is principal factor that causes warming for the past 50 years. Its concentration starts to increase from industrial era in 1700s due to burning of fossil fuels (coal, oil, and natural gas) and the clearing of forests. It added human activities are primary causes that increase greenhouse gases, such as methane, nitrous oxide, and halocarbons though out the world.

IPCC (2007) finding shows global GHG annual emission by human activities is grown between 1970 and 2004 about 80%, from 21 to 38 Giga tons (Gt), and represented 77% of total anthropogenic GHG emissions in 2004. The rate of growth the most common anthropogenic GHG carbon dioxide is much higher during the recent 10-year period of 1995-2004 (0.92 $GtCO_2$ - eq per year) than during the previous period of 1970-1994 (0.43 $GtCO_2$ - eq per year). This increment caused by energy supply, transport and industry, while residential and commercial buildings, forestry (including deforestation) and agriculture low growth rate.

According to GCCIUS (2009) explanation about this GHGs starting from methane concentration increased due to agriculture, raising of livestock (produce methane in their digestive tracts); mining, transportation, and use of certain fossil fuels, sewage and decomposing garbage in landfills. About 70% emission is related to human activities. Secondly, nitrous oxide concentration increase due to fossil fuel burning and fertilizer usage. Thirdly, halocarbon emission occurs from manufactured chemical like chlorofluorocarbons (CFCs) that used in refrigerator and other industrial processes. It is main cause for stratospheric ozone depletion. Fourth, ozone is greenhouse gas continuously produced and destroyed in the atmosphere. Its concentration increased by release of gases such as carbon monoxide, hydrocarbons, and nitrogen oxide reacted with gases produce ozone in the presence of sunlight. Fifth, water vapor it is important and abundant GHGs in the atmosphere. The abundance of GHGs leads atmospheric water vapor increment, since a warmer climate increases evaporation

and allows the atmosphere to hold more moisture that causes an amplified feedback loop leads to more warming. Additionally, aerosols are causes for climate change. During burn of coal produces emissions of sulfur-containing compounds. These compounds form sulfate aerosol particles that reflect some of the incoming sunlight away from the Earth, causing a cooling influence at the surface. Sulfate aerosols cause's clouds more efficient at reflecting sun-light and indirect cooling effect. Human activities changes the land surface in ways that alter heat reflected and absorbed by the surface. Also sun and volcanic eruptions are the two main natural factors influence climate. Those above mentioned activates and gases are cause of climate change for the past three decades.

2.4 Constructing Climate Scenarios for Impact Studies

Constructing climatic scenarios in the case of climate change helps to get information the future activity of human for alter the composition of atmosphere, its effects to global climate and natural systems (IPCC, 2001). It gives self-consistent outcome of future climate that used to investigate the potential consequences of anthropogenic climate projections, for example future climate simulated by climate models (Jones *et al.*, 2004). Figure 2 -1 shows the alternative data sources and main steps for constructing climate scenarios. Smith and Hulme (1998) suggested climatic scenarios have to be consistent with global projection, physical plausible, applicable in impact assessments (should describe change in sufficient number of variable), representative and accessible to be useful for impact researchers and police makers (IPCC, 2000).

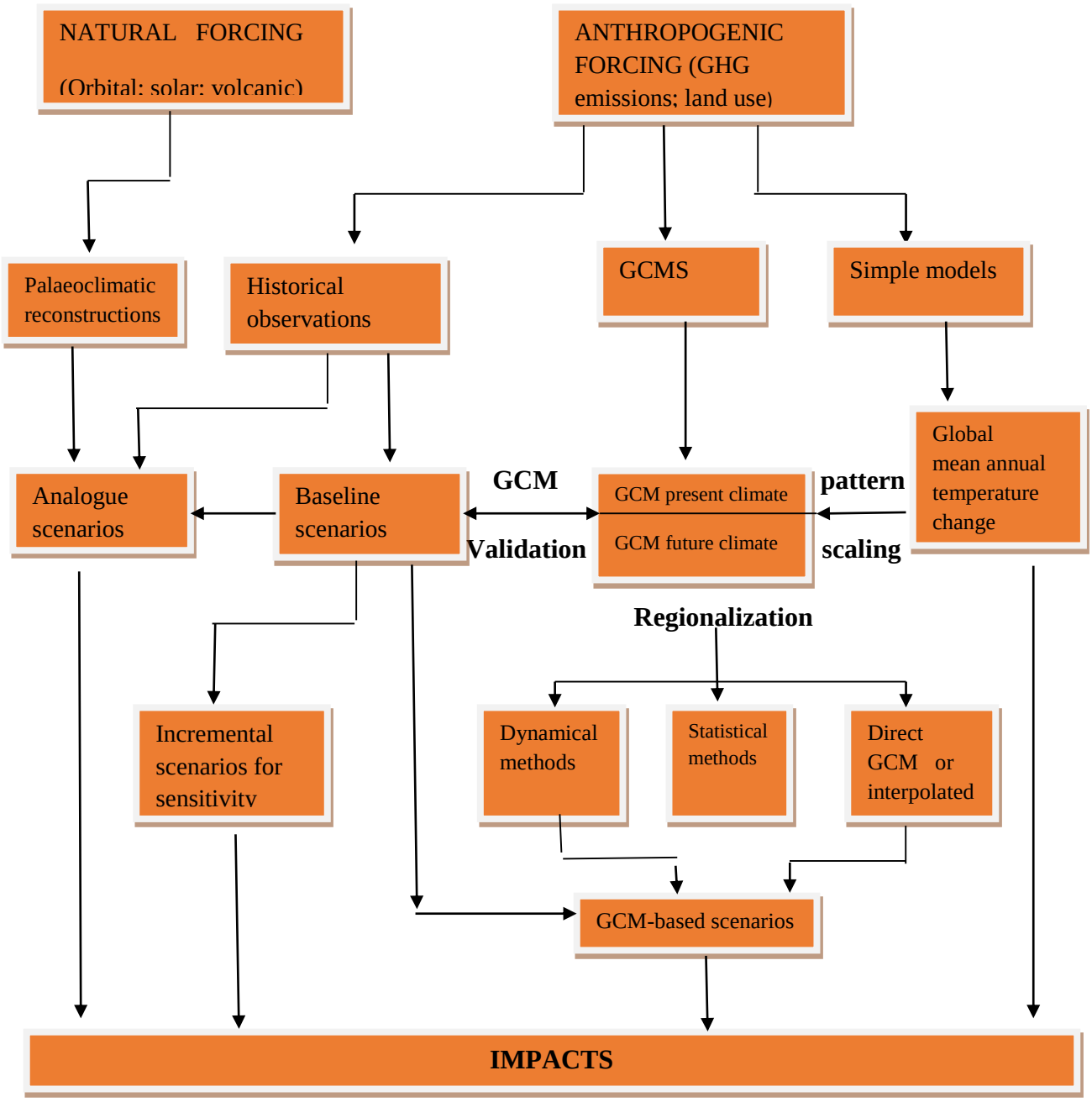

Figure 2-1:-Main sequences of steps for various types of climate scenarios are constructed (IPCC, 2001)

2.5 Special report on emission scenario

Scenarios are alternative images of how the future changes and appropriate tool for analyses how driving forces influence future emission outcomes and to assess the associated uncertainties. They assist in climate change analysis, including climate modeling, the assessment of impacts, adaptation, and mitigation and highly uncertain (IPCC, 2000).

Carter *et al*. (1999) explained about Specail Report on Emission Scenarios (SRES) are constructed to explore future developments of global environment with special reference to the production of greenhouse gases and aerosol emissions. They use the following terminology

• Storyline: a narrative description of a scenario (or a family of scenarios), highlighting the main scenario characteristics and dynamics, and the relationships between key driving forces.

• Scenario: projections of a potential future, based on a clear logic and a quantified storyline.

• Scenario family: one or more scenarios that have the same demographic, politico-societal, economic and technological storyline.

IPCC SRES (2001) stated in this report four different narrative storylines developed to describe consistent relationships between the forces driving emissions and their evolution and to add context for the scenario quantification. Although Shimelis *et al*. (2011) added this scenario families are (A1, A2, B1 and B2) that contain different development pathways, covering a wide range of demographic, economic and technological driving forces and resulting GHG emissions.

A1. The storyline and scenario family describes very rapid economic growth in the future world, global population that peaks in mid-century then declines and rapid introduction of new and more efficient technologies. This scenarios family develops three groups contains different type technological change in the energy system. This groups are distinguished by technological emphasis: fossil intensive (A1FI), non-fossil energy sources (A1T), or a balance across all sources (A1B) (where balanced is defined as not relying too heavily on one particular energy source, on the assumption that similar improvement rates apply to all energy supply and end-use technologies).

A2. This storyline and scenario family describes a very heterogeneous world. Fertility patterns across regions converge very slowly that results continuous increasing population. Economic development is primarily regionally oriented and per capita economic growth and technological change more fragmented and slower than other storylines.

B1. This storyline and scenario family describes a convergent world with the same global population, which peaks in mid-century and declines. Also the storyline indicates rapid change in economic structures toward a service and information economy, reductions in material intensity and the introduction of clean and resource-efficient technologies. The emphasis is on global solutions to economic, social and environmental sustainability, including improved equity, but without additional climate initiatives.

B2. This storyline and scenario family describes a world in which the emphasis is on local solutions to economic, social and environmental sustainability. In this scenarios family continuously increasing global population at a rate lower than A2, intermediate levels of economic development, and less rapid and more diverse technological change than in the A1 and B1 storylines. This scenario oriented towards environmental protection and social equity, it focuses on local and regional levels.

UNEP (1998) recommended climate change senarios seletion for impact assesment should meet the following four conditions

Condition 1. The scenarios should contain broad range global warming projections based on increased atmospheric concentration of greenhouse gases.

Condition 2. The scenarios should be physically plausible they should not violate the base laws of physics.

Condition 3. The scenarios should estimate sufficient number of variables on the spatial and temporal scale that allows for assessing impact.

Condition 4. The scenarios should reflect the potential range of future regional climate change on reasonable extent.

The selection of climatic change scenarios by considering the above four conditions that is recommended by UNEP (1998) for impact assessments. In this study SRES scenarios (A2 and B2) are used. It is because of the study area better related to this scenario families firstly, A2 considers economic development is primary regional oriented, per capita economic growth, technological change more fragmented and slower than other storylines and continuous increasing global population rate higher secondly, B2 is taken it considers intermediate levels of economic development, and less rapid and more diverse technological change are used explore future developments in the global environment with increment of greenhouse gas and aerosol emission.

2.6 General Circulation Model

Global Climate Models (GCMs) is a mathematical representation of the climate system based on the physical properties of its components, their interactions and feedback processes (Jones *et al.,* 2004). It is numerical weather prediction (NWP) and uses the same equation of motion for the purpose of numerical simulate change in climate due to boundary conditions (such as the solar constant) or physical parameters (such as the greenhouse gas concentration) (Fadil *et al.*, 2011). It represents physical processes in the atmosphere, ocean, cryosphere and land surface and the only available tool currently available for simulation the response of global climate system to increasing GHG concentration (Carter *et al.,* 1999). It is widely used for weather forecasting, understanding the climate, and projecting climate change (IPCC, 2007).

According to Bader *et al*. (2008) description GCMs are evolved from Atmospheric General Circulation Models (AGCMs) which widely used for daily weather prediction and Ocean General Circulation Model (OGCM) which used to simulate the circulation of oceans. AGCMs dynamically simulates the circulation of atmosphere, including the processes that regulate energy transport and exchange in the atmospheric flow. The atmospheric flow represented by fundamental equations that links the mass distribution and mass filed. This equations represent on a spherical spatial grid field that has many levels representing the depth of the atmosphere and modified by the representation of processes that occur on a scale below of the grid including such processes as turbulence, latent heat of condensation in cloud formation, and dynamic heating as solar and infrared radiation interact with atmospheric gases, aerosols, and clouds.

Although OGCM represent a dynamic thermal reservoir, through energy exchange with the atmosphere, dominates the evolution of the climate system. The specification of the processes that regulate heat, moisture, and momentum exchanges between the ocean and atmosphere is crucial to the integrity of a GCM. GCM is complex,gridded and three dimensional computer based models of climate system.

Carter *et al*. (1999) mentioned it have horizontal resolution of between 250 and 600 km, 10 to 20 vertical layers in the atmosphere and sometimes as many as 30 layers in the oceans and quite coarse relative to the scale of exposure units.

GCMs used for investigating interactions between processes of the climate system, simulating evolution of the climate system, and providing projections of future climate states under scenarios that might alter the evolution of the climate system (Bader *et al.,* 2008). GCMs are not useful for spatial scales climate impact and adaptation studies though lack of resolution is not necessarily a major factor to consider when constructing comprehensive climate scenarios for impacts studies. It is primary source of information for constructing climate scenarios and will always provide the basis of comprehensive assessments of climate change at all scales from local to global (Carter *et al.*, 1999; Jones *et al.*, 2004).

There are different souce of GCM detail on (IPCC, 2007; Carter *et al.,* 1999). Some of the future most commonly used once in which the output is archived in IPCC database(Table 2-1).

Table 2-1:- General Climate change Models of climate change held by IPCC data distribution center

Climatic model	**Atmospheric resolution**	**Country**	**Emission senarios**
BCCR-BCM2.0	2.8_×2.8_ (T63 L31)	Norway	A1B, B1
CCSM3	1.4_×1.4_ (T85 L26)	USA	A1B, A2, B1
CGCM3.1(T47)**	3.8_×3.7_ (T47 L31)	Canada	A1B
CNRM-CM3	2.8_×2.8	France	A1B,A2

CSIRO-Mk3.0	1.9_ x 1.9_ (T63 L18)	Australia	A1B, B1, A2
ECHAM5/MPI-OM MPIM	1.9_× 1.9_ (T63 L31)	MPIM-Germany	A1B, A2, B1
ECHO-G**	T30 L19	KMA-Korea and MPIM-Germany	A1B, A2, B1
GFDL-CM2.0	2_×2.5_ (L24)	USA	A1B, A2, B1
GFDL-CM2.1	2_×2.5_ (L24)	USA	A1B, A2, B1
GISS-EH	3_ ×4_(L12)	USA	A1B, B1
IPSL-CM4	2.5 x 3.75	France	A1B, A2, B1
MIROC3.2(hires)**	1.1_×1.1_ (T106 L56)	Japan	A1B, B1
MIROC3.2(medres)	2.8_×2.8_ (T42 L20)	Japan	A1B, B1
MRI-CGCM2.3.2	2.8_×2.8_ (T42 L30)	Japan	A1B, A2, B1
PCM	2.8_×2.8_ (T42 L26)	USA	A1B, A1
UKMO	2.75_×3.75	UK	A1B, A2, B1
UKMO-HadGEM1	1.25_×1.9	UK	A1B, A2

The data output from the above mentioned GCMs are rarely used in environmental impact assessment of climate change due to relative coarser spatial and have to be changed to finer scale compatible to selected hydrological model. The confidence of reliability of the output decrease moving from the global to the grid-box scale, from annual to monthly and ultimately in the daily time scale (IPCC, 2007). This study uses UK Hadley center for climate prediction and research (HadCM3). It has atmospheric part spatial resolution of 3.75° longitude by 2.5° latitude and 19 vertical levels. Also the ocean component of the model has horizontal resolution

of 1.25° longitude by 1.25° latitude with 20 vertical levels. According to Wilby & Dawson (2002) the predictor varables from HadCM3 are physically and conceptually sensible with respect to predictand, strongly and consistenly correlated with predicted and realitsic model by GCMs. Also the impact studied on (Wilby & Dawson, 2000; Shimelis *et al.*, 2011; Fadil *et al.*, 2011) are a good examples to show there is good correlation between the HadCM3 predictors and predictands on their region specally Shimelis *et al*. (2011) studied on Lake Tana impact assesment of climate change indicate there is good correlation between the two. Jones *et al.* (2004) added the Hadely center shows 10 year simulation captures about half of the variance of true region climate change response (i.e obtained with a simulation of infinite length). Due to the above mentioned reasons and contrain of time this study is conducted through the output of HadCM3 (UK Hadley center for climate prediction and research) and among the different Special Report on Emissions Scenarios (SRES), which were developed by the IPCC. This study uses the A2 (medium- high emission) and B2 (medium-low emission) scenarios for this climate change impact study.

2.7 Downscaling Model

2.7.1 Description of Statistical downscaling model

There is significant gap between large spatial resolution GCMs and regional and local watershed processes. The scale is mismatch and cause considerable problem in assessment of climate change impacts using the hydrological models. So siginficant attentions should be given during developemnt of downscaling methodologies for obtained coarse-resolution global climate models (Shimelis *et al.*,2011).

There are two main approaches for downscaling large spatial reolution GCM outputs to a fine spatial resolution: dynamical and empirical (statistical) downscaling. In dyanmical higher resloution climate models or regional climate models are forced using GCMs. This kind of downscaling is coarser resolution because of that fact there are limitations on simulating regional studies. Next is statistical (empirical) approach. It creates empirical relationship between GCM-resolution climate variables and local climate. It uses such relationship to resolve behavior in GCMs with climate in targeted area. This area can be small as single point. As long as this relationship occurs, it yields regional information for any desired variable such as precipitation and temperature, as well as variables not typically simulated in climate models.

It is very inexpensive compared to numerical simulation when applied to few locations or use simple techniques. Its lower costs, together with flexibility in targeted variables, have led to a wide variety of applications in assessment impacts of climate change. This approach encompasses a range of statistical techniques from simple linear regression to more-complex applications such as those based on weather generators, canonical correlation analysis, or artificial neural networks.

According to Wilby & Dawson (2002) mentioned from the types of statistical methods regression based downscaling have benfit on standardazation of predictor varables (by their respective mean and standard deviations) so that there is closer agreement between correspondent distribution of observed and GCM predictors. That ensure the future scenarios downscaled using GCM predictor variables are not compromised by system biases in climate model output and sufficent data will be available for calibration and validation.

SDSM is best described as a hybrid of the stochastic weather generator and regression-based methods. This is because large-scale circulation patterns and atmospheric moisture variables are used to linearly condition local-scale weather generator parameters (e.g. precipitation occurrence and intensity). Additionally stochastic techniques are used to artificially inflate the variance of the downscaled daily time series to better accord with observations. To date, the downscaling algorithm of SDSM has been applied to a host of meteorological, hydrological and environmental assessments (Wilby & Dawson, 2000).

SDSM can be expressed in the most general form as (Cherie, 2013);

$$R_t = F_Y(X_T, \theta); T \leq t \qquad (2\text{-}1)$$

Where

θ is the parameter set

F_Y is represents a multiple non linear regression function, that in many case reverts to a multiple linear regression model

R_t stands for the local downscaled predictand at a site,

X_T stands for the large scale predictor varaible(from the GCMs)

Several studies used to assese the impact of climate change as (Cherie, 2013; Fadil *et al.*, 2011; Shimelis *et al.*, 2011; Gebresenbet, 2015).

1. Prepare input data of predictands and GCM predictors at daily time scale.

2. Screen the most potential predictors.

3. Fit the SDSM to reanalyse predictors and observed predictands.

4. Drive this fitted SDSM with independent temporally reanalysis predictors.

5. Compare the statistical properties of the results of step 4 with those of observed predictands. A good agreement implies that the SDSM can reconstruct the climatology of the observed local variables well, when driven by large scale observation.

6. Drive the SDSM fitted to observed time series in step 3 with control GCM predictors and generates a simulated time series.

7. Compare the simulated time series in step 6 with observed time series. Good agreement implies that the GCM predictors can adequately simulate the local climate variables.

8. Drive the SDSM fitted to observed time series in step 3 with future GCM scenarios and generates a future simulated time series of climate variables.

Wilby & Dawson (2007) describe about the model structure and operation of SDSM 4.2 have seven major tasks: 1) quality control and data transformation; 2) screening of potential downscaling predictor variables; 3) model calibration; 4) generation of ensembles of present weather data using observed predictor variables; 5) statistical analysis of observed data and climate change scenarios; 6) graphing model output; 7) generation of ensembles of future weather data using GCM–derived predictor.

Wilby & Dawson (2007) outlines the purpose of each SDSM function as follows;

1) Quality control and data transformation

This part identifies gross data error, specification of missing data codes and outliers prior to model calibration. It can transform predictors by facilitating to choose the data file and apply

transformation (e.g., logarithm, power, inverse, lag, binomial, fourth and cube root etc.) or predict and prior to model calibration.

2) Screening of downscaling predictor variables

In center of statistical downscaling model it creates empirical relationship between gridded predictors (such as mean sea level pressure) and single site predictands (such as station precipitation). The main purpose of this step is selecting appropriate downscaling predictor variables and it is most challenging because of the choice of predictors largely determines the character of the downscaled climate scenario. Decision process is complicated due to the fact of explanatory predictor variables vary both spatially and temporally. This part facilitates to examine seasonal variations in predictor scale.

3) Model calibration

The specified predictand along with a set of predictor variables, and computes the parameters of multiple regression equation via an optimization algorithm (either dual simplex of ordinary least squares). It can be done monthly, seasonally or annually on the processes of conditional and unconditional models. Unconditional models mean direct link assumed between the predictors and predictand (e.g., local wind speeds may be a function of regional airflow indices). In conditional models, there is an intermediate process between regional forcing and local weather (e.g., local precipitation amounts depend on the occurrence of wet–days, which in turn depend on regional–scale predictors such as humidity and atmospheric pressure).

4) Weather generator

It generates ensembles of synthetic daily weather series based on observed (or NCEP re–analysis) atmospheric predictor variables. This step enables verification of calibrated models (using independent data) and the synthesis of artificial time series for present climate conditions. Synthetic time series are written to specific output files for later statistical analysis, graphing and/or impacts modelling.

5) Data analysis

This model examines both downscaled scenarios and observed climate data with the Summary Statistics and Frequency Analysis screens. It shows monthly/ seasonal/ annual means, measures of dispersion, serial correlation and extremes.

6) Graphical analysis

It is provided by SDSM 4.2 through the Frequency Analysis, Results comparison, and the Time Series Analysis screens. Frequency analysis plots extreme value statistics of chosen data file through Empirical, Gumbel, Stretched Exponential and Generalized Extreme Value distributions. Compared results are used to plot monthly statistics in bar and line charts. The Time Series Analysis screen is used to produce time series plots for five variables. The data is analyzed by monthly, seasonal, and annual or water year periods for statistics such as Sum, Mean, Maximum, and Winter/Summer ratios, Partial Duration Series, Percentiles and Standardized Precipitation Index.

7) Scenario generation

It produces ensembles of synthetic daily weather series given atmospheric predictor variables supplied by a climate model (either for present or future climate experiments), rather than observed predictors. Have identical function with weather generator but different model dates and source directory for predictor variables are used.

2.8 Hydrological Modeling

Modeling is defined as the process of organizing, synthesizing, and integrating component parts into a realistic representation of the prototype. The purpose of using a model is to establish baseline characteristics whenever data is not available and to simulate long-term impacts that are difficult to calculate (Lenhart *et al*., 2002). Hydrological modeling is use of physical or mathematical techniques to simulate the hydrologic cycle and its effect on a watershed. A watershed model simulates hydrologic processes in a more holistic approach

compared to many other models which primarily focus on individual processes or multiple processes at relatively small -or field-scale without full incorporation of a watershed.

Hydrological models are characterizations of the real world system. Modeling of the rainfall runoff processes of hydrology is needed for many different reasons the main reasons being limited range of hydrological measurement techniques and limited range of measurements in space and time (Beven, 1985). Therefore, it is necessary to develop a means of extrapolating from those available measurements in space and time to ungauged catchments and into the future to assess the likely impact of future hydrological changes. A wide range of hydrological models are used by the researchers, however, the applications of those models are highly dependent on the purposes for which the modeling is made. (Beven, 1985). Stated that many rainfall-runoff models are carried out purely for research purposes as a means of enhancing knowledge about hydrological systems He also added that other types of models are developed and employed as tools for simulation and prediction aiming ultimately to allow decision makers to improve decision making about hydrological problems. Before developing the hydrological models, it is very important to understand how the catchment responds to rainfall under different conditions.

2.8.1 Classification of Hydrologic Model

Hydrological models clasiified based on the component or method of repesentation of hydrological cycle as Emprical, conceptual or physical based (Chow, 1964). According to Getenet (2009) emprical (black box) model is based on mathematical relationship between input and output variables on catchment. The catchment is lumped they don't take account of spatial character of basin and parameters of the model is physically meaningless. Conceptual models most of them produce model output (stream flow) and not simulate other hydrological variables (groundwater level and infiltration e.t.c) less simple than emperical models. Physcally based models is based on theoretical equation relationship between the input and output varables by taking creating better understanding of physical process on the catchment. It use spatial distributed variables in order to take account spatial heterogeneity of the catchment. Their physical-based level in Figure 2-2.

MODELLING TYPES			
	Detail physically-Based models Partial physically-Based models	White box	Most model parameters Can be measured
	Conceptual model	Gray box	Model parameters need calibration (e.g. using measurements for model output variables)
	Empirical models Black-box models	Black box	Also the model structure building depend on the measurements for model output variables

Figure 2-2:- Schematic Overview of different model types (Willems, 2000)

Depends on the results behavior obtained from hydrological models can be classified as stochastic and deterministic or mixed (Chow, 1964) if one or more of the variables in mathematical model is random variables their distributions in probability the model is stochastic. If all the variables are considered free from a random variation, the model will be deterministic. Deterministic models provide reliable information on behavior of the system and use long data series comparing to stochastic.

Deterministic hydrologic model is classified into three as Lumped model, Semi-distributed model and Distributed model (Cunderlik, 2003; Chow, 1964).

Lumped model

The parameters of this model do not vary spatially in the basin and the basin response is evaluated at the outlet without considering the response of other sub basins. This parameter do not represent physical features of hydrological process and have certain degree of empiricism. This model is not used in event-scale process. It is selected because of having simple structure, requires minimum data, easily used, fast set up and calibration. Gives better result especially in

discharge prediction only also it provides good simulation as complex physically based model (Beven, 2000).

Semi-distributed model

Parameter of simplified distributed model are vary in space by dividing the basin into a number of smaller sub basins. This model contain two main type kinematic wave theory models (KV models, such as HEC-HMS) and probability distributed model (PD model, such as TOPMODEL). KV model is physical based model with simple version of surface or subsurface flow equation. PD model it use probability distribution of input parameter across the basin. The main advantage comparing to lumped model is physically based model and comparing to distribute it needs less data (Beven, 2000).

Distributed model

The parameters fully vary in space at resolution usually chosen by the user. Its approach is to mix data related to spatial distributed of parameter variations with computational algorithm to evaluate its effect of distribution on simulation precipitation-runoff behavior and requires large amount of data for parameterization in each grid cell. If the governing physical process modeled in detail and properly applied it provide higher degree of accuracy (Beven, 2000).

Although Cunderlik (2003) classified based on their time scale this hydrological models into event-driven models, continous-process models and models capable of simulating both short-term and continous events. According to his report event-driven models are desgined to simulate individual precipitation-runoff events their objective to evaluated direct runoff and give specail attention to infiltration and surface runoff. They are not suitable for the simulation of dry weather flows (drought analysis) because of lack of consideration of moisture recovery and storm events. The next is continous proecess models clearly consider all runoff components including direct and indirect runoff. They consider long term hydrologic abstract response for rate of moisture recovery during lack of precipetation also suitable for simulating daily, monthly and seasonal stream flow usually for long term runoff volum forcasting and estimating water yield.

2.8.2 Model selection criteria

Due to advance in hydrological science, geographical information system (GIS) and remote sensing many compressive spatially distributed hydrological models have been developed in the past decade. SWAT is one of the developed hydrological model According to Cunderlik (2003) report suggest the four criteria's to be considered during selection of hydrologic model are the model output purpose, models different hydrologic processes, availability of data and cost.

Fadil *et al.* (2011) described SWAT is a physical based and semi- distributed model operates continuously on a daily time step to produce efficient and reliable result in several area of the world. The biggest issue occurs on this model in developing countries is lack of data and efficient in semi-arid areas.

The soil and water assessment tool (SWAT) was chosen for this case study because it contain useful hydrological components and used to simulate water balance with additional watershed process such as water quality, climate change, crop growth, and land management practices. SWAT selected easily available model free in cost and needs less investment of money. This study is on impact of climate change on the hydrology of the catchment that concentrated on the climatic variables effect like temperature and precipitation on the hydrology by comparing their discharge difference after long period of years so SWAT requires less available data and gives long term results that is related with this study objective. Also literatures like (Fadil *et al.*, 2011; Tazebe *et al.*, 2009; Shimelis *et al.*, 2011) on climatic change assesment shows the model SWAT provide best correlation between observed and simulated also those output results are consides with IPCC finding in their study area but also they indicated this model is physical based do not consider landuse change, soil type and others.

Although Cherie (2013) added SWAT model is based on readily observed and measure information and it attempts to simulate many hydrological components, continuous time model and is capable of simulating long periods for computing the effects of climate change, thus allowing the computation of the effects of climate change, public domain with for free and online access, ease of data base management and linkage with sensitivity, calibration and uncertainty analysis tools.

Among these guidelines, the most common ones are listed below.

1) Accessebility of software: does the model is freely accessible?
2) Input data requirements: do the minimum input data required to make a run of model are available?
3) Computational efficiency: Does the model simulation of very large basins, a variety of management strategies and land use dynamics impact can be performed without excessive investment of time and money?
4) Capability to study long-term impacts: is the model a continuous time model, i.e. a long-term yield model.
5) Capability for interface with other software:does the model works in interface with other software?
6) Required model output: can the model best estimates output parameters required by the research?

2.9 Theoretical description of Selected Model

2.9.1 Soil and Water Assessment Tool (SWAT)

Soil and Water Assessment Tool (SWAT) is one of agro-hydrological watershed model created in Agricultural Research Services of United States Department of Agriculture, this model combine and analyze spatially by using GIS tool (Neitsch *et al.,* 2000). The model can be coupled with two GIS software as free additional extensions: ArcSWAT for ArcGIS and MWSWAT for Map-Window.

SWAT model is created in early 1990s used to predict the impact of land management practices on water, sediment and agricultural chemical yield in large, complex watershed with different soils, land use and management condition over long period of time. SWAT 94.2, SWAT 96.2, SWAT 98.1, SWAT 99.2, SWAT 2000, SWAT 2005, SWAT 2009 are significant improvement with additional model interface windows (Visual Basic), Arc View and ArcGIS. It is physical

based, semi-distributed, continuous time and operated on daily time step on river basins or watershed.

Based on the above criteria and taking into consideration of the following benefits of the model SWAT was selected as an appropriate model for this particular study. SWAT is free software, the model uses readily available inputs and the minimum data required to make a run of SWAT model are commonly available from government agency, is computationaly efficient for very large basins and perform well in predicting long term impact of land use dynamics without excessive investment of time and money, is applicable for large scale catchments and could best predict different parameters for catchments > 100 Km^2, is a continuous time model, i.e. a long-term yield model that enables users to study long-term impacts,works in interface with Geographic Information System (GIS), allowed topographical, land use and management differences.

SWAT embedded with ArcGIS interface called Arc SWAT used to evaluate the climate change in the hydrology of Megech watershed. According to Neitsch *et al.,* (2000) this model uses hydrolgical response unit (HRUs) to describe spatail heterogenity interms of land cover, soil type, slope within watershed and simulate the hydrology of the watershed by land and routing phases.

2.9.2 Hydrological Component of the SWAT Model

SWAT allows different physical processes simulated in watershed or river basin. It divides the watershed in to sub basin or sub watersheds. It create different watershed area have different soil property, land use and slope used to determine impact on hydrology. The input information's are grouped in climate, hydrological response unit or HRU, pond / wetlands, ground water and main channel or reach, draining the sub basins. It simulate the watershed by two separated division. First is land phase process it control the amount of water, sediment, nutrients and pesticide loading to the main channel in each basin. Then the second division is water or routing phase of hydrological cycle that defines the amount of water, sediment, nutrients and organic chemicals through the channel network of the watershed to the outlet.

Land phase of Hydrologic Cycle

The hydrologic cycle as simulated by SWAT is based on the water balance equation.

$$SWt = SWo + \sum_{i=1}^{t}(Rday - Qsurf - Ea - Wseep - Qgw) \qquad (2\text{-}2)$$

Where SWt is the final soil water content (mm H_2O),

SWo is the initial soil water content on day l (mm H_2O),

t is time (days), $Rday$ is amount of precipitation on day l (mm H_2O),

Ea is amount of evapotranspiration on day l (mm H_2O),

$Wseep$ is amount of water entering to vadose zone from the soil profile on day l (mm H_2O),

Qgw is amount of return flow on day l (mm H_2O),

$Qsurf$ is amount of surface runoff on day l (mm H_2O).

Surface runoff

Surface runoff is rate water applied to the ground surface exceed rate of infiltration. The infiltration rate decrease as the soil becomes wetter but when water initially applied to dry soil the infiltration rate increases. If application rate is higher than infiltration rate, surface depression fills and cause surface runoff. SWAT have two methods that estimate surface runoff; the SCS Curve number procedure (SCS, 1972) and the Green & Ampt infiltration method (1911). Neitsch *et al.* (2000) added SCS Runoff equation is an empirical model developed 1950s used estimating the amount of runoff under varying land use and soil type.

The Green-Ampt infiltration method is based on the principles of Green and Ampt (1911) and Mein and Larson (1973). It needs sub-daily precipitation data and depends on the wetted front matric potential and effective hydraulic conductivity of the soil profile (Ksat).

According to Getnet (2009) Green - Ampt infiltration method needs intensive data and is not feasible for large watersheds compared to SCS curve number method. The disadvantage

of SCS curve number method that it lumps canopy interception in the term of initial abstraction and also needs a slope adjustment.

For this study the SCS curve number procedure is preferred over the Green & Ampt infiltration method. The Green & Ampt infiltration method assumes that there is excess water at the surface at all times is invalid assumption in the study area. Although the Green and Ampt infiltration method requires sub-daily precipitation data and it other limitation to use this method. Because of above reasons this case study is conducted by using SCS curve number.

SCS Curve number equation is (SCS, 1972)

$$Qsurf = \frac{(Rday - Ia)^2}{(Rday - Ia + s)} \qquad (2\text{-}3)$$

Where: $Qsurf$ is the accumulated runoff or rainfall excess (mm H_2O),

$Rday$ is the rainfall depth for the day (mm H_2O),

Ia is initial abstract which include surface storage, interception and infiltration prior to runoff (mm H_2O),

s is a retention parameter (mm H_2O). Retention parameter varies due to change in soil, land use, management, and slope and temporally due to change in soil water content.

Retention parameter defined as

$$S = 25.4\left(\frac{1000}{CN} - 10\right) \qquad (2\text{-}4)$$

Where CN is the curve number for day,

Initial abstract,Ia, is commonly approximated as $0.2S$ and Equation 3-2 become

$$Qsurf = \frac{(Rday - 0.2S)^2}{(Rday - 0.2S)^2} \qquad (2\text{-}5)$$

Runoff always occur when $Rday > Ia$

Peak Runoff

SWAT calculate the peak runoff based on the modification of rational formula. It assumed that a rainfall of intensity i begins at time t = 0 and continues indefinitely, the rate of runoff will increase until the time of concentration, t = t conc. Time of concentration is calculated by manning formula by considering both overland and channel flow. To adjust total volume of runoff reach the bigger channel of sub basin Surlag (surface runoff lag coefficient) incorporated.

SWAT calculate peak runoff by modified rational formula

$$q\ peak = \frac{\alpha\ tc\ * Q\ surf * Area}{3.6 * t\ conc} \qquad (2\text{-}6)$$

Where $q\ peak$ is the peak runoff rate (m^2s^{-1}),

α_{tc} the fraction of daily runoff that occur during the time of concentration,

i is the runoff intensity (mm/hr), $Area$ is the sub basin area (km^2),

$Q\ surf$ is surface runoff (mm H_2O),

t_{conc} is time of concentration for sub basin (hr) and 3.6 is a unit conversion factor.

SWAT estimates the value α tc using

$$\alpha_{tc} = 1 - exp(2 * t_{conc} * ln(1 - \alpha_{0.5})) \qquad (2\text{-}7)$$

Where α_{tc} is the fraction of daily rain falling in the half-hour highest intensity rainfall

t_{conc} is time of concentration for the sub basin (hr).

Time of concentration

As Neitsch *et al.* (2000) discribion it is the amount of time from beginning of rainfall event until the entire sub-basin area is contributing to flow at the outlet. It can be calculated by summation of overland flow time (time takes flow from the remote point in the sub basin to

reach the channel) and channel flow time (time it takes for flow in the upstream channel to reach the outlet). It can be calculated by

$$t_{conc} = t_{ov} + t_{ch} \qquad (2\text{-}8)$$

Where t_{conc} is time of concentration for the sub basin (hr),

t_{ov} is the time of concentration for overland flow (hr),

t_{ch} is the time of concentration for channel flow (hr).

Overland flow time is the time taken for water travel from the furthest point in the sub basin in to stream channel.

Overland flow time (t_{ov}) is calculated by:-

$$t_{ov} = \frac{L_{slp}}{3600 * v_{ov}} \qquad (2\text{-}9)$$

Where: L_{slp} is the average sub basin slope length (m),

v_{ov} is the overland flow velocity (m/s), & 3600 is a unit conversion factor.

Overland flow velocity for a unit width along the slope is calculated by using the Manning's equation:

$$v_{ov} = \frac{q_{ov} * 0.4 * slp}{n^{0.6}} \qquad (2\text{-}10)$$

Where: q_{ov} is the average overland flow rate (m3/s),

slp is the average slope of the sub basin (m/m), and

n is Manning's roughness coefficient of the sub basin.

Channel flow time of concentration, t_{ch} can be computed by:

$$t_{ch} = \frac{L_C}{3.6 * v_c} \qquad (2\text{-}11)$$

Where: L_C is the average flow channel length (km),

v_c is the average flow velocity (m/s), and 3.6 is a unit conversion factor.

Average flow channel length is calculated as:

$$L_C = \sqrt{L * L_{cem}} \qquad (2\text{-}12)$$

Where: L is the channel length from the furthest point to the sub basin outlet (km),

L_{cem} is the distance along the channel to the sub basin centroid (km).

Soil Water - Percolation, Bypass Flow, and Lateral Flow

Neitsch *et al.* (2000) explained water enter to the soil move along one of several different pathways. The water removed from the soil by plant uptake or evaporation in addition it can be percolate pass to the bottom of the soil profile and recharge aquifer. Final option is water may move laterally in the profile and contribute to stream flow. From the different pathways, majority of water taken by plant than enter to plant uptakes soil profile.

Percolation is the downward movement of water in the soil. SWAT calculates percolation for each soil layer in the profile Water is allowed to percolate if the water content exceeds the field capacity water content for that layer and the layer below is not saturated. When the soil layer frozen, no water flow out of the layer. Getnet (2009) mentioned bypass flow is vertical movement of free water along macro pores through unsaturated soil horizons and that occurs in dominate vertic soil area. It occurs when the rate of rainfall or irrigation exceeds vertical infiltration rate. In simulation of bypass flow SWAT calculate the crack volume of soil matrix for each day of simulation. On days in which precipitation events occur, infiltration and surface runoff are first calculated for the soil peds. Part of the surface runoff equivalent to the cracks volume enters the soil profile as bypass flow, and the rest remains overland flow

Lateral flow is common in areas with high hydraulic conductivities in surface layers and an impermeable or semi-permeable layer at a shallow depth. Rainfall will percolate vertically up to the impermeable layer and develops a saturated zone stored above this layer and called a perched water Table; it is the source of water for lateral subsurface flow. Lateral flow occurs when water stored in the shallow aquifer exceeds a threshold value. SWAT incorporates a kinematic storage model for the calculation of subsurface flow.

Routing phase of the hydrologic cycle

Neitsch *et al.* (2000) describe SWAT determines the loading of water, sediment, nutrients and pesticides to the main channel, the loading are routed through the stream network of the watershed.

Main Channel Routing

The four basic elements routed in the main channel are: water; sediments; nutrients and organic materials. Water is routed in the model with the assumptions of an open channel flow with a trapezoidal shape. The velocity of flow in the channel calculated by Manning's equation. SWAT gives two alternatives for routing of water through: variable storage and the Muskingum routing methods.

Muskingum routing method the storage volume in the channel length as a combination of wedge and prism storage. To calculate the water balance in the channel flow, transmission and evaporation are considered by the model.

The variable storage routing method was developed by Williams in 1969, this study also use this method of SWAT

For given reach segment, storage routing is based on continuity equation

$$\Delta V_{stored} = V_{in} - V_{out} \qquad (2\text{-}13)$$

Where V_{in} the volume of inflow during the time step (m^3H_20),

V_{out} the volume of outflow during the time step (m^3H_20),

ΔV_{stored} is the change in volume storage during the time step (m^3H_20).

$$V_{storage,2} - V_{storage,1} = \Delta t * \left(\frac{q_{in,1}+q_{in,2}}{2}\right) - \Delta t * \left(\frac{q_{out,1}+q_{out,2}}{2}\right) \qquad (2\text{-}14)$$

Where: Δt is the length of the time step (s),

$q_{in,1}$ is the inflow rate at the beginning of the time step (m^3/s),

$q_{in,2}$ is the inflow rate at the end of the time step (m^3/s),

$q_{out,1}$ is the outflow rate at the beginning of the time step (m^3/s),

$q_{out,2}$ is the outflow rate at the end of the time step (m^3/s),

$V_{storage,2}$ is the storage volume at the beginning of the time step (m^3 water), and

$V_{storage,1}$ is the storage volume at the end of the time step (m^3 water).

Travel time is computed by dividing the volume of water in the channel by the flow rate.

$$TT = \frac{V_{storage}}{q_{out,1}} = \frac{V_{storage,1}}{q_{out,1}} = \frac{V_{storage,2}}{q_{out,2}} \quad (2\text{-}15)$$

Where: TT is the travel time (s),

$V_{storage}$ is the storage volume (m^3 water), and

$q_{out,2}$ is the discharge rate (m^3/s)

CHAPTER THREE

3 MATERALS AND METHODS

General

This study involved the use of semi-distributed hydrological model and climatic models that required extensive hydro-meteorology and spatial data at finer temporal and spatial resolution the included metrological data's are: precipitation, temperature, relative humidity, wind speed, solar radiation, and hydrological data are: stream flow, soil data, land use/land cover types and digital elevation models.

The methods and procedures used in this research work for assessment of climate change impact on the hydrology of the catchment go through the following key steps to achieve the outlined objectives:-

1. Collection of required data's according to the model requirement such as meteorological and hydrological data, DEM, soil map, land use/cover map and other related data's of the study area.
2. Preparation and assessment of data sets (using homogeneity and consistency test).
3. Use Global circular model (GCMs) that provides future global climate scenarios under the effect of increasing greenhouse gases by using the latitudinal and longitudinal location of study area.
4. Use statistical downscaling model (SDSM 4.2) to downscale the coarser scale to finer scale compatible and arrange the fine scale data found from SDSM 4.2 (maximum and minimum temperature, precipitation) in two emission scenarios to make it compatible with SWAT model.
5. Checking the significance of downscaled precipitation, minimum and maximum temperature results using Mann Kendell trend.
6. Model setup and simulation of SWAT using the corrected Megech River inflow after construction of Megech dam (inflow of Megech dam) and generating the flow at the dam site from near to end of the century.
7. Result analysis is bounded with the outlined objective.

3.1 Conceptual Frame work of the study

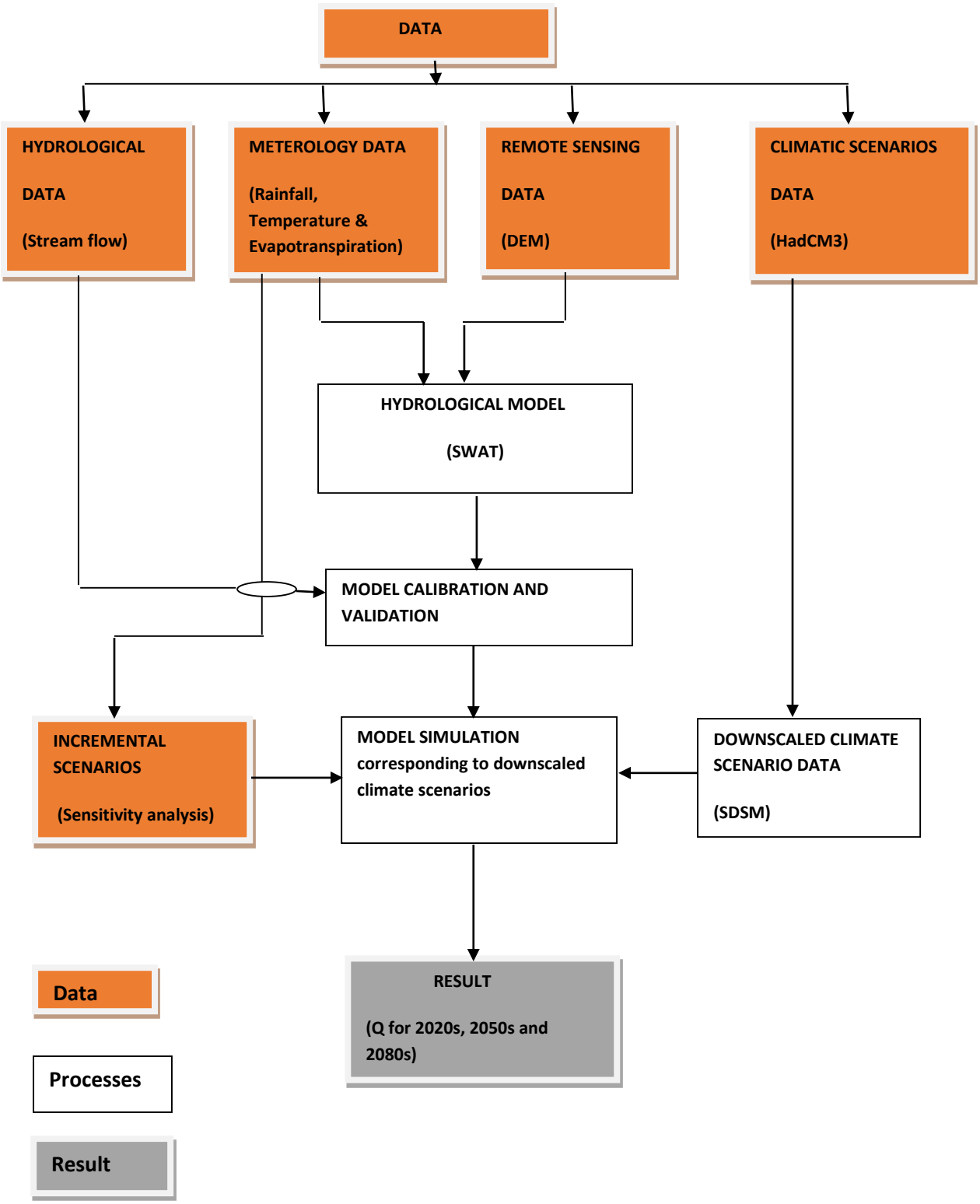

Figure 3-1:- Conceptual framework of the research

3.2 Description of the study area

Lake Tana sub-basin is the beginning of Blue Nile River. The major rivers feeding Lake Tana are the Gilgel Abay, Ribb, Gumara, and Megech. Megech River catchment is situated in the northern portion of the sub-basin in geographic location b/n latitude of 12⁰46’ 0’’ to 12⁰28’0’’ and longitudes 37 ⁰24’ 0’’to 37⁰38’0’’ with catchment area of 700 Km².

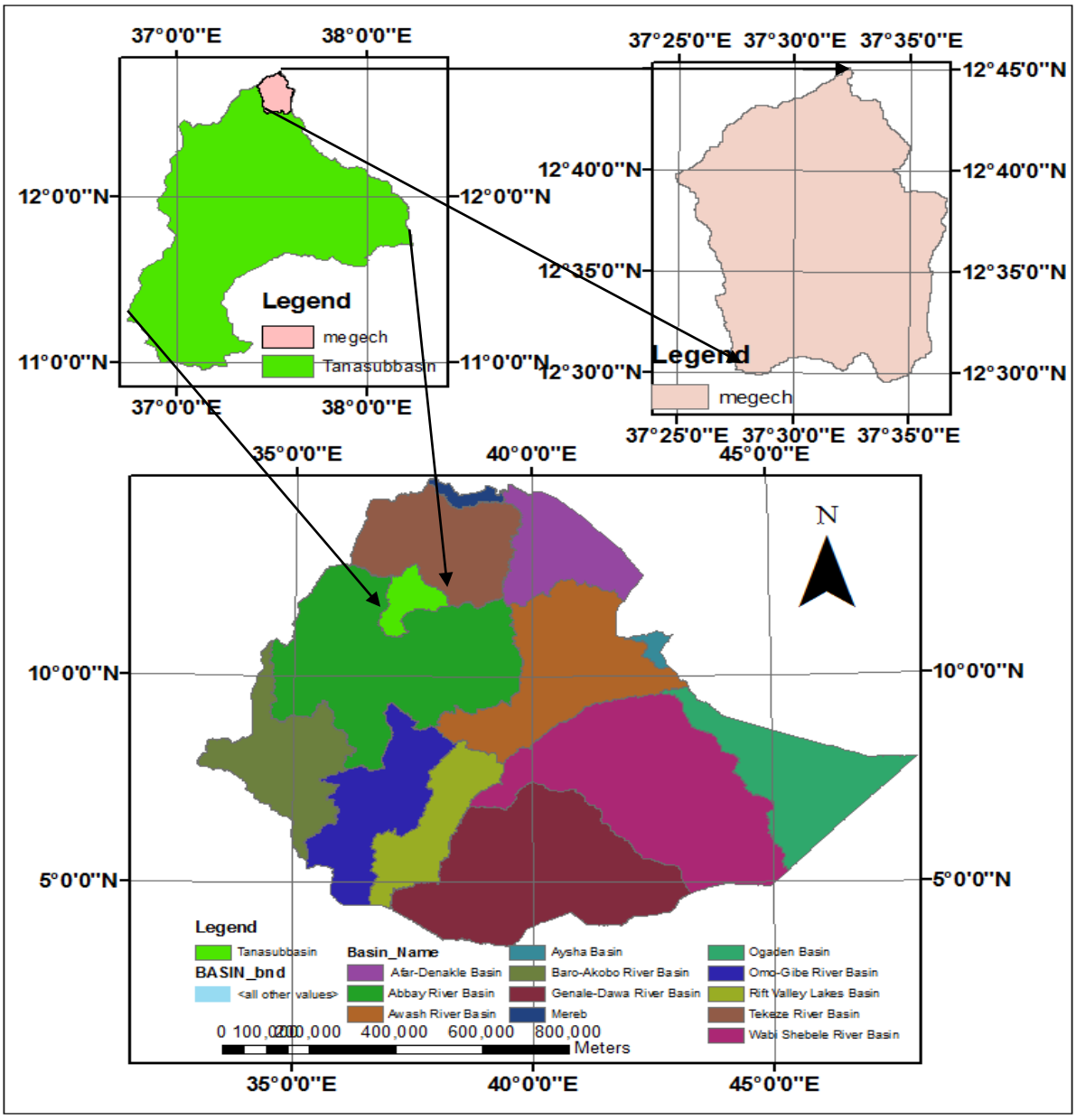

Figure 3-2: - location map of Ethiopia basins and Megech watershed (shape file from ministry of water, Irrigation and Energy)

3.2.1 Digital Elevation Model (DEM)

Topography is defined by a Digital Elevation Model (DEM). Megech watershed is characterized as a steep mountainous watershed with circular shape. The elevation range in the watershed varies between 1878 m and 2945 m above mean sea level. The watershed highest elevation is 2,945 m in its north-eastern part with mean elevation of 2338.194 m above mean sea level. Table 3-1 shows the watershed elevation range.

Table 3-1:-Elevation range of Megech watershed with area percentage coverage

Elevation Range (m)	Area (%)
1878 - 2030	9.83
2030 - 2182	18.6
2182 - 2334	22.21
2334 - 2486	21.76
2486 - 2638	16.13
2638 - 2790	9.92
2790 - 2945	1.56

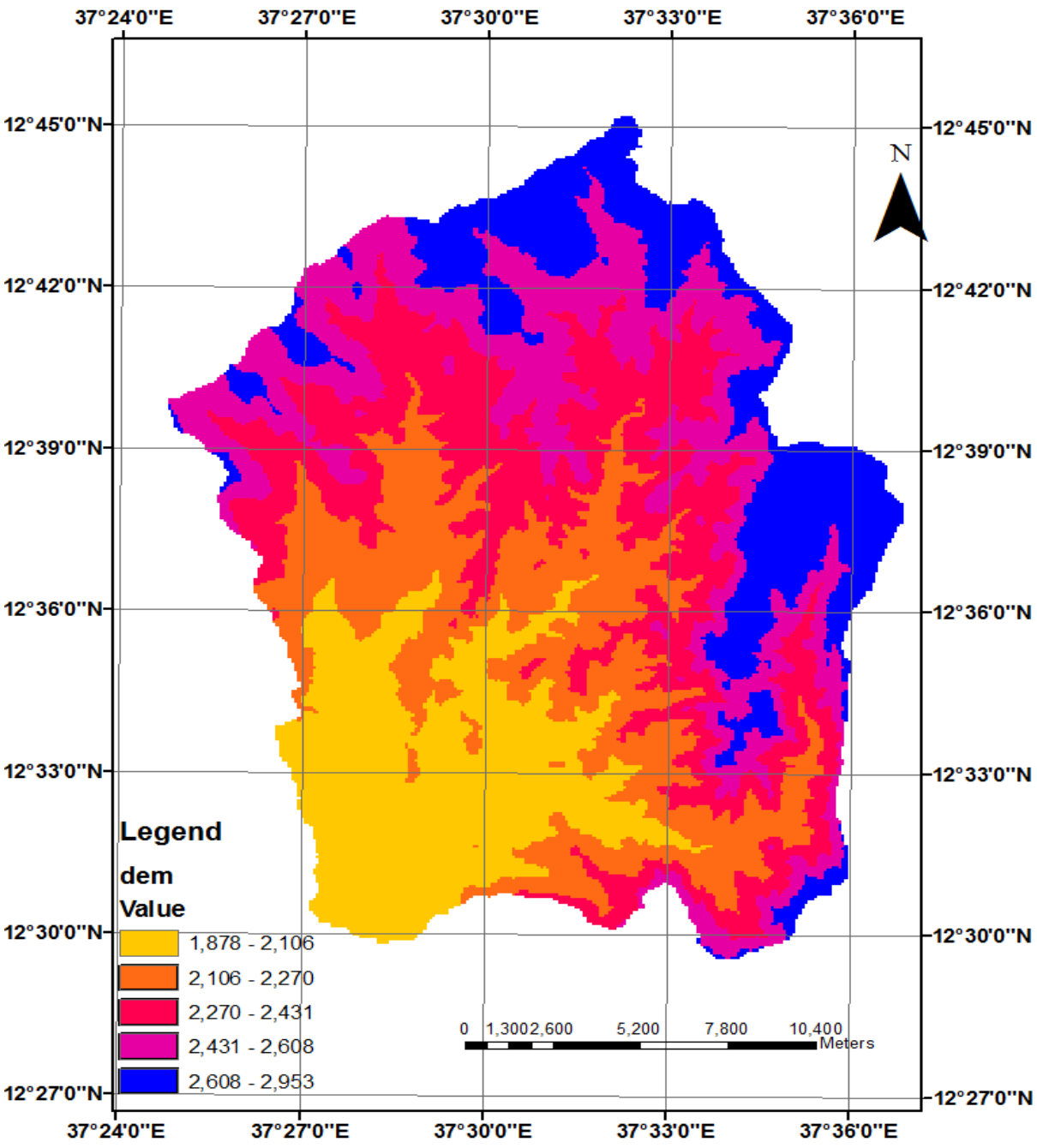

Figure 3-3:- DEM of Megech watershed (shape file of ministry of water, Irrigation and Electricity)

3.2.2 Soil Map

Megech watershed is covered by five major FAO/UNESCO soil groups; Eutric Cambisols (84.35 %), Haplic Nitisols (9.47 %), Chromic Luvisols (3.77 %), Eutric Fluvisols (1.38 %) and Urban (1.04 %). This watershed area more than 75 % is covered by Eutric Cambisols soil. This soil unit is characterized by brownish sandy clay loams and sandy loam developed on metamorphic rocks.

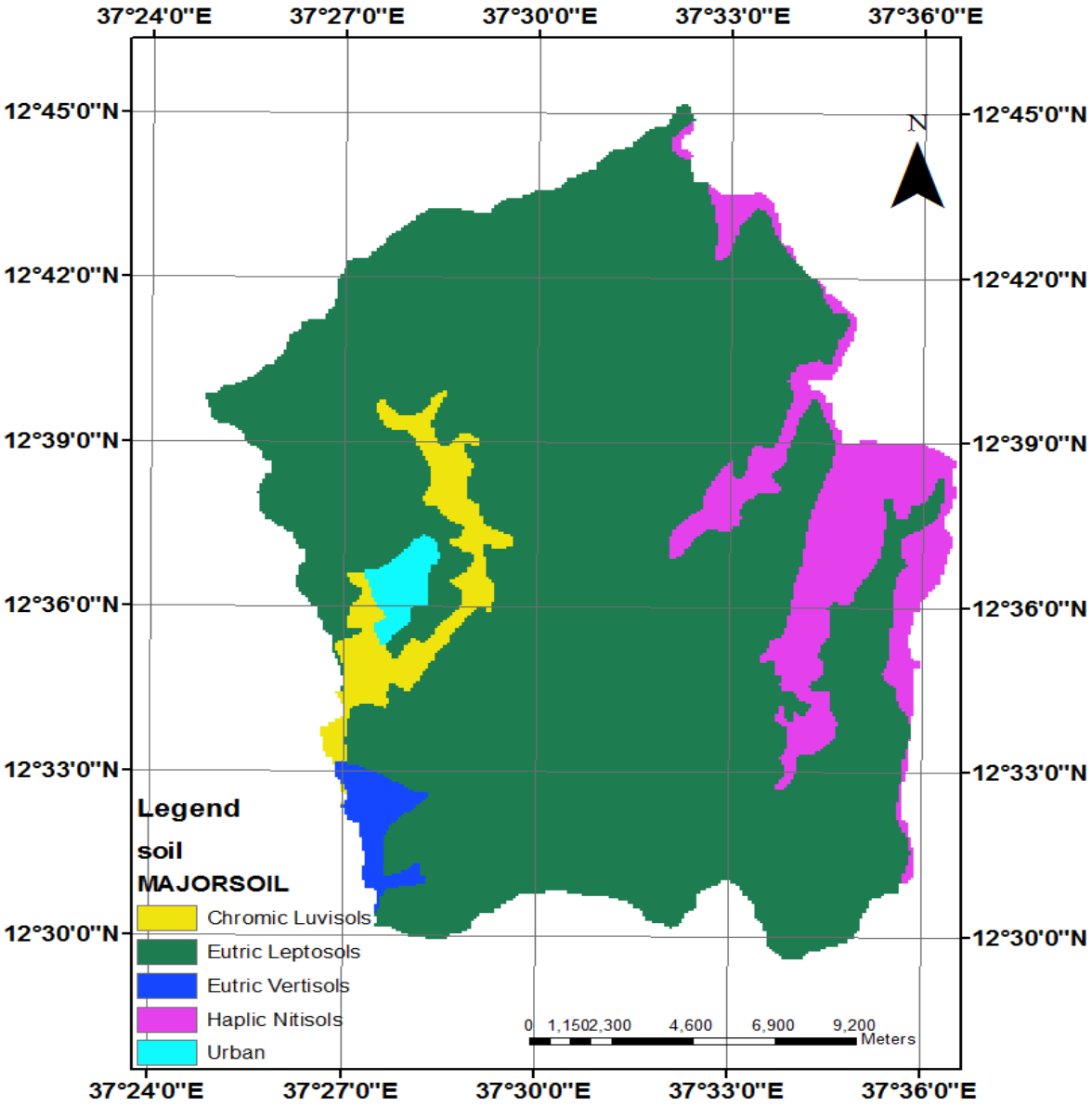

Figure 3-4:- Megech watershed soil map (shape file of ministry of water, Irrigation and Electricity)

3.2.3 Land Use/Land Cover data

The land use map of the study area was obtained from Ministry of Agriculture. The map is available on chapter two of study area description. Spatial distribution and specific land use parameters were required for modeling. SWAT has predefined land uses identified by four letter codes and it uses these codes to link land use maps to SWAT land use databases in the GIS interface. Therefore for my land uses to be configured by SWAT its prepared look up table and land use types were made compatible with the input needs of the model. After all the classified land use map and its attribute were adjusted to the SWAT model requirement format and database. Finally the land uses were re- classified by 4-letter SWAT code for both land use map and their spatial distribution were prepared as follows. SWAT model code reclassification of the land use/ land cover of 2008 that used to generate stream flow of the watershed (Figure 3-5). In addition 1984 LULC and 2008 LULC were compared using SWAT model to observe the land use/ land cover change on the past 24 years using the above mentioned method.

Table 3-2:- Distribution and Area Coverage of land use/cover in Megech Watershed

Land use	SWAT code	**Area coverage (ha)**	**Percentage of cover of watershed (%)**
Cultivated land	AGRC	25358.37	64.34
Plantation	FRSE	469.09	1.19
Grass land	PAST	3074.70	7.80
Shrub land	RNGB	8116.41	20.59
Bare land	URLD	1162.87	2.95
Urban	URHD	1237.76	3.14

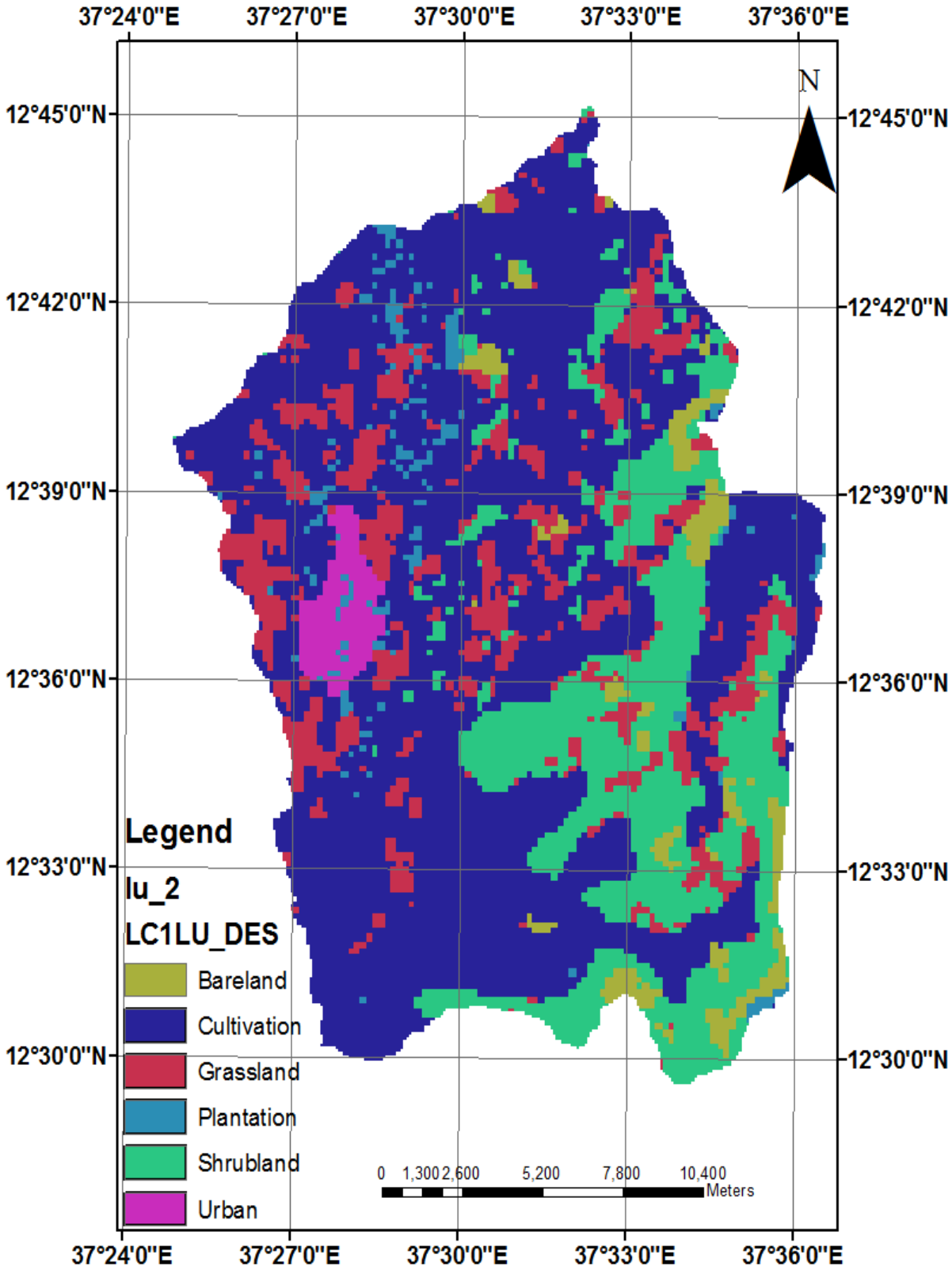

Figure 3-5:- Land Use /land cover map of Megech watershed in 2008 (shape file of Ministry of Water, Irrigation and Energy

3.2.4 Climate

The climate of the Megech watershed is marked by a rainy season from May to October, with monthly rainfall varying from 67 mm in October to 306 mm in July. Mean annual precipitation is about 1,100 mm in the upper part and about 1,000 mm in the lower part. Rainfall over the Megech watershed is mono-modal with nearly 79 % of the annual rainfall occurring in the period June – September. The dry season, from November to April, has a total rainfall of about 8% of the mean annual rainfall. Dependable rainfall (85%) varies from less than 1.2 mm during the dry season to 88–225 mm/month during the period of June to July/August, equivalent to 55–75% of the average values. Maximum temperatures vary from 23 ºC in July to 30 ºC in March, whereas minimum temperatures range from 11.5 ºC in January to 15.6 ºC in April & May. Humidity varies between 39% in March and 79% in August. Wind speed is low, thus minimizing potential evapotranspiration values between 101 mm/month in July and 149 mm/month in March (WWDSE, 2008).

3.3 Data availability and analysis

3.3.1 Meteorology data collection

There are six meteorological observation stations within and around the Megech watershed namely Aykel, Gondar, Ambagiorgis, Chewahit, Gorgora and Maksegnit. For each gauging stations the required daily Meteorology data (daily precipitation, daily maximum and daily minimum air temperature, daily solar radiation, daily wind speed, and daily relative humidity) were collected from National Meteorology Agency of Ethiopia (NMA) for the period of 1993-2013 G.C.

Precipitation

The daily rainfall data for all six gauging stations (Aykel, Gondar, Ambagiorgis, Chewahit, Gorgora and Maksegnit) were collected for the period of 1993-2013. These data later prepared in the dbf format required by the model. The observed stations around Megech watershed with their geographical location and Areal weightage of each stations (Figure 3-6 & Table 3.3).

Estimation Areal Rainfall

Rain gauges represent point sampling of the areal distribution of a storm. In practice, hydrological analysis requires knowledge of the rainfall over an area. Arithmetic mean, thiessen polygon, Isohyetal methods are some of the methods used to convert point (gauged) rainfall values at various stations into an average value over a catchment. However, Thiessen polygon is used for this study due to its simplicity and the average rainfall over the catchment is calculated by:

$$pave = \sum_{i=1}^{n} \frac{(p_i * A_i)}{At} \qquad (3\text{-}1)$$

Where, $pave$ is average areal rainfall (mm),

P1, P2, P3….Pn precipitation of station 1,2,3…n, respectively and

A1,A2, A3….An is area coverage of station 1,2,3…n Respectively in the thiessen polygon.

Table 3-3:-List of meteorological stations and areal weightage of Megech watershed.

Station name	Latitude (^{o})	Longitude (^{o})	Elevation (m)	Areal weightage
Aykel	12.54	37.06	2254	0.082914708
Gonder	12.52	37.44	1973	0.240640363
Maksegnit	12.39	37.56	1912	0.131562083
Ambagiorgis	12.77	37.6	2900	0.163125406
Chewahit	12.33	37.22	1925	0.220645572
Gorgora	12.25	37.3	1830	0.161111869

Temperature:

Excluding Chewahit the daily temperature were collected for all other five gauging stations (Aykel, Gonder, Ambagiorgis, Gorgora and Maksegnit). These data were collected for the Period of 1993-2013 except Gorgora which is from 1994-2013 G.C.

Relative humidity, solar radiation and wind speed data:

Relative humidity, solar radiation and wind speed data were available only for principal stations or class-1 (Aykel and Gondar) from the year 1993- 2013 G.C. In this case SWAT can generate data for the rest stations by using weather generator.

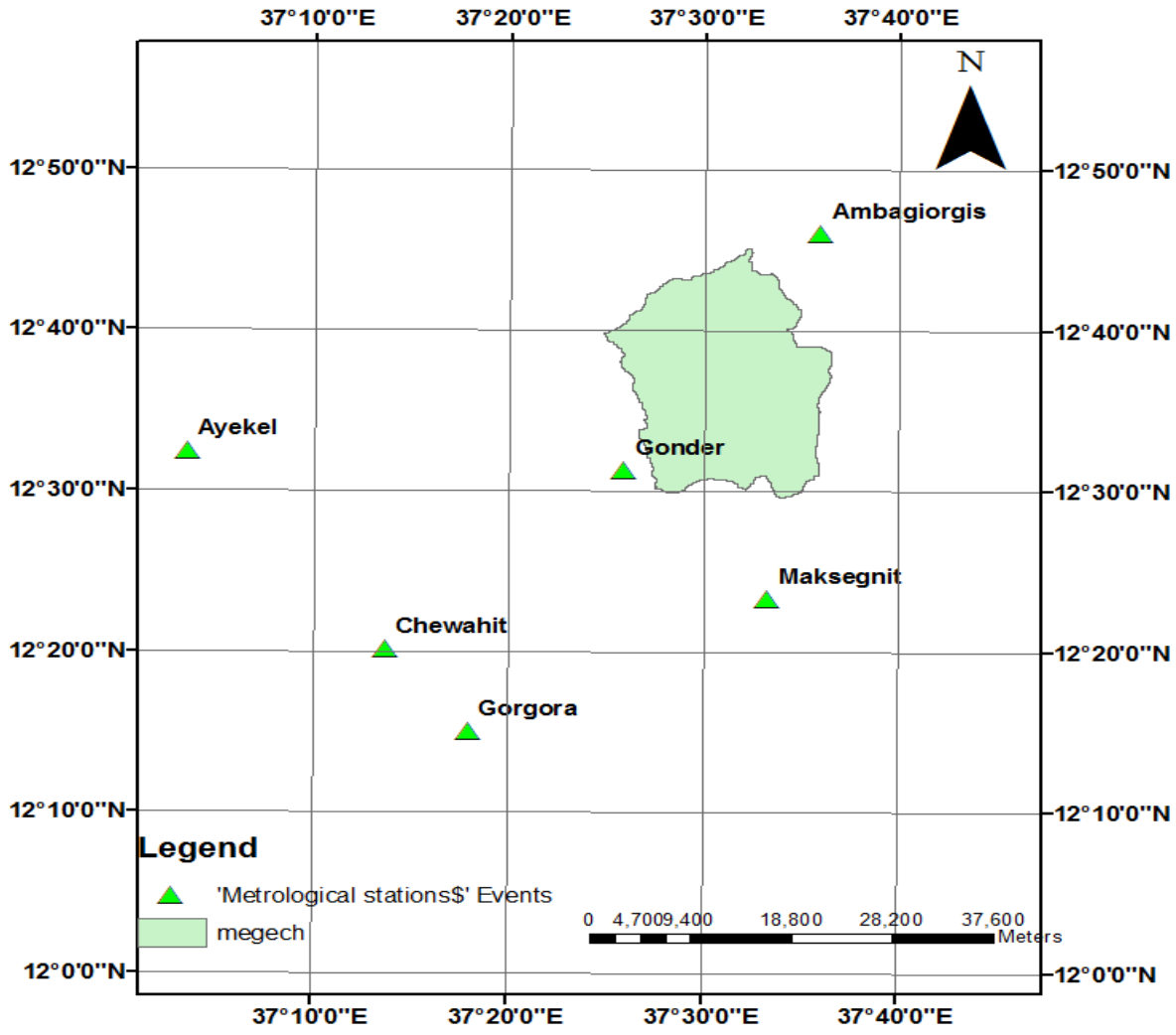

Figure 3-6:- Distribution of selected station's over the Megech watershed (source from Ministry of Water, Irrigation and Electricity)

3.3.2 Filling missed meteorology data

Rainfall is key meteorology variable that mostly affects the hydrological regime of the study area. Daily rainfall data of six stations for which data was obtained and have less than 30 % missing data in the analysis period were used. Data for the missing period was filled using estimation technique. Arithmetic mean, Normal ratio are the most commonly used methods for estimation of missing rainfall & temperature data sets.

Simple Arithmetic mean method was used where the mean monthly rainfall of all the index stations is within 10% of the station under consideration (station x) and calculated the missing data by Equation 3.1. Whereas the mean monthly rainfall of one or more of the adjacent (index) stations differs from that of station x by more than 10% then the normal ratio method was used (Equation 3.2).

$$P_x = \frac{P1+P2+P3}{3} \qquad (3\text{-}2)$$

$$P_x = \frac{1}{3}\left[p1\frac{N_X}{N_1} + p2\frac{N_X}{N_2} + p3\frac{N_X}{N_3}\right] \qquad (3\text{-}3)$$

Where P_x is the precipitation for the station with missed record,

$p1, p2, p3$ ……, pN are the corresponding precipitation at the index stations,

N_1 , N_2, N_3 ……,N_N are the long term mean monthly precipitation at the index stations and at station x under consideration respectively.

3.3.3 Data Quality Assessment

Water resources development and management needs accurate data of hydrological and meteorology data of the study area. These data should be stationary, consistent, and homogeneous when they are used for frequency analysis or to simulate a hydrological system. Accordingly in this study, the data quality assessment goes through the following key tests.

Test for Homogeneity

The data qualities with regard to possible temporal and spatial variations or errors should have to be investigated by checking homogeneity and consistency of selected stations. Non-homogeneity is a change in the statistical properties of the time series. It's caused by either natural or man-made. Reliable measurements of this data are important foundation for quantitative climate analysis. There are several factors affecting the quality of climate data and those factors are considered for scientific and climatic analysis. There are universally accepted standards/recommendations for instrument installation and observations. Measurement practice and instruments may differ from one station to others in a given country and in addition there is change in an individual station from time to time. These mentioned factors cause variation in the result of stations time series.

The homogeneity of the stations checked by:

$$P_i = \frac{P_{i,av}}{P_{av}} * 100 \qquad (3\text{-}4)$$

Where P_i Non-dimensional value

$P_{i,av}$ is over years mean monthly rainfall,

P_{av} is over year's annual average rainfall, i is month.

Time series rainfall of six stations conducted through Equation 3-4. The homogeneity test plot shows that all of the rainfall stations used for this particular study were homogeneous and their rainfall pattern was found to be mono-modal with high rainfall season from July to September and low rainfall season from February to March.

This study area have mono-modal rainfall pattern in non-dimensional graphical plot (Figure 3-7). The plot shows that all stations are homogeneous without showing any sign of inhomogeneity.

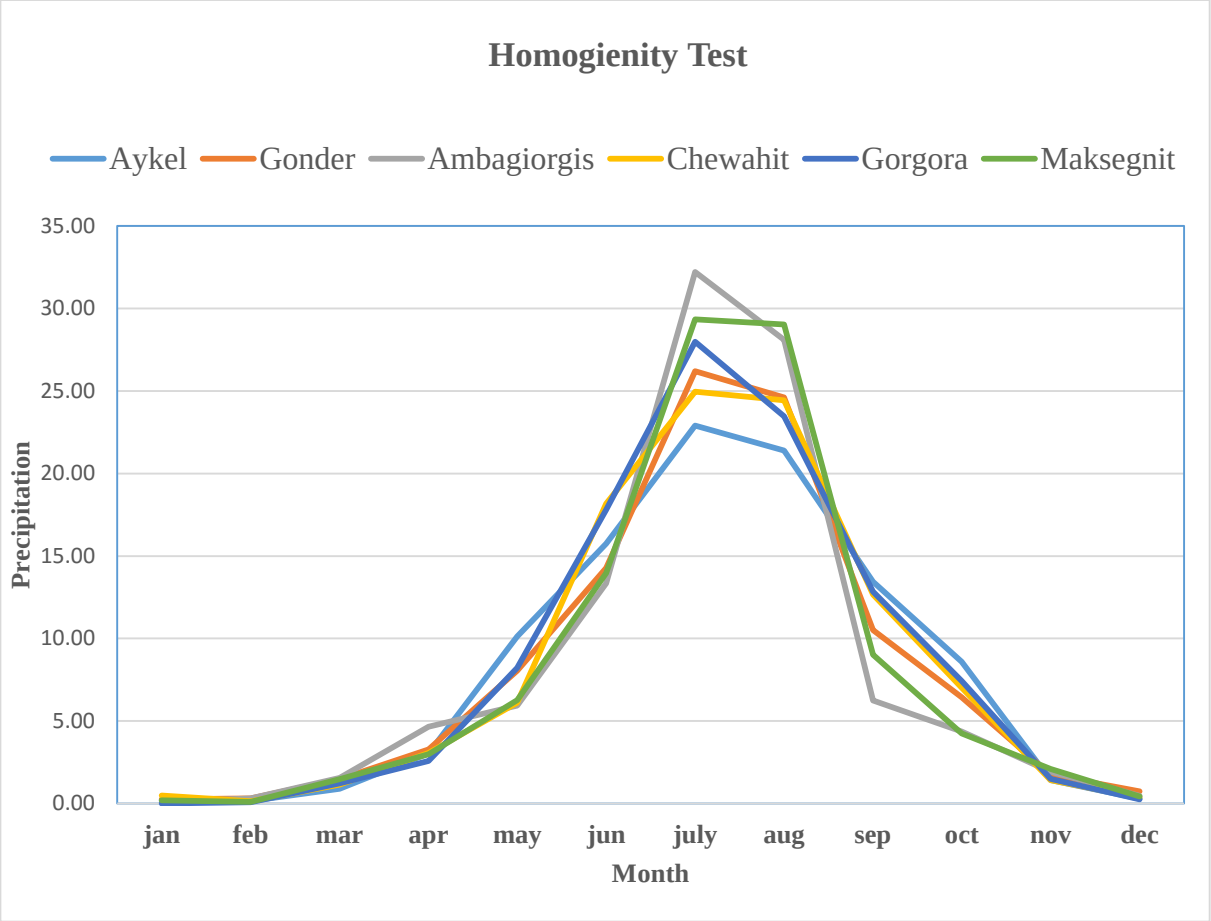

Figure 3-7:- Result of relative homogeneity test for selected rainfall stations

Test for Consistency

Consistent record is a record not changed with time. Adjusting gage consistence involves estimation of effect rather than missing value. Consistency of the stations is checked by double mass curve analysis. This analysis is a graphical method for identification and adjusting inconsistency in a stations recording by comparing its time trend with adjacent stations. If the conditions relevant to the recording of a rain gauge station have undergone a significant change during the period of record, inconsistency would arise in the rainfall data of that station. This inconsistency can be differentiated from the time the significant change took place. If significant change in the regime of the curve is observed, it should be corrected using Equation 3-5. The stations used in this study have not undergone a significant change during the base line period (1993-2013) of the study.

$$P_{CX} = P_X * \frac{M_C}{M_a} \qquad (3\text{-}5)$$

Where: P_{CX} is corrected precipitation at any time period,

P_X is original recorded precipitation at time period,

M_C is corrected slope of the double mass curve and

M_a is original slope of the double mass curve .

Summary of rainfall data for each rain gauge stations

The spatial analyses of rainfall for gauging stations were made for this study period from 1993 to 2013 using the mean annual of each observed gauging station. The spatial analysis result of the six meteorological station.

By comparing the two principal station (Figure 3-6). Gonder station was found good representative of Megech watershed than Aykel and other stations have a lot of missed data. Because of the above mentioned case Gonder station was selected.

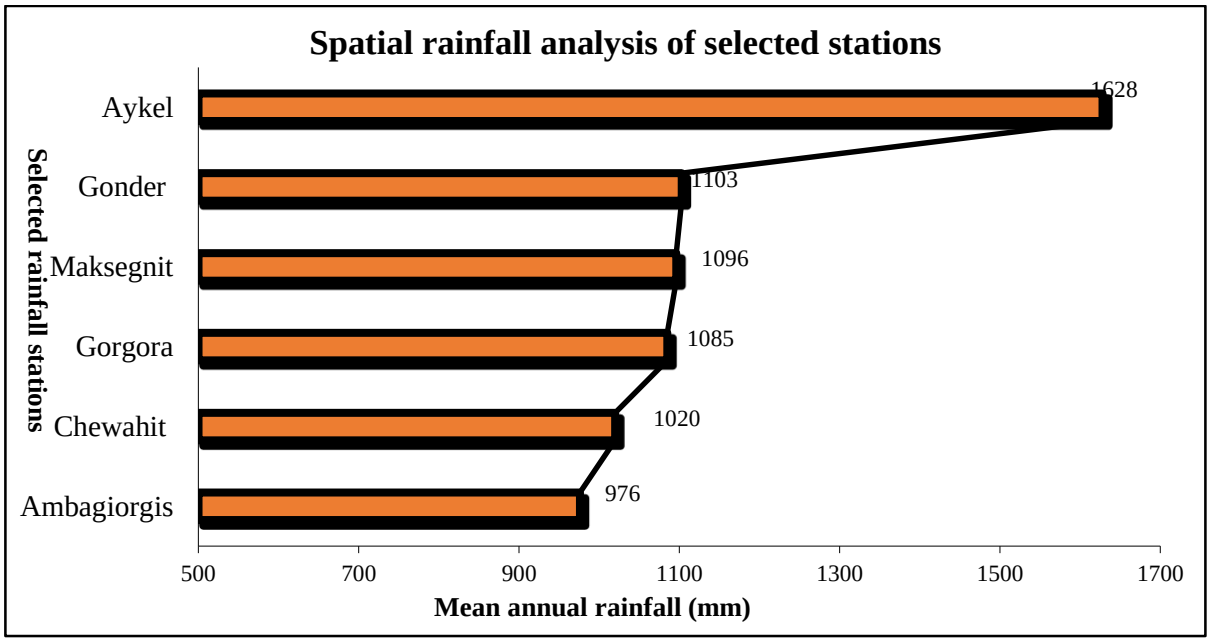

Figure 3-8:- Observed rainfall magnitude for each gauging stations from 1993 – 2013.

3.3.4 Hydrological data analysis

Filling of Missing Stream Flow

Unlike rainfall, stream flow shows strong serial correlation; the value of one day is closely related to the value on the previous and following days especially during periods of low flow or recession. Flow in the Megech River depends on the rainy season that occurs from June to September and also light rains are experienced in other seasons and it has good stream flow records with a small number of missing data in the study baseline period (1993-2008). The location and mean monthly annual stream flow data of Megech gauge of the River is presented in **Appendix 4.**

Filling of the missing data was made into two divisions; for wet season missing data filled by using linear regression between consecutive wet season months; and for the dry season the recession curve method was used to fill the gaps by using Equation 3-6.

$$Q_t = Q_{t_o}\, exp\left(-\frac{t-t_o}{k}\right) \qquad (3\text{-}6)$$

Where: Q_t is the missed flow data (m^3/s) in day,

Q_{t_o} is a specified initial daily mean discharge (m^3/s),

k is the watershed characteristics and it is the inverse of flow recession (α) or also also called reaction factor.

K value is calculated by the slope of the logarithmically transformed flow series data values of the flow last before the gap at time t_o (Q_{t_o})and the first flow value after the gap at time t_1 (Q_{t_1}) as follows:

$$\frac{1}{K} = \alpha = \frac{lnQ_{t_0} - lnQ_{t_1}}{t_1 - t_0} \qquad (3\text{-}7)$$

For this study all the missing data were observed only during wet seasons (August 1998 and June 2007). Due to this only the first method (linear regression method) was used for this study. A total of 12 daily missing data, five in August 1998 and seven in June 2007 were filled. The monthly flow of Megech River near the Megech dam site (Figure 3-9).

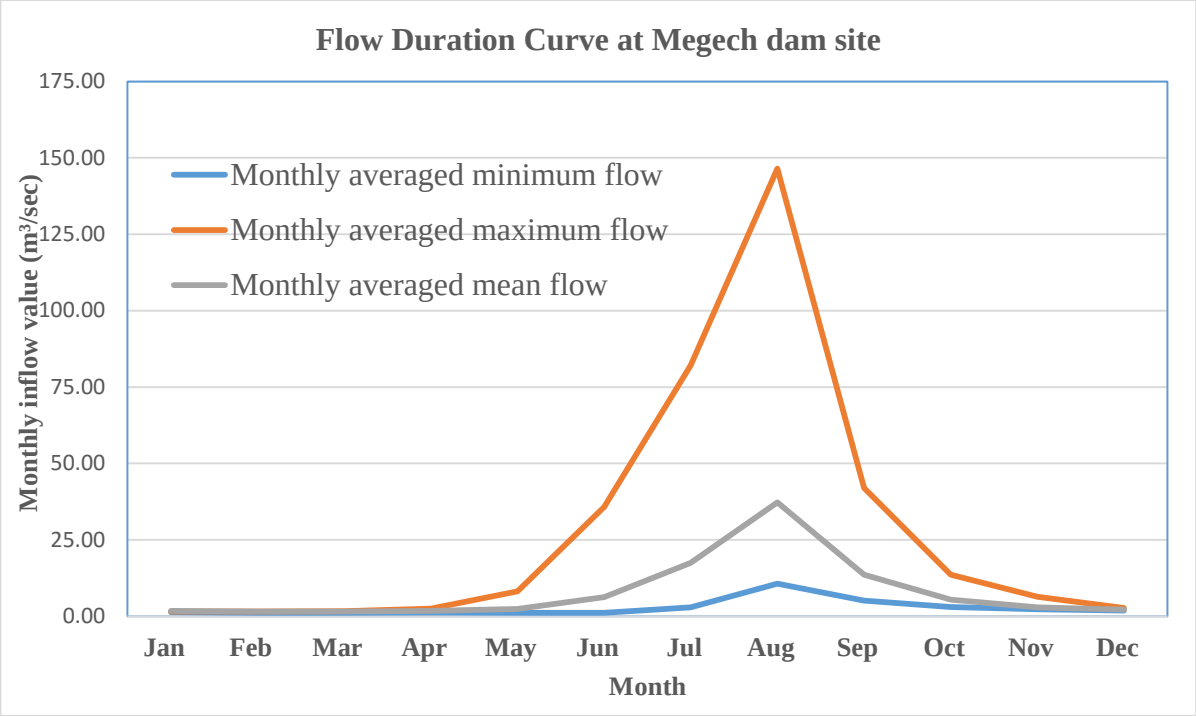

Figure 3-9:- Changed Flow duration curve of Main Megech River at Megech dam site after construction of the Dam (1993 – 2008)

3.4 Mann-Kendall test for trends

It is non-parametric test for looking at trend in time series which is robust even for highly skewed hydro metrological data described by Mann, although the test lately proved by Kendall in 1975 as a special case for testing of correlation between two data serious (Y, X) using Kendall's τ. Because of this it called Mann-Kendell test and measures whether data value (Y) tends to increase or decrease with time (T) (Cherie, 2013).

Mann-Kendell test is a statistical test widely used for the analysis of trends in climatological and in hydrological time serious. It has two advantage of using it. First, it is non-parametric test and doesn't require the data to be normally distributed. Secondly the test has low sensitivity to abrupt break due to inhomogeneous time serious (Karmeshu, 2012).

3.4.1 Non-seasonal Mann-Kendall Test

According to this test, the null hypothesis H0 assumes there is no trend (the data was independent and randomly ordered) and this is tested against the alternative hypothesis H1, which assumes that there is a trend.

Mann-Kendall test considers the time series of n data points T_i and T_j as two subsets of data where i = 1,2, 3,……,n-1 and j = i+1,i+2, i+3,……,n. The data values are evaluated as an ordered time serious. If a data value from a later time period is higher than a data value from an earlier time period, the statistic S is incremented by 1. On the other hand, if the data value from a later time period is lower than a data value sampled earlier, S is decremented by 1. The net result of all such increments and decrements yields the final value of S.

The Mann-Kendall S Statistic is computed as follows:

$$S = \sum_{i=1}^{n-1} \sum_{j=i+1}^{n} sign(Y_j - Y_i) \qquad (3\text{-}8)$$

$$sign(T_j - T_i) = \begin{cases} 1 \; if \;\; Y_j - Y_i > 0 \\ 0 \; if \;\; Y_j - Y_i = 0 \\ -1 \; if \; Y_j - Y_i < 0 \end{cases} \qquad (3\text{-}9)$$

Where T_j and T_i are the annual values in years j and i, j > i, respectively.

It can be simplified as;

$$S_g = P - M \qquad (3\text{-}10)$$

Where

$T_j > T_i$

P = the number of times the Y's increase as $Y_j > Y_i$

M = the number of times the Y's decrease as $Y_j < Y_i$

It can be shown that is asymptotically normally distributed with the mean of E(S) =0 and standard deviation = $(variance^{1/2})\delta_s$ given by

$$\delta_s = \sqrt{\frac{n}{18}\left[(n-1)(2n-5) - \sum_{t_i=1}^{g} t_i(t_i-1)(2t_i+5)\right]} \qquad (3\text{-}11)$$

Where: g is the number of tied groups

t_i the number of ties of extent$i$.

The normality distribution of S is even guaranteed for small numbers of data points (n<10) if one use the standardized variable Z defined as

$$z = \begin{cases} \frac{S+1}{\delta_s} \; if \; S < 0 \\ 0 \; if \;\; S = 0 \\ \frac{S-1}{\delta_s} \; if \; S > 0 \end{cases} \qquad (3\text{-}12)$$

For n ≤ 10, given the level of significance (α) determine the critical z directly from the table of any standard statistical book. But for n > 10 and with the presence of ties, since the tied values of Y_i and Y_j produces 0 instead of +1 or -1 hence ties do not contribute to either P or M.

Kendall's τ can be defined as:

$$\tau = \frac{S}{D} \qquad (3\text{-}13)$$

Where: D is the maximum possible value of S, when all data points are monotonically

increasing and is given in Hipel and McLeod (1993).

When no ties exist, D is a constant, so that the statistics of S and τ are the same.

The null hypothesis Ho stated above (no trend exists) is tested through the significance of S or τ, being significantly different from zero, i.e. the null hypothesis is rejected at a significant level X (significant trend exist in the time series) if the computed value

$$|Z_s| \geq Z_{1-\frac{\alpha}{2}} \qquad (3\text{-}14)$$

Where:

$Z_{1-\frac{\alpha}{2}}$ is the value of the standard normal distribution with the probability of exceedance

Of $\frac{\alpha}{2}$.

For 5% significance level, the critical $Z_{1-\frac{\alpha}{2}}$, value which is computed from any

Standard normal distribution table is 1.96.

The trend analysis was done for annual observed time series of precipitation, maximum and minimum temperature for the study area using statistical software XLSTAT, this trend analysis was done for the downscale results of SDSM 4.2 from 1993 to 2099 to show the trend results increasing or decreasing. On running the Mann-Kendall test on observed temperature and precipitation data, the following result are for Gonder station (Table 3-4).

Table 3-4:- Mann-Kendall test result for precipitation, maximum and minimum temperature of Gonder station

	Mann-Kendall test result			
variables	**Z_S**	**$Z_{crit,.05}$**	**Son slope**	**Test interpretation**
Precipitation	-1.11	> 1.96	0.08	Accepted Ho (no statistical significant rainfall trend)
Maximum temperature	2.70	> 1.96	0.054	Reject Ho (there is statistical significant maximum temperature trend)
Minimum temperature	0.83	> 1.96	0.04	Accepted Ho (no statistical significant minimum temperature trend)

If $Zcrit_{,.05}$ value is greater than Z_S the Ho is accepted. Rejecting Ho indicates that there is a trend in the time series, while accepted Ho indicates was detected. On rejecting the null hypothesis the result is said to be statistically significant. Mann-Kendall test shows a trend for rejected and accepted Ho with their statistical significance. Table 3-4 maximum temperature was only indicates statistical significant increasing trend. In case of precipitation and minimum temperature shows statistical insignificant trend. The Mann-Kendall test results for mean annual of precipitation, maximum and minimum temperatures (Table 3-5). Mean annual

maximum temperature trend is statistical significant increasing trend the rest is insignificant trends (Figure 3-11).

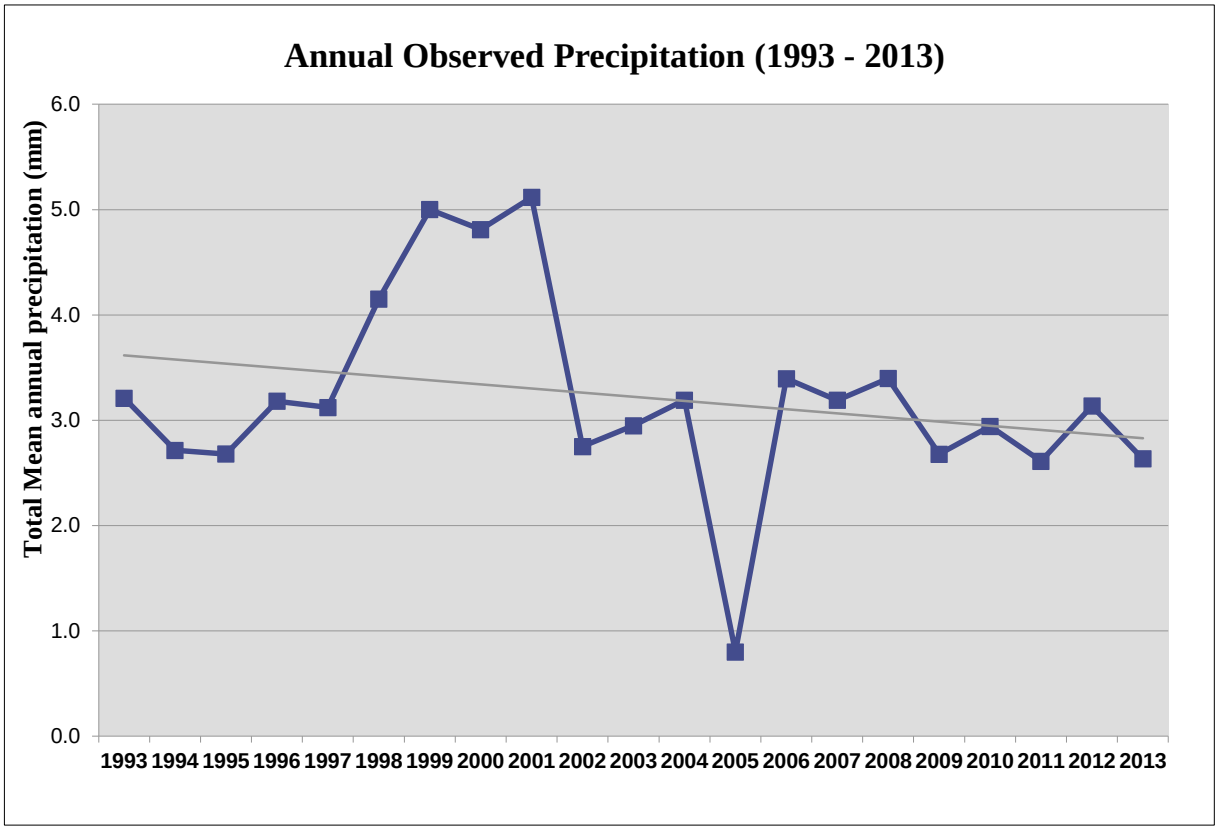

Figure 3-10:- Annual observed time series for precipitation of Megech watershed from 1993 – 2013 in Mann-Kendall trend test

The Mann-Kendall result of precipitation shows that the observed period (1993-2013) is not sufficient to conclude either increasing or decreasing. The trend of mean annual precipitation highly change in observed time period. The minimum mean annual precipitation observed in 2005 by 0.8 mm and the maximum precipitation observed in 2001 by 5.1mm (see Figure 3-10).

If null hypothesis is accepted in some case that doesn't mean there is no trend rather it is statement of the available observed period is not sufficent to conclude there is no trend (Helsel and Hirsch, 2002; Cherie, 2013). Statistical insignificant trends that neither increase nor decreases for mean annual minimum temperature and precipitation may due to the available data is not sufficient to conclude there is no trend (Figure 3-10 and Figure 3-12).

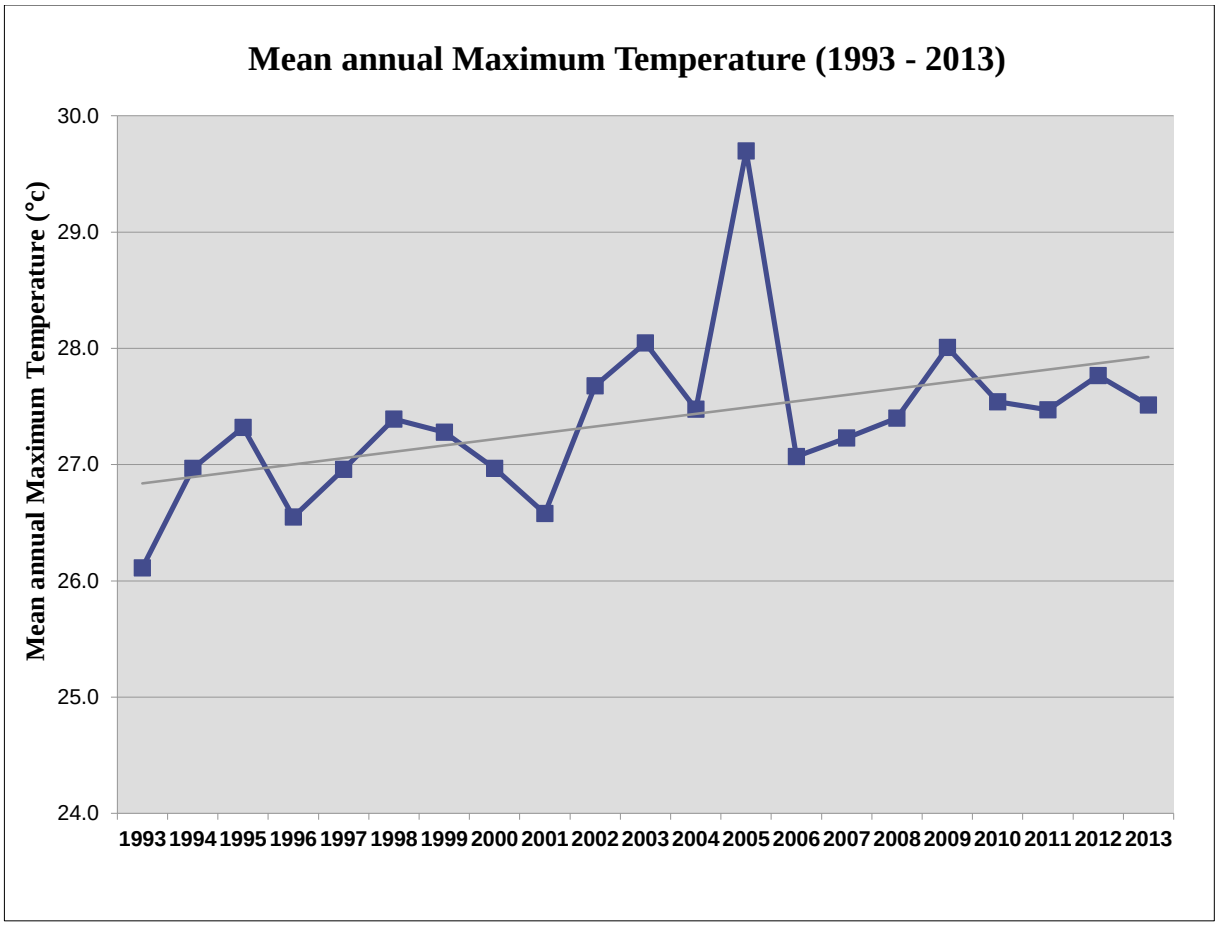

Figure 3-11:- Annual observed time series for Maximum Temperature of Megech watershed from 1993 – 2013 in Mann-Kendall trend test

The Mann-Kendall trend test result of mean annual maximum temperature shows positive difference is higher than the negative difference. The test conclude its increasing though observed time period. Mean annual maximum temperature shows increasing and decreasing trend in observed time period. The maximum mean annual temperature observed in 2005 by 29.7 °c and the minimum observed 1993 by 26.1°c (see Figure 3-11).

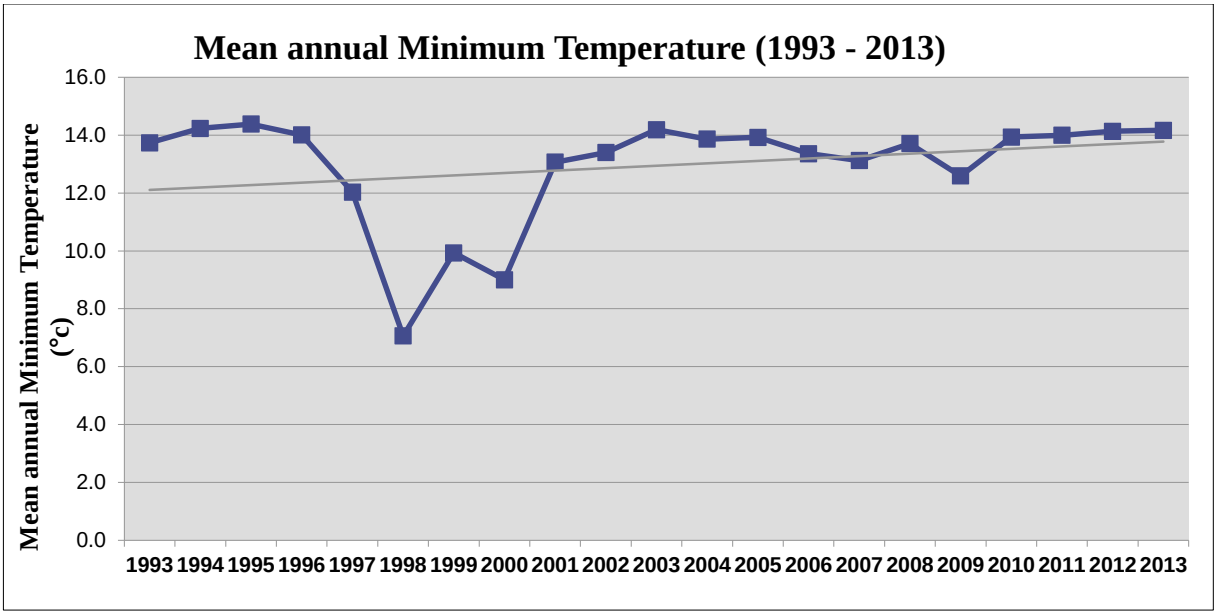

Figure 3-12:- Annual observed time series for Minimum Temperature of Megech watershed from 1993 – 2013 in Mann-Kendall trend test

Mean annual minimum temperature shows similar trend in most of observed time period except 1996 to 2001. The lowest mean annual minimum temperature observed in 1998 by 7 °c and the higher is observed in 1995 by 14.4 °c. The mann-kendall trend test result of mean minimum temperature is not sufficient to conclude that it increases or decreases (see Figure 3-12).

Table 3-5:- Mann-Kendall trend test results of precipitation, maximum and minimum temperate

	Mann- Kendall trend result		
	Precipitation	Maximum Temperature	Minimum Temperature
Observed time series (1993 – 2013)	No trend	Sign (+)	No trend

"**No**" implies there is no statically significant trend, "**Sign**" represents the presence of statically significant trend, and **(+)** increasing trend and **(-)** decreasing trend with the values of X which is the time series

3.5 Methodology

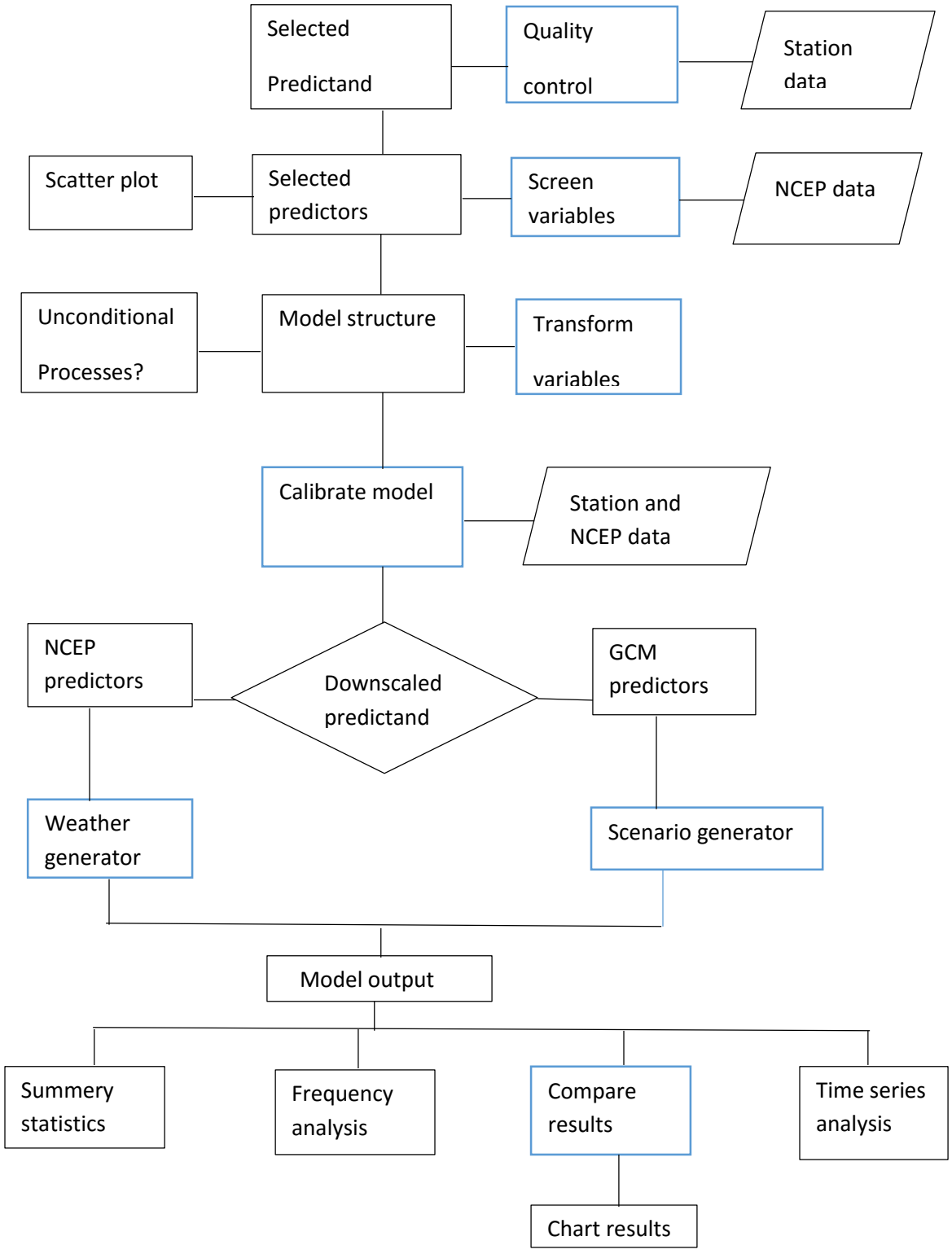

Figure 3-13:- SDSM 4.2 climate scenario generation process (Wilby & Dawson, 2007)

a) SDSM model input

The SDSM procedure begins with the preparation of same time period predictor and predictand data sets. Predictands are individual daily weather series, obtained from meteorological observations at single stations (daily precipitation, maximum or minimum temperature). Among the stations in the study area, from Section 3.3.3 spatial analysis of rainfall for selected station (Figure 3-8). Gonder station was founded to be best representative of Megech watershed than other stations. In addition it have long available data and good quality comparing to the other stations. Gonder station is class 1 metrological station and available inside the Megech watershed area so this study use this station as predictand for downscaling due to limited time to use more than one stations.

The predictors may be obtained for any global land area of a data portal maintained by the Canadian Climate Impacts Scenarios Group. The Web-site is accessed from http://tools.pacificclimate.org/select. After registered e-mail, then predictors were selected from the available GCMs (currently HadCM3 were used for this study), given the latitude and longitude of the nearest grid-box to the study region. All data files, including NCEP predictors, were then downloaded directly for immediate deployment by SDSM.

The downloaded zipped file contained three directories:

NCEP_1961-2001: This directory contains 41 years of daily observed predictor data; derived from the NCEP reanalyzed and normalized (with respect of mean and standard deviation) over the complete 1961-1990 period. These data were interpolated to the same grid as HadCM3 (3.75^0 longitude by 2.5^0 latitude) before normalization.

H3A2a_1961-2099: This directory contains 139 years of daily GCM predictor data; derived from HadCM3 A2 (a) experimented and normalized over the 1961-1990 period.

H3B2a_1961-2099: This directory contains 139 years of daily GCM predictor data; derived from HadCM3 B2 (a) experimented and normalized over the 1961-1990 period.

For model calibration, the source is the National Centre for Environmental Prediction (NCEP) re–analysis data set. The data is re–gridded to conform to the grid system of HadCM3. All predictors (with the exception of the geostrophic wind direction, see below) is normalized with

respect to the 1993 to 2013 average. However, daily predictors are also supplied for the period 1961–2000. There are 26 available predictors on NCEP and HadCM3 (in A2 & B2 scenarios). The potential daily predictor available at NCEP predictors are shown in Table 2-1.

Table 3-6:- Type of predictor variables available at NCEP and HadCM3

No	Predictor code	Predictor variable	No	Predictor code	Predictor variable
1	mlsp	Mean sea level pressure	14	Pzhaf	500hpa divergence
2	P_faf	Surface air flow strength	15	P8_faf	850 hpa airflow strength
3	P_uaf	Surface zonal velocity	16	P8_uaf	850 hpa zonal velocity
4	P_vaf	Surface meridional velocity	17	P8_vaf	850 hpa meridional velocity
5	P_zaf	Surface voriticity	18	P8_zaf	850 hpa voriticity
6	P_thaf	Surface wind direction	19	P850af	850 hpa geopotential height
7	P_zhaf	Surface divergence	20	P8thaf	850 hpa wind direction
8	P5_faf	500 hpa airflow strength	21	P8zhaf	850 hpa divergence
9	P5_uaf	500 hpa zonal velocity	22	r500af	Relative humidity at 500 hpa
10	P5-vaf	500 hpa meridional velocity	23	r850af	Relative humidity at 850 hpa
11	P5-zaf	500 hpa voriticity	24	rhumaf	Near surface relative humidity
12	P500af	500hpa geopotential height	25	shumaf	Surface specific humidity

13	P5thaf	500 hpa wind direction	26	tempaf	Mean temperature at 2m

b) Settings adjustment of SDSM 4.2

Year length: - calendar day is 366 days allowing 29 days in February every four years (i.e., leap year) used in observed data or predictand but NCEP predictors and HadCM3 use model year consisting of 360 days. Therefore in scenario generation the default day of 366 days had to be changed to 360 days.

Standard Start/End Date: - In this part, the model recommends to use for 30 years, but due to availability of data the study used 20 years (starting date is 1993 and the ending date is 2013).

Allow Negative Values: - The model by default allows simulation of negative values. Unconditional processes for temperature used the default button and Conditional processes for rainfall are unaffected by this button.

Event Threshold: - the parameter stated for daily precipitation is 0.3 mm/day, i.e. days with a rainfall less than this value are treated as dry days. It is to remove the linear dependencies in the regression equation. In the case of temperature this value is 0.

Model Transformation: - The transformation is applied to the predictand in conditional models. In advance setting no transformation was applied for predictand normally distributed in daily temperature and Fourth root was used in skewed data of daily precipitation.

Variance Inflation: - Controls the magnitude of variance inflation in downscaled daily weather variables. The default value (i.e. 12) produces approximately normal variance inflation prior to any transformation was applied to maximum and minimum temperature. For precipitation, this parameter is adjusted to 18.

Bias Correction: - Compensates for any tendency to over– or under–estimate the mean of conditional processes by the downscaling model. The default value is 1.0, indicating no bias correction used in maximum and minimum temperature. For precipitation the parameter is adjusted to 0.9.

The variance inflation and bias correction was adjusted to give higher percentage of explained variance. For precipitation both adjustments are higher comparing to temperature.

c) Quality control and Data transformation

The model by itself checks the quality of data entered from the study area metrological stations. There is no missing data at the end as all missed data was filled in temperature and precipitation. During data transformation, Wrap is selected (for Lag n) enter "–1" in the box then last value is used as the first value in the lag transformation in the case of temperature and fourth powers is used in precipitation.

d) Screening Downscaling Predictor Variables

The purpose of the Screen Variables option is to help the choice of appropriate downscaling predictor variables by identifying an empirical relationship between predictors and predictands. It was challenging in which it needs a good experience in selecting the appropriate downscaling variables. Otherwise the output of the model totally depends on the selected predictors that can determine the character of the downscaled climate scenario. The other challenge in selection of the downscaling variables is individual predictor variables vary both spatially and temporally which makes the decision process complicated.

In this part SDSM performs three supporting tasks: seasonal correlation analysis, partial correlation analysis, and scatterplots that help to select appropriate predictor variables from NCEP 1961-2001.

Steps followed to select appropriate predictors variables;

Step 1: Analyze button used to investigate the percentage of variance explained by specific predictand – predictor pairs. The model allows selecting and analyzing 12 variables in the same time out of 26 predictor variables. By making different groups of these variables (12 variables together in a group) and then selecting the predictor variables have high explained variance. (Default Significant level is $P < 5\%$)

Step 2: Correlation button used to investigate inter-variable correlations for specified sub–periods and also reports partial correlations between the selected predictors and predictand. The

predictors have high explained variance (the strong correlated variables are indicated in red), and correlation with other predictor variables in the list is dropped. (Significant level is P < 5%)

By follow these steps, predictors are selected described (Table 3-7). They have higher percentage explained variance with this predictor combination relative to the other combination for Megech watershed. The predictors selected for the precipitation, maximum and minimum temperature (Table 3-7). Detail description of the name of predictor's symbols (Table 2-1).

Table 3-7:- Selected predictor variables from NCEP correlation with precipitation, maximum and minimum temperature.

Predictands	**Predictors symbols**	**Pearson's correlation**	**Predictors symbols**	**Pearson's correlation**
Maximum Temperature	mslp	0.10	P_uaf	0.03
	P_zaf	0.02	P5-uaf	0.07
	P500af	0.05	P8_faf	0.47
	P8-uaf	0.58	rhumaf	0.45
	shumaf	0.04	ptempaf	0.43
Minimum Temperature	mslp	0.22	P_zaf	0.44
	P5_uaf	0.01	P500af	0.03
	P_zhaf	0.54	P5_vaf	0.51
	P8_zaf	0.02	r500af	0.49
	r850af	0.03		
Precipitation	mlsp	0.32	P5_faf	0.19
	P8_uaf	0.48	P8_vaf	0.41
	P850af	0.02	shumaf	0.01

e) Model Calibration

The SDSM-model calibration process serves to establish the general transfer- or regression function (Eq. 2.1) between a particular weather data (predictand) and a set of screened large scale predictors to construct downscaled models. For this purpose, the model structure by choosing the time steps monthly, and the process either unconditional or conditional were defined based on the type of predictand.

For calibartion of maximum and minimum temperature, unconditional process was selected because direct link is assumed between predictor and predictand. Whereas for precipitation, conditional process was selected since there is intermediate process between regional forcing and local climate (e.g., local precipitation amounts depend on the occurrence of wet-days, which in turn depend on regional–scale predictors such as humidity and atmospheric pressure).

In addition, Wilby *et al* (2000) describes this percentage of explained variance shows the daily variations in the local predictand and are determined by regional force. For spatially conservative variables like temperature 70%+ explained variance is not unusual and for heterogeneous variables such as daily precipitation occurrence/amounts < 40% is more likely. This study used model calibration period from 1993-2002 using NCEP, but the remaining years have also been used for validation.

f) Weather Generation

This enables the verification of calibrated models (assuming the availability of independent data) as well as the synthesis of artificial time series representative of present climate conditions and also used to reconstruct predictands or to infill missing data. By using the calibration data (or the parameter of regression model) the validation period (i.e. 2003 to 2013) was generated by the weather generator part. The validation of this model is done by comparing the 20 mean ensembles generated by the model SDSM 4.2 and observed station data at the same period.

g) Scenario generation

It produces 20 ensembles of synthetic daily weather series using atmospheric predictor variables supplied by a GCM (either under present or future greenhouse gas forcing). After comparing

the model weather generate validation period (2003-2013) with the same year of observed metrological station. Adjusting the setting to 360 days, start/end date, use input the model calibration period (or parameter file) and select from the GCM directory (can be HadCM3A2a or HadCM3B2a) then the scenario generation produces twenty ensembles. The mean of the twenty generated ensembles of maximum temperature, minimum temperature and precipitation are used for the hydrological model SWAT. This part generates the ensembles for 2020 (2011 – 2040), 2050(2041 -2070) and 2080(2071 -2099).

3.6 SWAT Model Setup and Inputs

There are two types of model algorithms developed in SWAT model which vary in their process of computing surface runoff called SWAT CN and SWAT WB. The earlier developed algorithm (SWAT_CN) models on the occurrence of runoff from infiltration excess processes and the new version SWAT _WB models runoff generated strictly from saturation-excess processes; no surface runoff will be generated with this algorithm until the soil becomes sufficiently saturated (Neitsch *et al,* 2000).

Infiltration excess method of runoff computation is used. Channel water routing method in the reaches and Potential evapotranspiration calculation by SWAT model in this study using, a default settled variable routing and Hargreaves method respectively. Skewed normal distribution for rainfall distribution during the simulation was selected.

3.6.1 Model set-up

The model setup involves five steps: (A) Data preparation, (B) Sub basin discretization, (C), HRU definition, (D) parameter sensitivity analysis and (E) calibration and model performance.

A. Data preparation and Sub basin discretization

The first step in initializing a watershed simulation in SWAT model is to delineate the watershed and partition into sub basins. Digital Elevation Model (DEM) was used to delineate the watershed and analyze the drainage pattern of land surface terrain.

The land use / Land cover special data were classified into SWAT land cover/plant types. Lookup table was created to link the Land cover/Land use map of the study area and SWAT data base using SWAT codes. The soil map was linked with the soil data base which is a soil data base designed to hold data of the study area soils not included in the U.S. The watershed and sub watershed delineation was done using DEM data. The watershed delineation process include five major steps, DEM setup, stream delineation, outlet and inlet definition, watershed outlet selection and definition and calculation of sub basin parameters. For the stream definitions the threshold based stream definition option was used to define the minimum size of the sub basins. The Arc SWAT interface allows the user to fix the number of sub basins by deciding the initial threshold area. The threshold area defines the minimum drainage area required to form the origin of a stream. Subdividing the sub watershed into areas having unique land use, soil and slope combinations made it possible to study the differences in evapotranspiration and other hydrological conditions for different land covers, soil and slopes. The land use, soil and slope data sets were imported overlaid and linked with the SWAT database. Megech watershed was divided into 29 sub-basins with a total of 944 grid cells and the model automatically delineates a watershed area of 39419.2 ha (Figure 3-14).

A. HRU definition

Hydrologic response units (HRUs) are lumped land areas within the sub-basin that comprised of unique land cover, soil and management combinations. HRUs enable the model to reflect differences in evapotranspiration and other hydrologic conditions for different land covers and soils. The runoff is estimated separately for each HRU and routed to obtain the total runoff for the watershed. This increased the accuracy in flow prediction and provided a much better physical description of the water balance.

To define the hydraulic response unit (HRU), both single and multiple HRU definition options are available. The HRU distribution in this study was determined by assigning multiple HRU to each sub-watershed. In multiple HRU definitions, a threshold level was used to eliminate minor land uses, soils or slope classes in each sub-basin. Land uses, or soils which cover less than the threshold level are Eliminated. After the elimination process, the area of the remaining land use, or soil was reapportioned so that 100% of the land area in the sub-basin is modeled.

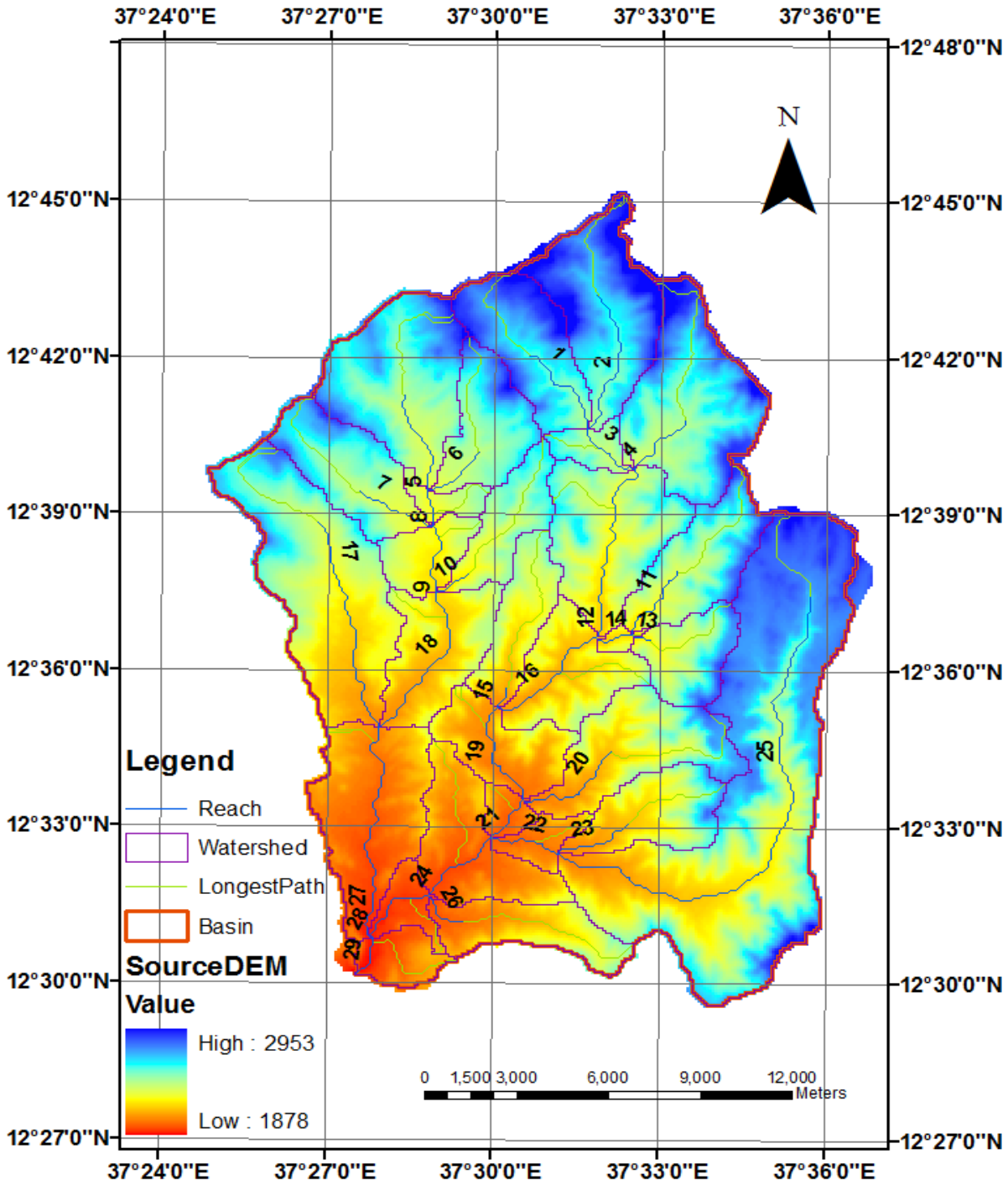

Figure 3-14:- Megech watershed delineated (from SAWT Model)

The threshold levels set is a function of the project goal and amount of detail required. In the SWAT user manual it is suggested that it is better to use a larger number of sub-basins than larger number of HRUs in a sub-basin; a maximum of 10 HRUs in a sub-basin is recommended. Hence, taking the recommendations into consideration 5%, 15% and 20%

threshold levels for the land use, and soil were applied, respectively so as to encompass most of spatial details.

The third step in HRU definition is selection of slope classification option (single or multiple) and if multiple slope option is selected then it defines the range of the slope. For this study, multiple slope option (an option for considering different slope classes for HRU definition) was selected and the slope class was classified to three with range 3 % between each of them 0 - 3%, 3 - 9 % and above 9 %. Lastly, after defining the HRUs within a watershed was completed, the HRU was setup. For this study the option of multiple HRU was selected. 5 %, 20% and 20% were used as threshold area of land use, soil and slope in each HRU to the sub-basin respectively. The reason for taking these threshold values was in order to keep the HRUs to a reasonable and manageable number and also considering computer processing time required. Even though, application of these thresholds eliminate the land uses and soils that covered relatively small areas in the watershed. It created a total of 133 HRUs for 29 sub-basins.

Table 3-8:- Summary of HRU analysis result of SWAT model

Maps in HRU analysis	**% of overlaps with delineated watershed**	**No of sub basins**	**No of HRUs**
LULC maps of 2008	100%	29	133
Soil map	100%	29	133

B. Write Input Tables

Next to Hydrologic Response Units analysis, SWAT model follows with writing all input tables. Arranging the batch file that contain the location and elevation of weather generator gauge stations, rainfall gauge stations, temperature gauge stations, relative humidity gauge stations, solar gauge stations and wind gauge stations were loaded sequentially. Then SWAT connected each meteorology data related to each arranged batch file and write it to the database for each sub-basin.

C. Weather Generator

Daily values of precipitation, maximum and minimum temperature, solar radiation, relative humidity and wind speed are required by SWAT model. A weather generator WXGEN model is included in SWAT that generate the above stated data or fill the gap of measured recording. The inside model is based on the contiguous U.S. condition. However this case study crates its own data base (userwgn.dbf) according to the local conditions. This study creates it data base for weather generator by using WGN maker (Excel Macro Solver) and soil data base by using SPAW.

D. Simulation, Sensitivity Analysis, Calibration & Validation

Acccording to Agizew (2010) the main objective of hydrological model is prediction of the hydrological cycle. The prediction power and uncertainty of the model are involved with the predicted result that must be known before making meaningfull judgment on the impact of proposed study. Uncertainty of model depends on quality of input data and the nature of the model. It can be reduced by optimization of model parameter. It is also important to know the sensitivity of these different paramters with respect of model output inaddition to their prediction power tested by statistical and graphical techniques.

Sensitivity Analysis

Sensitivity analysis is used to estimate the rate of change of model output with respect to the input. It is usefull to understand how the model depends on the information fed into it and provides better understanding on the behavior of the system being modelled such as model parameters and applicability, thus it increases the confidence level of the model and its predictions (Getnet, 2009). Although Fadil *et al*. (2011) added SWAT model have large number of parameters and outputs. An initial parameter selection makes the calibration process easier and reduces the uncertainties related to different parameters. Automatic sensitivity analysis tool is applied to SWAT based on One-factor-At-a Time (OAT) design and the Latin Hypercube (LH) sampling techniques. The LH simulation is based on the principles of Monte Carlo with a stratified sampling. Each parameter is subdivided into 'N' ranges with a probability of occurrence of 1/N. The OAT design uses the LH samples as an initial points and one parameter is changed at a time. For N intervals with 'm' parameters, a total of N* (m+1) runs

are done. The objective functions are: the change of the mean value of the output variables (e.g. mean flow, sediment and etc.) for the case of non-observed data; and the sum of the squared of errors (SSQ) between the observations and the simulations when there is an observed data for the required output variables. Currently, model sensitivity analysis is done with a default number of 26 parameters and 280 runs.

For this study the sensitivity analysis was performed using SWAT interface for a period of 1/ 1/ 1995 to 12/31/2001 in which the first two years (1993 and 1994) was taken as warm up period. After running sensitivity analysis, the sensitive parameters were categorized in to four classes based on their mean relative sensitivity (MRS). Based on this classification, flow parameters with mean relative sensitivity value of medium to very high had been selected for calibration. For Megech watershed 7 parameters for flow. Whereas 8 parameters for flow to be sensitive for recent land use (2008 LULC phase). According to Lenhart *et al*. (2002) the sensitivity of a flow to a parameter can be categorized into four classes as describe in the Table 3-9 and the sensitivity class for the governing parameters was taken in consideration by the specified values.

Table 3-9:- Sensitivity class assigned in SWAT Model

Class	Mean Index	Category of Sensitivity
1	$0 \leq MRS \leq 0.05$	Small to negligible
2	$0.05 \leq MRS < 0.2$	Medium
3	$0.2 \leq MRS < 1$	High
4	$MRS \geq 1$	very High

Model calibration

According to Neitsch *et al*. (2000) model calibration is to mean adjusting by fine tuning model parameters to match with observed data as much as possible, with limited range of deviation accepted. Similarly, model validation is testing of calibration model results with independent

data set without any further adjustement at different spatail and temporal scale. Also parameter estimation for calibration is technique designed to reduce the uncertainty in the estimation of process parameters. Typical approach is to select an initial estimate for the parameters, inside the ranges previously specified. The parameter values are then adjusted more closely to match model behavior of the watershed. **Appendix 13** shows the most common parameters used in SWAT model for runoff generation. Moriasi *et al*. (2007) discribed there are three types of calibration procedures that can be differentiated as:

1. Trial-and-error, manual parameter adjustment;

2. Automatic, numerical parameter optimization;

3. A combination of (1) and (2).

Manual method is most common and especially recommended for the application of more complicated models when good graphical representation is needed. It checks water balance contribution, then calibrate stream flow. The minimum recommended values are embraced by the model that is $R^2 > 0.6$, NSE > 0.5 and PBIAS < ±15 (Moriasi *et al.*, 2007).

For this study, the manual calibration was applied due to its simplicity. Figure 4-14 shows the process of manual calibration done on the SWAT model. It is trial-and-error process of parameter adjustment; after each parameter adjustment is made, the simulated and observed hydrographs were visually compared to see if the match is improved. The match is checked by the R^2, NSE and PBIAS values. In simulation of the Megech River flow done at the outlet of the Megech watershed (29 sub-basin) the observed period is divided in to three zones, the first is for warm up the model (1993-1994) and the second is to calibration (1995- 2003) and the last is validation (2004-2008) . In this process, model parameters varied until recorded flow patterns were accurately simulated.

Model Validation

It is comparison of the model outputs with an independent dataset without value parameter adjustment. To utilize the predictive watershed model for estimating the effectiveness of future potential management practices, the model must be first calibrated to measure data and tested (without further parameter adjustment) against an independent set of measured data. So model

validation is testing the model independent data set. Model calibration determines the best or least reasonable, parameter set while validation ensures calibration parameters set performs reasonably well under an independent data set. During calibration and validation phase, the model can be used with confidence for future prediction under different management scenarios.

Model validation period was used in this study from 01/01/2004 to 30/12/2008 for the watersheds, due to absence of stream flow data after 2008 in the study area. The validation was carried out using the coefficient of Determination (R^2), Nash-Sutcliffe simulation efficiency (NSE) and Percent Bias (PBIAS).Flow validation was carried out similar to the calibration.

Performance Evaluation of the model

According to Moriasi *et al* (2007) there are range of methods grouped in to three are error index, dimensional and regression based models. Error index is the commonly used and includes Mean Absolute Error (MAE), Mean Square Error (MSE), Root Mean Square Error (RMSE), and Mean Square Error to standard deviation (RSR) and percentage bias (PBIAS). Nash-Sutcliffe simulation efficiency (NSE) widely used dimensionless measurement. Coefficient of determination (R^2) is commonly used regression based models. This case study use model evaluations described below.

Coefficient of determination (R^2):- Estimates combined dispersion against single dispersion of observed with predicted series and gives the correlation between observed and simulated time serious. This value occurs between 0 and 1 the result that gives 0 indicates there is no correlation if it is 1 that show perfect correlation Moriasi *et al.* (2007).

The formula below use to calculate the result;-

$$R^2 = \left[\frac{\left[\sum_{i=0}^{n}[(Q_{sim}-\bar{Q}_{sim})(Q_{obs}-\bar{Q}_{obs}]^2\right]}{[\sum_{i=0}^{n}(Q_{obs}-\bar{Q}_{obs})^2 \sum_{i=0}^{n}(Q_{sim}-\bar{Q}_{sim})^2]}\right] \qquad (3\text{-}15)$$

Where n is the number of observation during simulation,

Q_{obs} is the ith observation (stream flow),

Q_{sim} is the ith simulated value with respect of time

$\bar{Q}_{sim}$ & $\bar{Q}_{obs}$ arithmetic mean of observed and simulated

Nash-Sutcliffe simulation efficiency (NSE):- defined as one minus the sum of absolute square differences between predicted and observed value normalized by the variance of the observed values during period under investigation (Fadil *et al.*, 2011). Perfect match of the model indicated by 1.0 and 0.0 shows the model performance as good as the mean of observed data. It NSE is less than zero unsuitability of the model.

$$NSE = 1 - \left[\frac{\sum_{i=0}^{n}(Q_{obs}-Q_{sim})^2}{\sum_{i=0}^{n}(Q_{obs}-\bar{Q}_{obs})^2}\right] \qquad (3\text{-}16)$$

Percent Bias: - Percent bias (PBIAS) measure the average tendency of simulate data to be larger than observed counterparts. The optimal value is 0.0 with low magnitude values that indicate accurate model simulation. The positive value indicate the model underestimation bias and negative also shows overestimation (Moriasi *et al.*, 2007).

PBIAS estimated by the following formula: -

$$PBIAS = \frac{\sum_{i=0}^{n}(Q_{obs}-Q_{sim})}{\sum_{i=0}^{n} Q_{obs}} * 100 \qquad (3\text{-}17)$$

3.7 Determination of Climate Change Impact on Stream Flow

Neitsch *et al.* (2000) mentioned SWAT model is capable of simulating a number of climate customization options and simulates orographic impact on temperature and precipitation for watershed in mountainous regions. It also modifies climate inputs for simulating that are observed as impacts of climate change on watershed and allows weather forecasting period incorporated into simulation to study the effect of weather prediction on the watershed.

SWAT can simulate climate change by using climate inputs like precipitation, temperature, solar radiation, relative humidity, wind speed, potential evapotranspiration and weather generator parameters. According to different reports there are two common ways to assess effect of climate change on the hydrology of a catchment using SWAT. The first one is manipulating the climatic input data (mainly temperature and precipitation) in to hydrological

model SWAT (Cherie, 2013 and Fadil *et al.*, 2011) and the second is adjustment and alternation of the weather data of the sub basin (Gebresenbet, 2015).

Gebresenbet (2015) mentioned the second method is less time consumig and straight forward method in climate change assesement by adjusting factors of various climatic inputs namely precipitation, temperature, solar radiation, relative humidity and level of carbon dioxide of each sub basin. Also this case study used the second method due to it simplicity and less time consuming. SWAT model adjust various inputs as follow. Allows the user to adjust precipitation, temperature, and solar radiation, relative humidity, and carbon dioxide levels in each sub basin. The alteration of precipitation, temperature, solar radiation, relative humidity are straight forward

$$R_{day,adj} = R_{day} * \left(1 \frac{adj_{PCP}}{100}\right) \quad (3\text{-}18)$$

Where $R_{day,adj}$ is the adjusted precipitation of the sub-basin on a given day (mm H_2O),

R_{day} is the precipitation falling in the sub basin on a given day (mm H_2O),

adj_{pcp} is the % change in rainfall.

$$T_{mx,adj} = T_{mx} + adj_{tmp} \quad (3\text{-}19)$$

Where $T_{mx,adj}$ is the adjusted daily maximum temperature (^{0}c),

T_{mx} is daily maximum temperature (^{0}c),

adj_{tmp} is the change in temperature (^{0}c).

$$T_{mn,adj} = T_{mn} + adj_{tmp} \quad (3\text{-}20)$$

*W*here $T_{mn,adj}$ is the adjusted daily maximum temperature (^{0}c),

T_{mn} is daily maximum temperature (^{0}c),

adj_{tmp} is the change in temperature (^{0}c).

SWAT allows the adjustment terms to vary from month to month so that it enables to simulate seasonal changes in climate condition. This study considered the precipitation and temperature impact of climate change only.

CHAPTER FOUR

4 RESULTS AND DISCUSSIONS

4.1 Downscaling Climatic Variables

4.1.1 Selection of Predictor Variables

The potential predictor strength done with the help of internal screening facility of SDSM was observed in monthly basis, red mark shows relatively strong correlation. It was obtained between the predictand and predictor for each month.

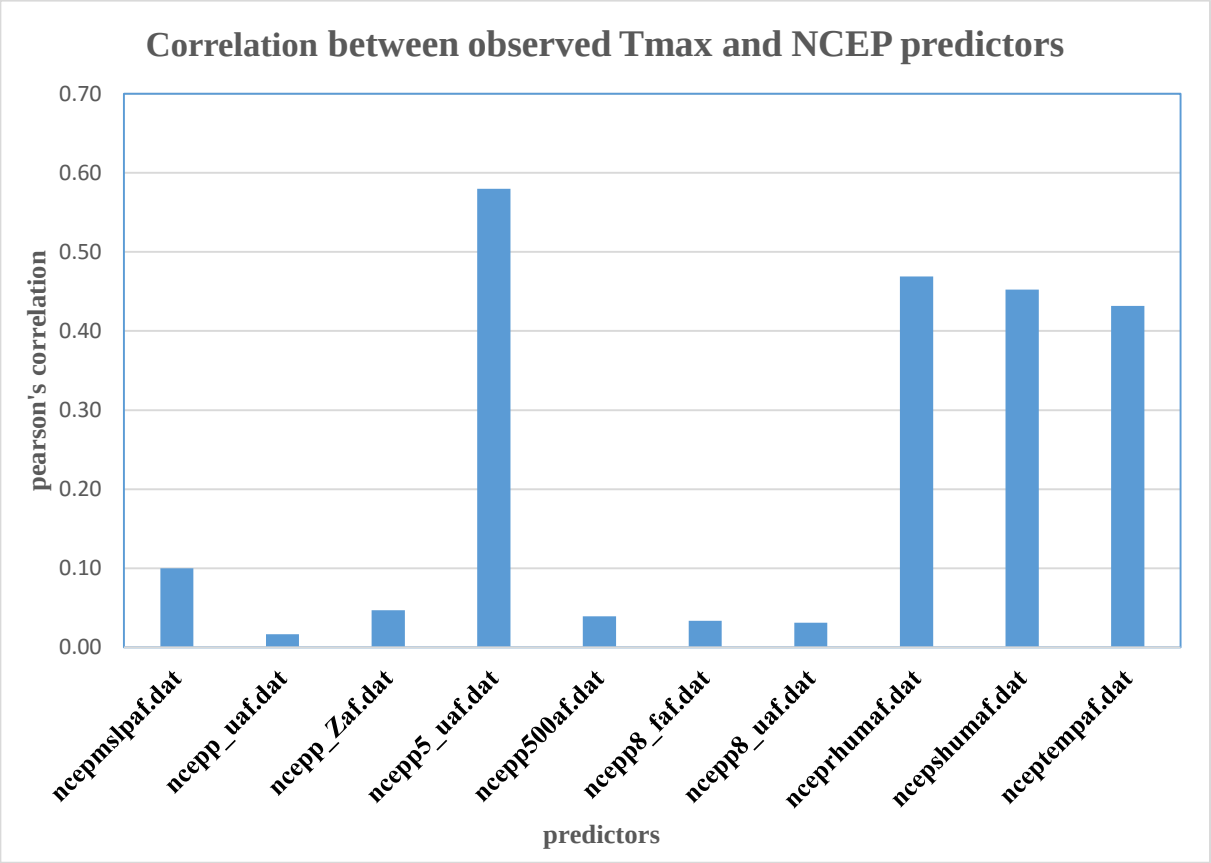

Figure 4-1:- Correlation between observed maximum temperature and NCEP predictors for Gonder station

Figure 4-1 shows the correlation of maximum temperature and NCEP predictors strongly correlated with 500hp zonal velocity (ncepp5-uaf.dat). In addition, near surface relative humidity (nceprhumaf.dat), mean temperature at 2m (nceptempaf.dat) and surface specific humidity (ncepshumaf.dat) shows better correlation than the others predictors.

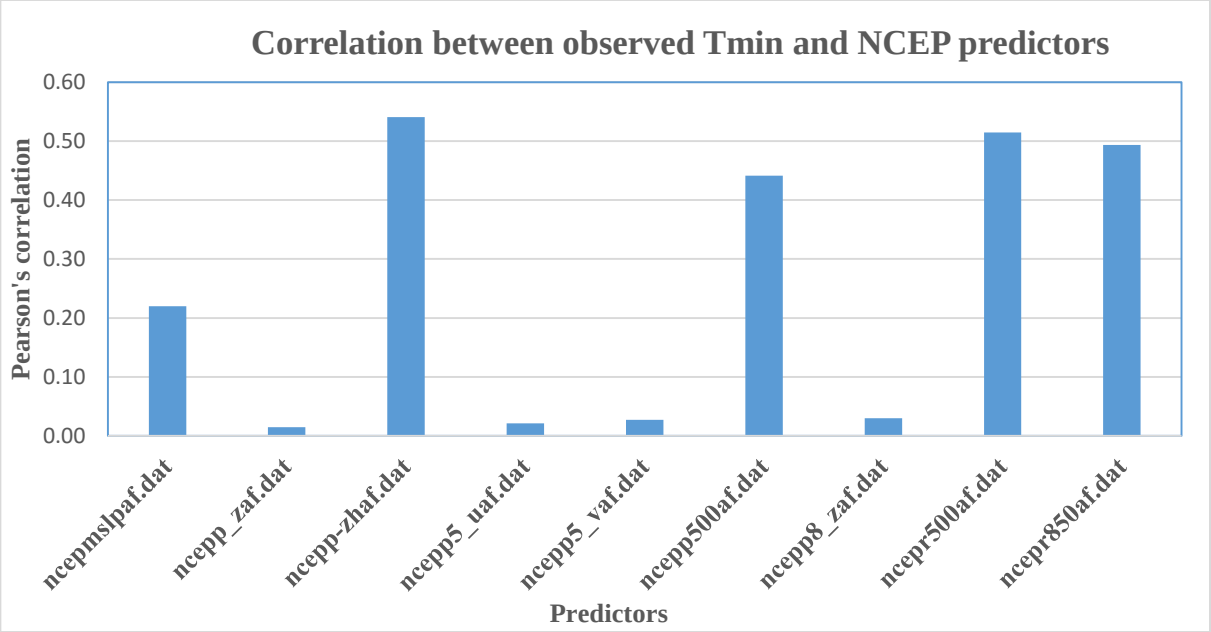

Figure 4-2:- Correlation between observed minimum temperature and NCEP predictors for Gonder station

Observed minimum temperature and NCEP predictors shows strongly correlated with surface divergence (ncepp-zhaf.dat), relative humidity at 850hpa (ncepr850af.dat), relative humidity of 500hpa (ncepr500af.dat) and 500hpa geopotential height (ncepr500af.dat).

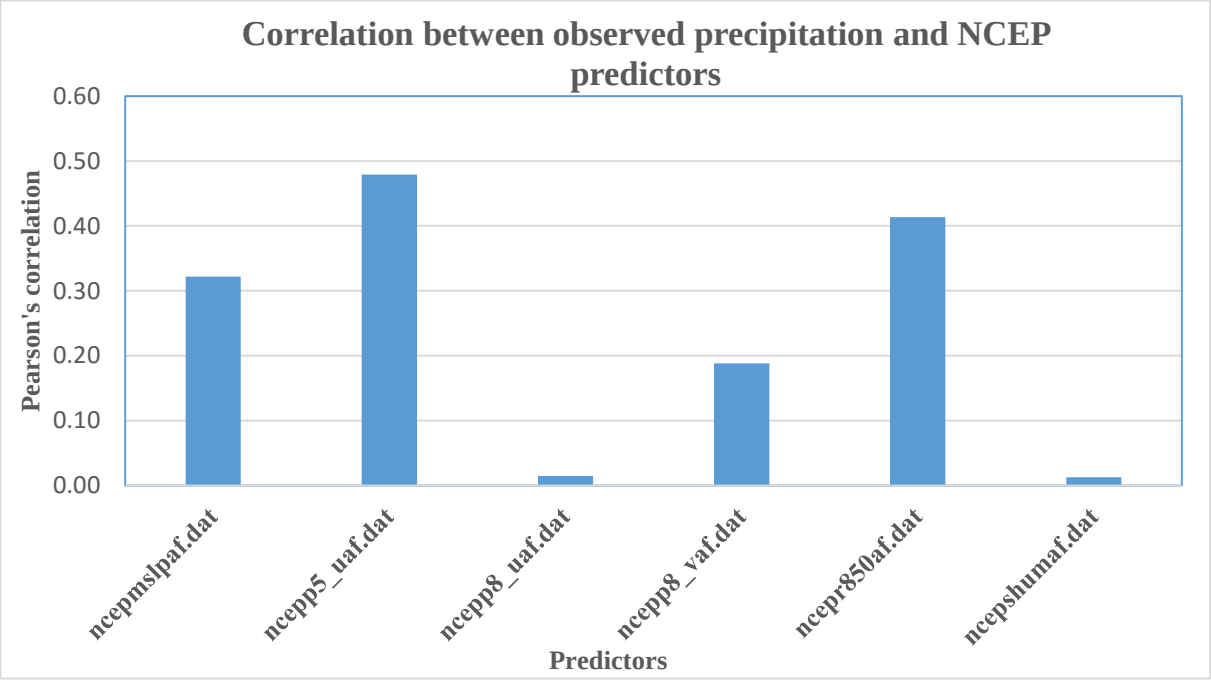

Figure 4-3:- Correlation between observed precipitation and NCEP predictors for Gonder station

Observed precipitation of Gonder station and NCEP predictors shows strong person's correlation with 500hpa zonal velocity (ncepp5_uaf.dat). In addition 850hpa (ncepr850.dat) and 850hpa merdional velocity (ncepp8_vaf.dat) have good correlation (Figure 4-3).

4.1.2 Calibration and Validation

It develops multiple regression equations between the metrological station data (predictand), regional scale and atmospheric (predictor) variables. Then calibration of climatic predictors from 1993-2002 periods followed, coefficient of determination R^2 that measures the percentage of the explained variance between modeled and observed variables is 51 %, 69 % and 71% for precipitation, maximum and minimum temperature. The weather generator generates twenty ensembles of synthetic daily weather series by using calibration .PAR file and NCEP-reanalysis data from the 1/1/2003 to 31/12/2013. Then mean of those 20 ensembles generated by weather generator for remaining 11 years used for validation gives 64 %, 75 % and 80 %.

Table 4-1:- Calibration and validation R^2 values of SDSM 4.2 downscaled for precipitation, maximum and minimum temperature

	R^2		
	Precipitation	Maximum temperature	Minimum temperature
Calibration (1993-2002)	0.51	0.69	0.71
Validation (2003-2013)	0.64	0.75	0.80

Maximum and minimum temperature values gives a better R^2 values, inferring that future projections would also be well replicated. But the result of precipitation is unsatisfactory

because of its conditional nature. Although different literatures (Fadil *et al.,* 2011 ,Cherie, 2013 , Shimelis *et al.,* 2011) indicates the downscaling of precipitation is problematic, it is either misunderstanding climatic governing fine scale processes or misrepresentation physics of precipitation itself in global climate models. According to Wilby *et al.* (2004) downscaling of precipitation in tropics is challenging, because of ocean atmospheric coupling and relationship between large scale predictors and local variables very strongly within the annual cycle. The calibration results in the Table 5-1 is acceptable according to Wilby *et al.* (2000) statement of temperature less than 70 % and heterogeneous variables such as daily precipitation occurrence/amount not more than 40 % more likely accepted. Lower R^2 value exhibited for precipitation because of limited available long time series observed data and courser resolution of climate data.

4.2 Comparison of Downscaled GCM with Observed data

There is a significant gap between the large spatial resolution GCMs and regional and local watershed processes. This scale mismatch causes a considerable problem for the assessment of climate change impact using hydrological models. Hence, significant attention should be given to the development of downscaling methodologies for obtaining high-resolution climate or climate change information from relatively coarse-resolution global climate models (GCMs). After model calibration of SDSM by adjusting the output using event threshold, bias correction and variance inflation, it is important to compare the GCM simulation that represent present day conditions with observed climate. According to IPCC (2000) statement on the performance of GCM depends critically on the size of region (i.e. small regions at sub grid scale are less likely described than large regions in continuous scale), on its location (i.e. the level of agreement between GCM outputs varies at continental scale), on the variable being analyzed (for instance, regional precipitation is more variable and more difficult to model than regional temperature). Because that above mentioned reasons IPCC recommends it better to include most valuable function of a model intercomparison with observed in estimating the future climatic variables. The main assumption of this statistical relation is to identify the current climate statistics and it will remain valid under change in future condition (Abouabdillah *et al.,* 2010). To evaluate the performance of simulated outputs of downscaled model, SDSM offers comparison of downscaled model scenarios and observed climate data using statistical tool of

analytical data screen. The most common statistical parameter delivered by the model are daily/ monthly/ seasonal/ annual means, maxima, minima, sums and variance.

This study compared downscaled model scenarios and observed climate data using mean and variance although check the model error between the downscaled scenarios.

I. Maximum Temperature

The monthly mean maximum temperature downscaled for A2 and B2 scenarios in the observed (baseline) period.

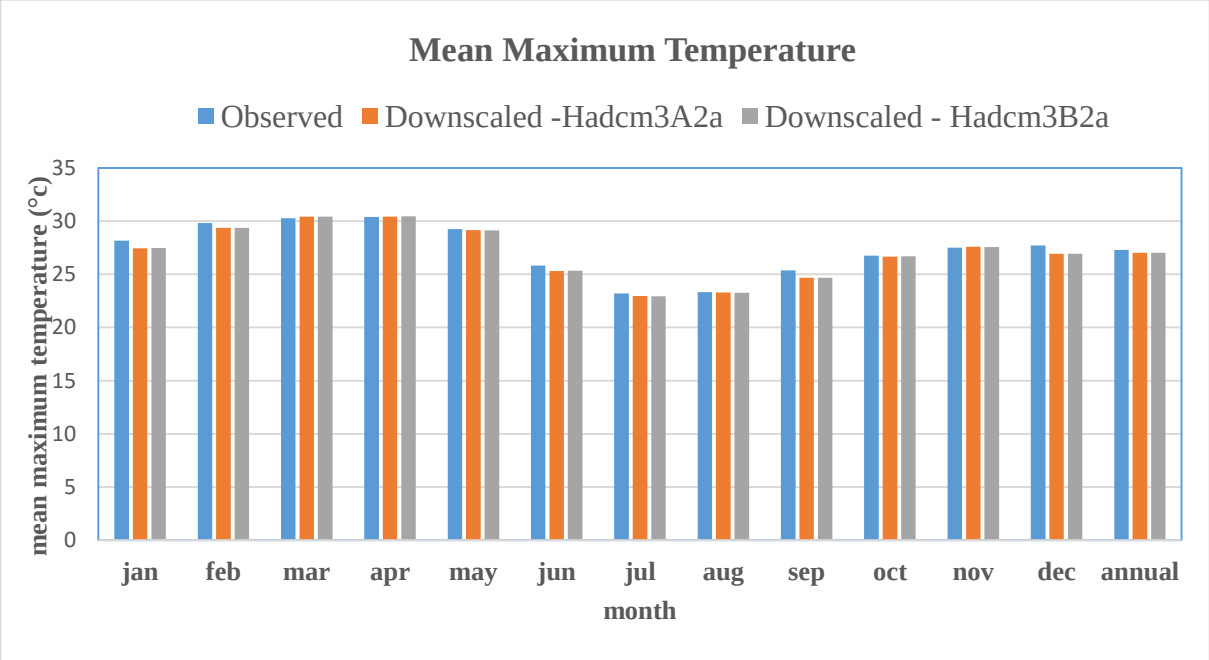

Figure 4-4:- Observed and downscaled mean monthly maximum temperature for baseline period (1993-2013)

Figure 4-4 and Table 4-2 shows the mean monthly HadCM3A2a and HadCM3B2a emission scenarios SDSM model generated result have good similar with mean and variance of observed baseline maximum temperature. The mean monthly value of generated HadCM3 was greater in spring (only March & April) and autumn (only November) although the rest was lower than observed. The mean values of observed temperature have slight higher results compared to HadCM3A2a and B2a emission scenarios in most of the month (see Table 4-2).

Table 4-2:- Baseline period comparison of observed and GCM (HadCM3) downscaled results of Gonder station; using mean, variance and model error results for observed maximum temperature (1993-2013)

Month	**Observed**		**Downscaled HadCM3A2a**			**Downscaled HadCM3B2a**		
		Variance $(^{o}c)^{2}$		**Variance** $(^{o}c)^{2}$	**Model Error** (^{o}c)		**Variance** $(^{o}c)^{2}$	**Model Error** (^{o}c)
January	28.15	1.6	27.45	1.48	0.49	27.46	1.49	0.47
February	29.81	2.3	29.36	1.46	0.20	29.36	1.46	0.21
march	30.27	3.9	30.41	1.70	0.02	30.43	1.75	0.03
April	30.39	4.1	30.43	3.04	0.00	30.44	3.07	0.00
May	29.25	5.4	29.15	2.80	0.01	29.14	2.79	0.01
June	25.83	4.3	25.30	4.68	0.27	25.32	4.61	0.26
July	23.19	2.4	22.96	1.84	0.05	22.94	1.86	0.06
August	23.32	2.4	23.29	1.60	0.00	23.27	1.63	0.00
September	25.37	2.3	24.67	4.32	0.49	24.66	4.34	0.51
October	26.74	1.9	26.66	1.66	0.01	26.69	1.59	0.00
November	27.51	1.4	27.58	0.81	0.00	27.57	0.81	0.00
December	27.70	0.9	26.94	1.21	0.58	26.93	1.29	0.59
Annual	27.28		27.02			27.02		

The variance of observed monthly maximum temperature is slightly higher than downscaled HadCM3A2a and HadCM3B2a from January to May. Although the variance of monthly

maximum temperature of observed value is similar trend with downscaled value from all months from July to December. There is similarity of general trend between the observed and downscaled mean monthly temperature for both A2a and B2a scenarios (Figure 4.5). May is the month shows maximum variance difference in compared with HadCM3A2a and HadCM3B2a emission scenarios (see Table 4-2).

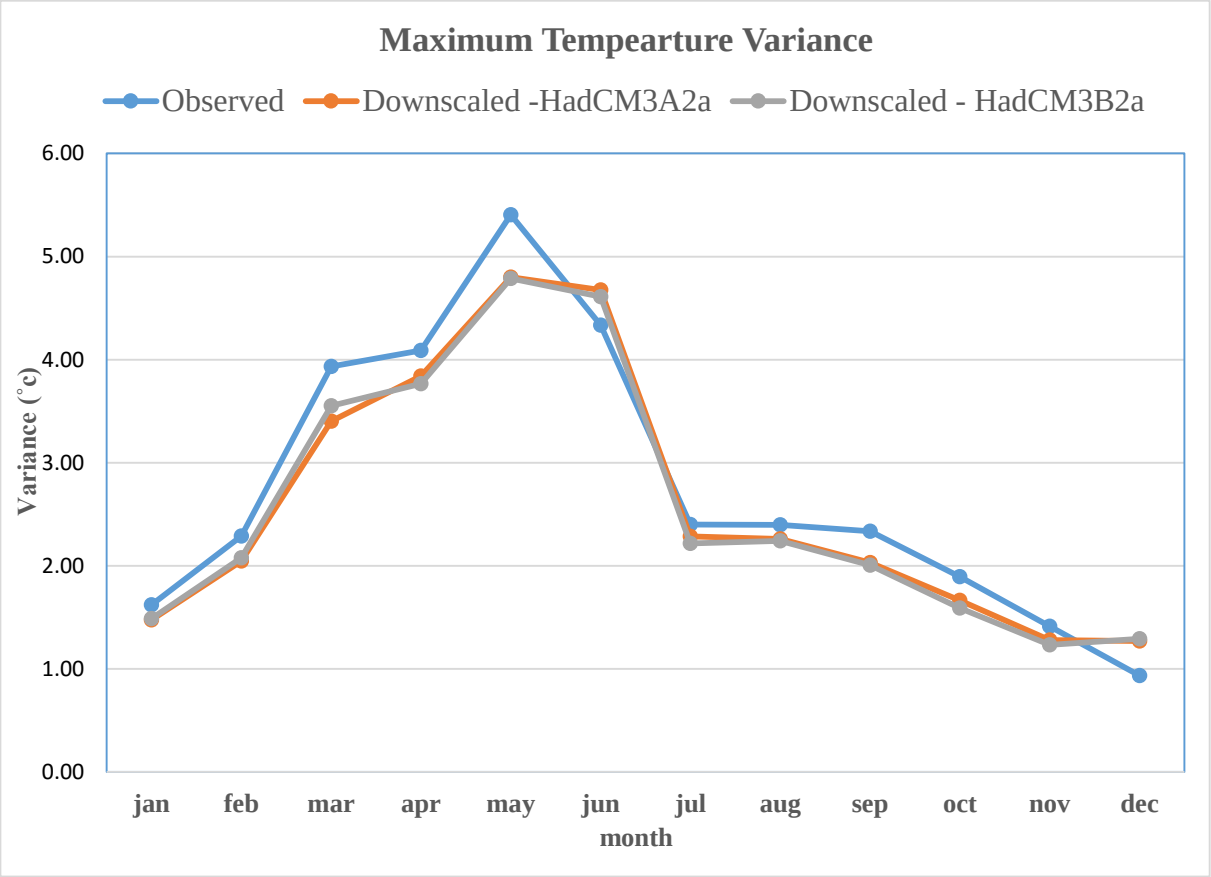

Figure 4-5:- Variance of observed and downscaled mean monthly temperature for observed (baseline period).

The monthly absolute model error of the downscaled maximum temperature for the baseline period shows almost similar result for both A2a and B2a emission scenarios. Figure 5-6 shows absolute model error in estimation of mean monthly downscaled temperature of both emission scenarios compared with observed data is less than 0.5 ^{0}c in most of the months. The maximum absolute model error occurred at December with 0.58^{0}c. March, April, May, August, October and November are the months that shows less model error compared to maximum temperature (see Table 4-2 model error values and Figure 4-6).

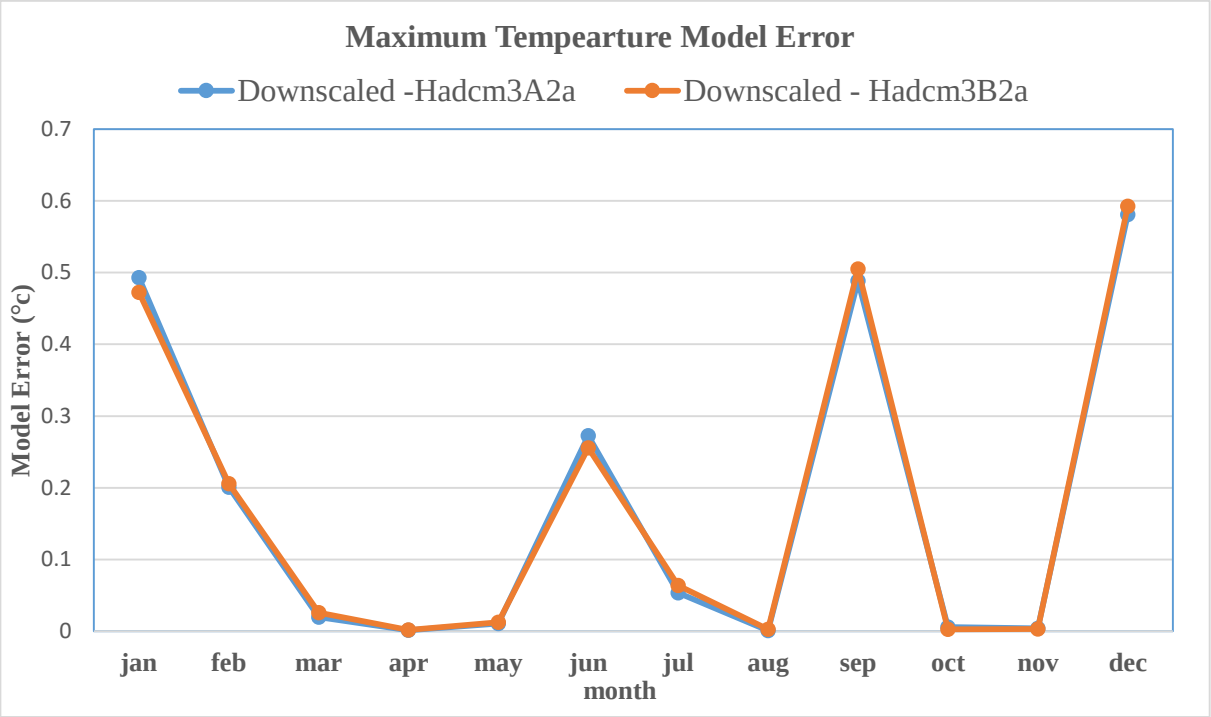

Figure 4-6: - Absolute model error occurred in estimated mean monthly temperature A2 and B2 scenarios compared with observed (baseline) period.

II. Minimum Temperature

The mean monthly temperature of GCM (HadCM3) for both scenarios was less than mean values in compared with the observed mean monthly result without including March (Table 4-3 and Figure 4-7). It shows similar trend of increasing and decreasing in all months. The variance of GCM (HadCM3) for A2 and B2 scenarios was greater in winter (only December & January), autumn and summer (only August) in comparing to the observed minimum temperature variance.

Like that of the maximum temperature the downscaled minimum temperature also shows a reasonably good agreement with the observed minimum temperature for all months both under A2a and B2a emission scenarios. All mean monthly observed minimum temperature is higher than downscaled A2a and B2a except March (Figure 4-7).

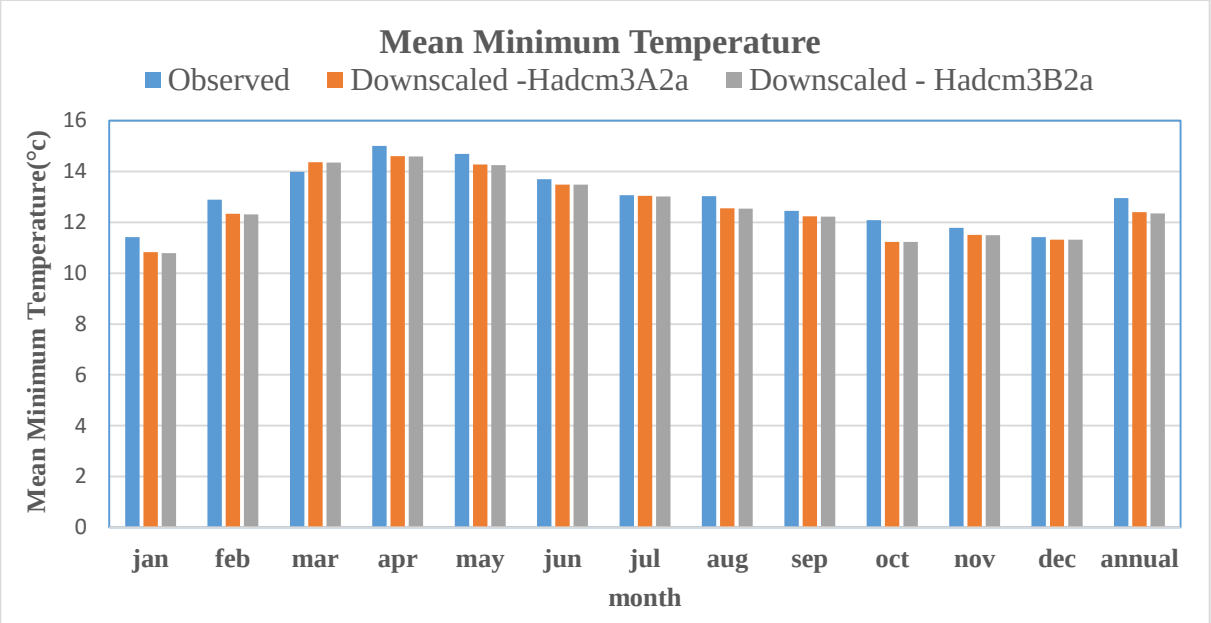

Figure 4-7:- Observed and downscaled mean monthly minimum temperature for baseline period (1993-2013)

The general trend between the observed and downscaled mean monthly temperature for both A2a and B2a scenarios identical to that of maximum temperature and have slight similar values. The variability of monthly minimum temperature of observed is well preserved in downscaled value in most of the months except from May to July.

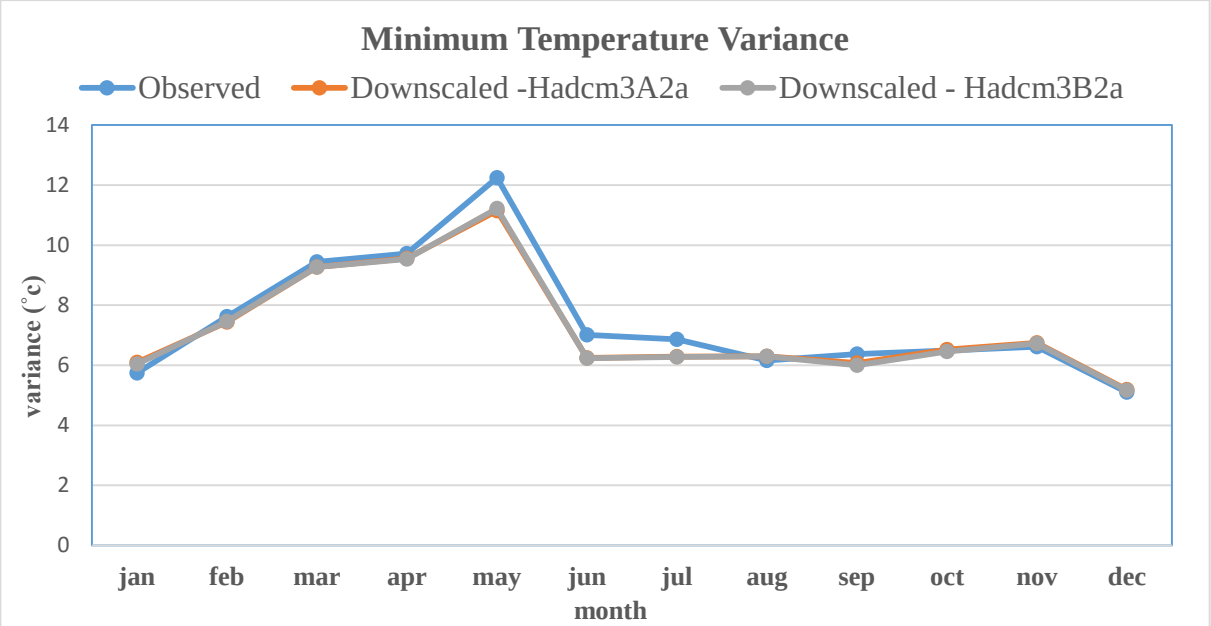

Figure 4-8:- Variance of observed and downscaled mean monthly temperature for observed (baseline period)

The rest of all months from January to April and August to December shows slight variances difference between observed minimum temperature and downscaled A2a and B2a scenarios (see Figure 4-8).

Table 4-3:- Baseline period comparison of observed & GCM (HadCM3) downscaled results of Gonder station; using mean, variance and model error results for minimum temperature

Month	**Observed**		**Downscaled HadCM3A2a**			**Downscaled HadCM3B2a**		
		Variance ($^{o}c)^2$		**Variance ($^{o}c)^2$**	**Model Error (^{o}c)**		**Variance ($^{o}c)^2$**	**Model Error (^{o}c)**
January	11.41	5.74	10.82	6.94	0.35	10.79	6.94	0.38
February	12.89	7.62	12.34	6.43	0.31	12.31	6.46	0.34
march	13.99	9.44	14.36	6.71	0.14	14.35	6.70	0.13
April	15.00	9.72	14.60	7.56	0.16	14.58	7.54	0.17
May	14.69	12.24	14.28	11.14	0.17	14.25	11.22	0.20
June	13.70	7.01	13.48	6.25	0.05	13.48	6.23	0.05
July	13.07	6.86	13.04	6.29	0.00	13.02	6.28	0.00
August	13.03	6.16	12.55	7.30	0.22	12.54	7.29	0.24
September	12.45	6.39	12.24	12.08	0.05	12.23	12.00	0.05
October	12.08	6.49	12.23	7.53	0.74	12.22	7.46	0.73
November	11.78	6.62	11.51	7.75	0.07	11.49	7.72	0.08
December	11.42	5.10	11.32	5.19	0.01	11.31	5.17	0.01
Annual	12.96		12.39			12.35		

The absolute model error of mean monthly minimum temperature and downscaled HadCM3A2a and B2a scenarios is less than 0.4^{0}c in most of the months for both HadCM3 emission scenarios except October. Maximum absolute error occurred in October by 0.73 ^{0}c. Less absolute model error observed in July and December comparing to other months (Figure 4-9 and Table 4-8).

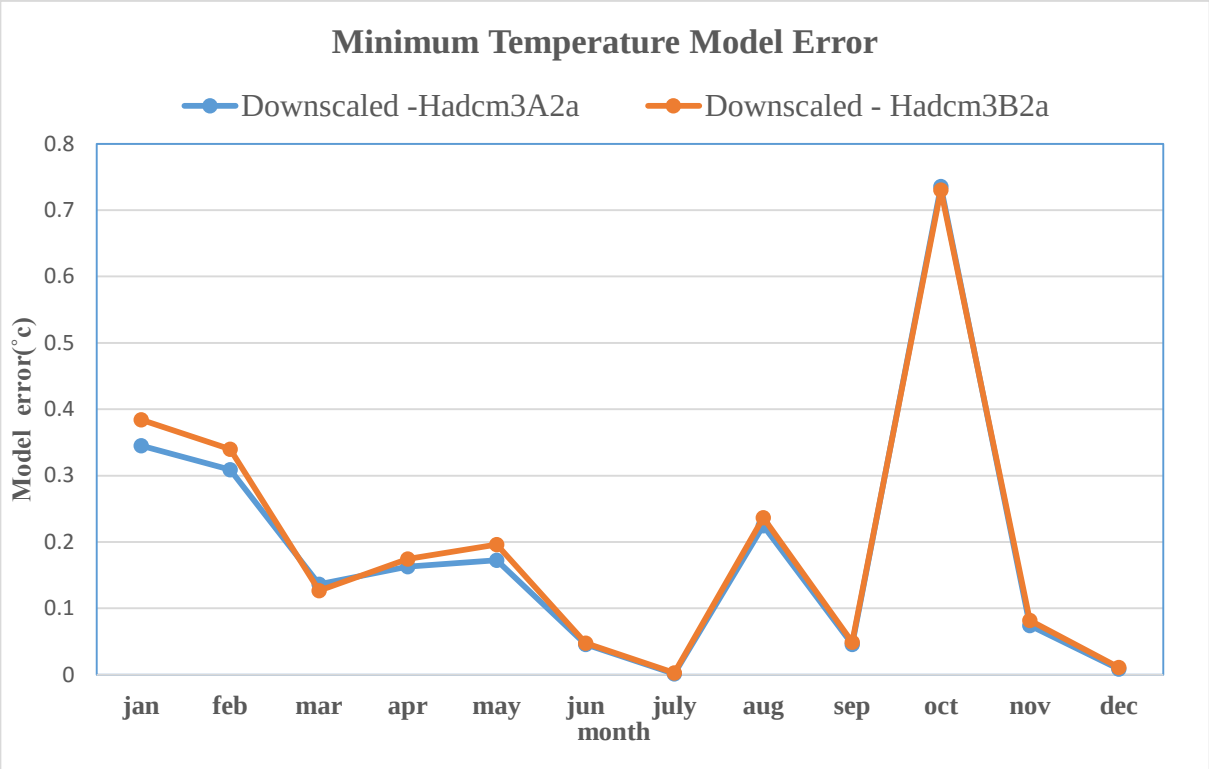

Figure 4-9:- Absolute model error occurred in estimated mean monthly temperature by A2 and B2 scenarios compared with observed (baseline) period

III. Precipitation

Daily precipitation amount at individual station continue to be the most problematic variable to downscale, this arise because of the generally low predictability of daily precipitation amount at local scale by regional forcing factor (Dawson, 2007). All observed mean daily precipitation is greater than GCM generated in both scenarios in all months except in summer (only July) and autumn (only November) (see Figure 4-10 and Table 4-4). The mean monthly precipitation shows more difference comparing to the variance and absolute model error of observed and downscaled A2a and B2a emission scenarios.

Table 4-4:- Baseline period comparison of observed and GCM (HadCM3) downscaled results of Gonder station; using mean, variance and model error results for precipitation

Month	**Observed**		**Downscaled HadCM3A2a**			**Downscaled HadCM3B2a**		
		Variance $(mm)^2$		**Variance $(mm)^2$**	**Model Error (mm)**		**Variance $(mm)^2$**	**Model Error (mm)**
January	0.12	1.33	0.10	0.91	0.00	0.09	0.85	0.00
February	0.11	0.75	0.09	0.51	0.00	0.09	0.48	0.00
march	0.46	6.02	0.38	4.15	0.01	0.37	3.85	0.01
April	1.06	11.59	0.88	7.99	0.03	0.84	7.42	0.04
May	2.85	44.37	2.36	30.57	0.23	2.28	28.40	0.32
June	6.40	110.18	6.31	75.90	0.01	6.02	70.51	0.14
July	10.64	136.43	11.63	320.48	0.97	11.60	311.11	0.92
August	10.29	129.25	9.02	261.15	1.61	8.70	250.71	2.51
September	3.88	48.49	3.22	33.41	0.44	3.11	31.40	0.60
October	2.84	62.71	2.36	43.20	0.23	2.28	40.13	0.32
November	0.71	9.72	1.75	19.08	1.08	1.70	17.79	0.99
December	0.27	4.22	0.23	2.90	0.00	0.22	2.70	0.00
Annual	3.33		2.86			2.76		

The monthly precipitation downscaled for the baseline period (Figure 4-10). July and November are the only month's higher mean monthly precipitation of downscaled HadCM3A2a and B2a compared to observed mean monthly precipitation. Observed mean monthly precipitation of August, September and October slight higher than downscaled mean monthly precipitation HadCM3A2a and B2a scenarios.

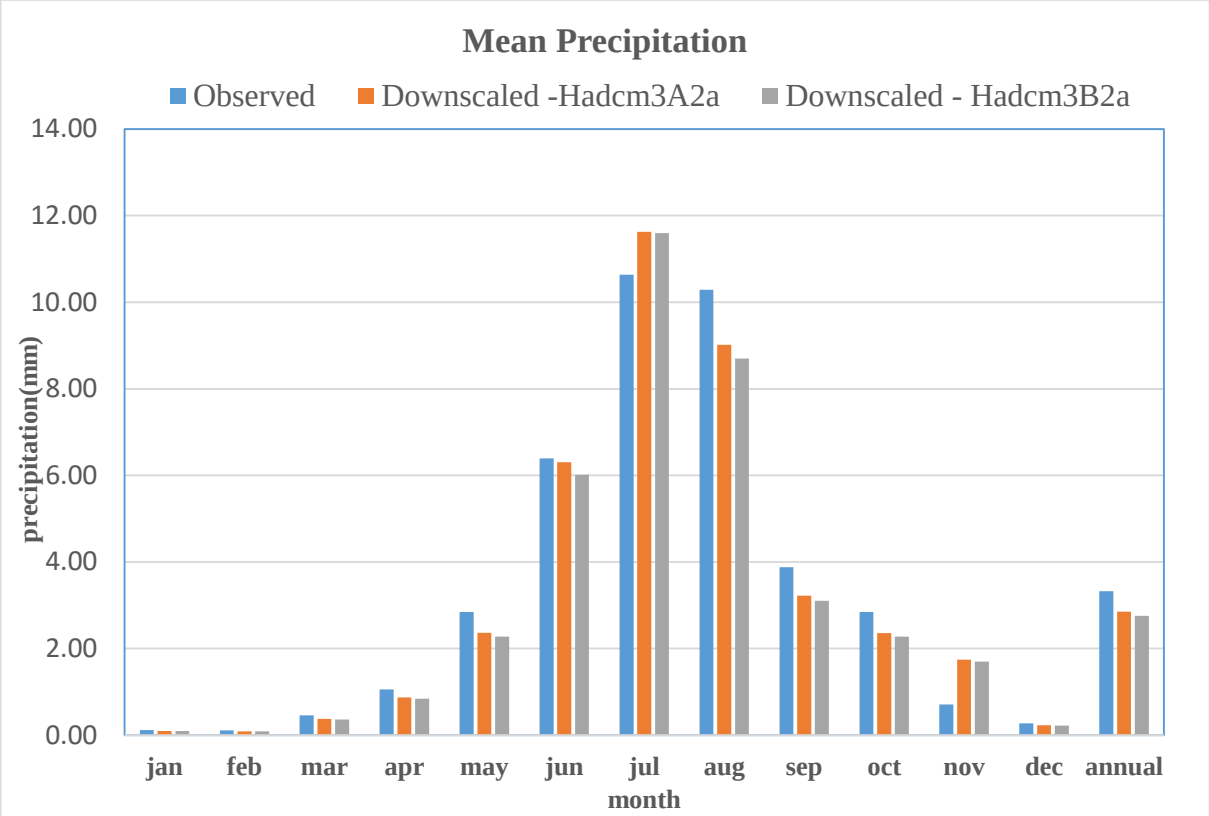

Figure 4-10:- Observed and downscaled mean daily precipitation for baseline period (1993-2013)

Comparing to maximum and minimum temperature the precipitation could not able to replicate the historical (observed data). This is due to the variability in space and time and complicated nature of precipitation process (Figure 4-10 and Table 4-4).

Variability of observed and downscaled precipitation for both scenarios shows similarity in variance in many months however, the variance of observed precipitation higher than downscaled GCM (HadCM3) scenarios except November. In general the variance of mean monthly precipitation shows more identical trend of increasing and decreasing than the mean monthly precipitation (Figure 4-11).

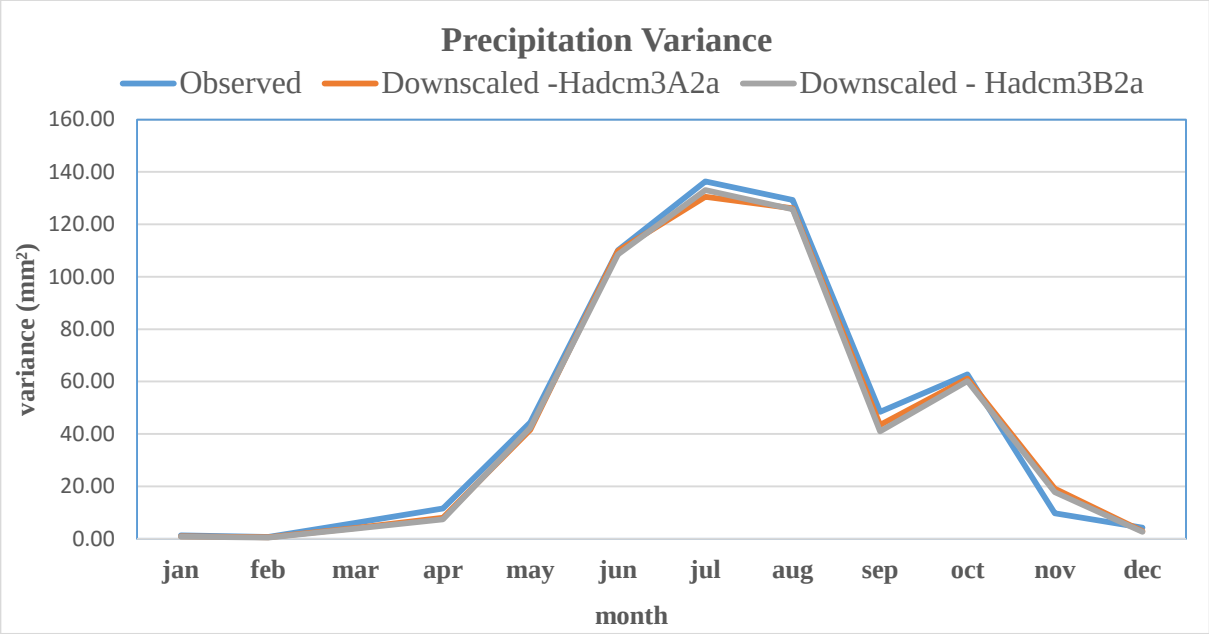

Figure 4-11:- Variance of observed and downscaled mean monthly precipitation for observed (baseline period)

The absolute model error shows very less model error from January to April and December. Maximum absolute model error observed in August month. Downscaled HadCM3B2a scenarios shows slight higher absolute model error than HadCM3A2a. The rainy seasons from June to September shows more model error in comparison to other months (Figure 4-12).

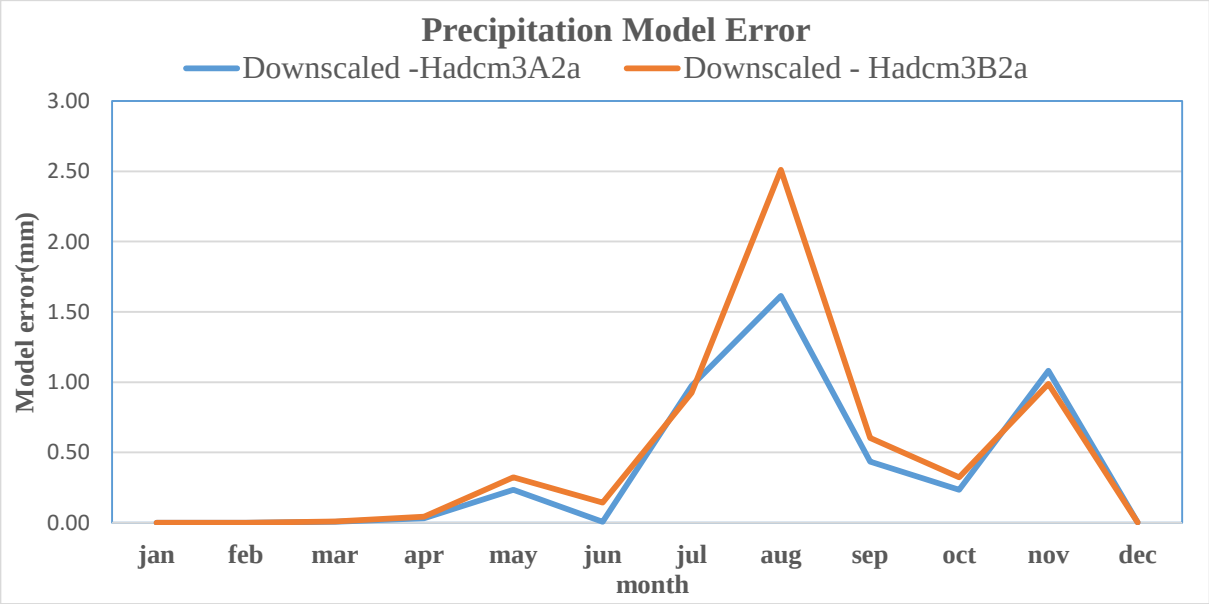

Figure 4-12:- Absolute model error occurred in estimated mean monthly precipitation by A2 and B2 scenarios compared with observed (baseline) period

4.3 Downscaling of the GCM for future Scenario

The climatic scenario for future period was developed by statistical downscaling of the GCM predictor variable for the two emission scenarios for 100 years based on the mean of 20 ensembles and the analysis was done based on three 30 years period. The impacts of both A2 and B2- SRES scenarios are simulated for three future time periods 2011 - 2040 (2020s), 2041 - 2070 (2050s) and 2071 - 2099 (2090s) and compared with model results for the 1993 - 2013 baseline period.

Future result of Maximum Temperature

The projected maximum temperature shows an increase trend for all time horizons. Maximum temperature increases for all seasons (Figure 4-13 and Table 4-5). Relatively, a larger absolute monthly difference from the baseline temperature is found in summer seasons for both A2 and B2 emission scenario.

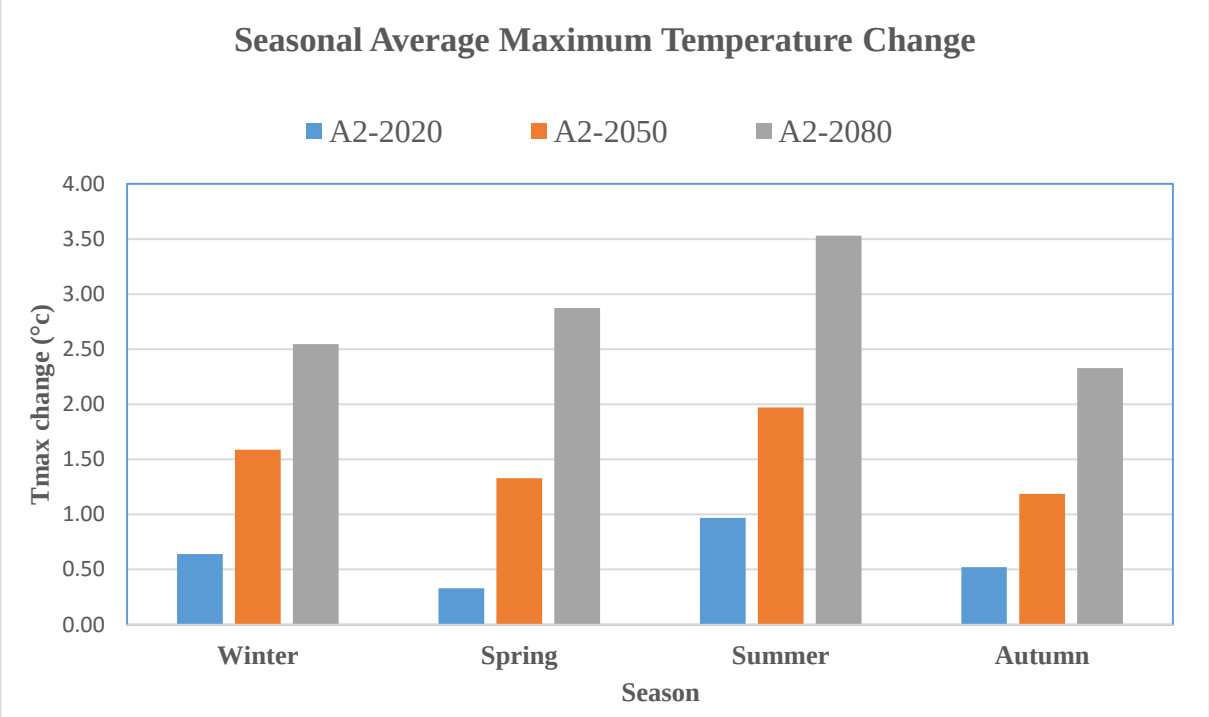

Figure 4-13:- Seasonal average absolute change in mean monthly maximum temperature change for the future HadCM3A2a emission scenarios

Compared downscaled future maximum temperature for both scenarios with observed baseline period, an overall increase of maximum temperature range from 0.52 ⁰c to 2.94 ⁰c. Form this range the maximum change is observed in HadCM3A2a scenarios. Less increment of maximum temperature observed in 2020 by 0.33 ⁰c and from mid to end of the century less increment is observed in autumn. In 2080s maximum temperature increases in summer season by 3.53 ⁰c and minimum increment by 2.33 ⁰c in autumn for HadCM3A2 emission scenarios. Annual seasonal average maximum temperature increases by 0.61⁰c, 1.52⁰c and 2.94⁰c for A2 scenarios (Table 4-5 and Figure 4-13).

Table 4-5:- Seasonal average absolute change in maximum temperature change for the future HadCM3A2a and B2 emission scenarios

	A2-2020	**A2-2050**	**A2-2080**	**B2-2020**	**B2-2050**	**B2-2080**
Winter	0.64	1.59	2.55	0.63	1.27	2.04
Spring	0.33	1.33	2.87	0.34	1.01	1.92
Summer	0.97	1.97	3.53	1.04	1.72	2.69
Autumn	0.52	1.19	2.33	0.48	0.91	1.49
Annual	0.61	1.52	2.94	0.52	1.23	2.03

Like HadCM3A2a scenarios HadCM3B2a senarios average seasonal maximum temeparture change shows similar trend of increasing and decreasing except the range of change is less in HadCM3B2a senarios (Figure 4-14). The smallest seasonal average absolute change in mean monthly maximum tempearture change occures at 2020s in spring seasons by 0.34 °c and the largest maximum temperature change observed in summer season by 2.69 °c. 2050 and 2080 summer seasons shows the maximum change compared to the others seasons. The Annual seasonal average absolute change in mean monthly maximum temperature increases by 0.52°c, 1.23°c and 2.03°c for B2 scenarios is indicated in numerical value on Table 4-5.

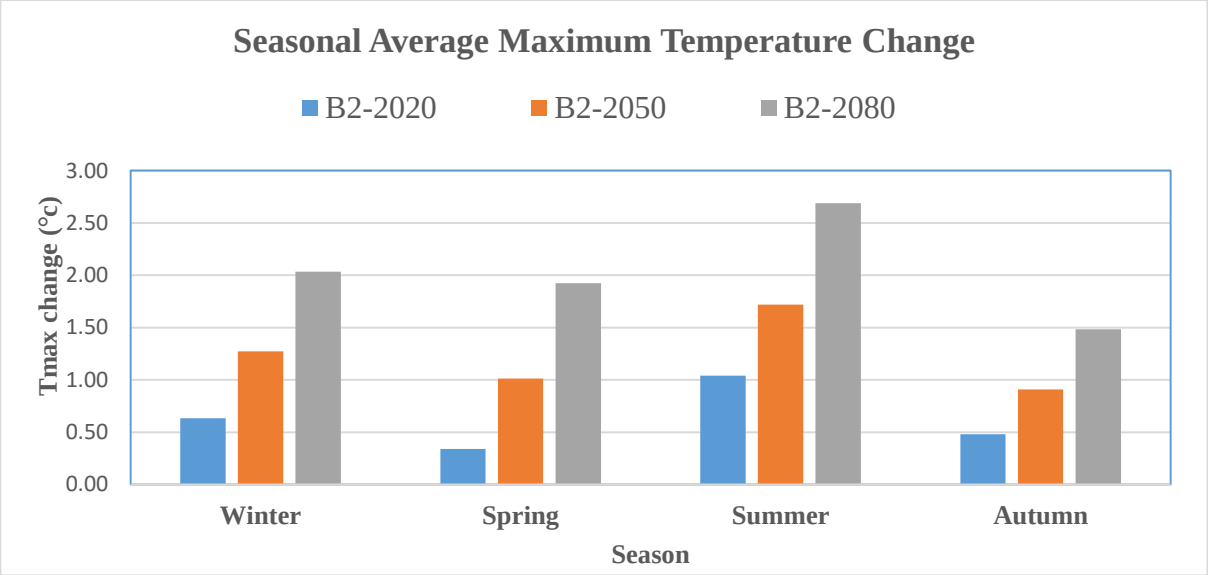

Figure 4-14:- Seasonal average absolute change in mean monthly maximum temperature change for the future HadCM3B2a emission scenarios

Future result of Minimum Temperature

The generated minimum temperature shows an increasing trend from near to end of century. Seasonal average absolute change in mean monthly minimum temperature for both HadCM3A2a and B2a emission scenario increases in range from 0.60 °c to 3.93 °c.

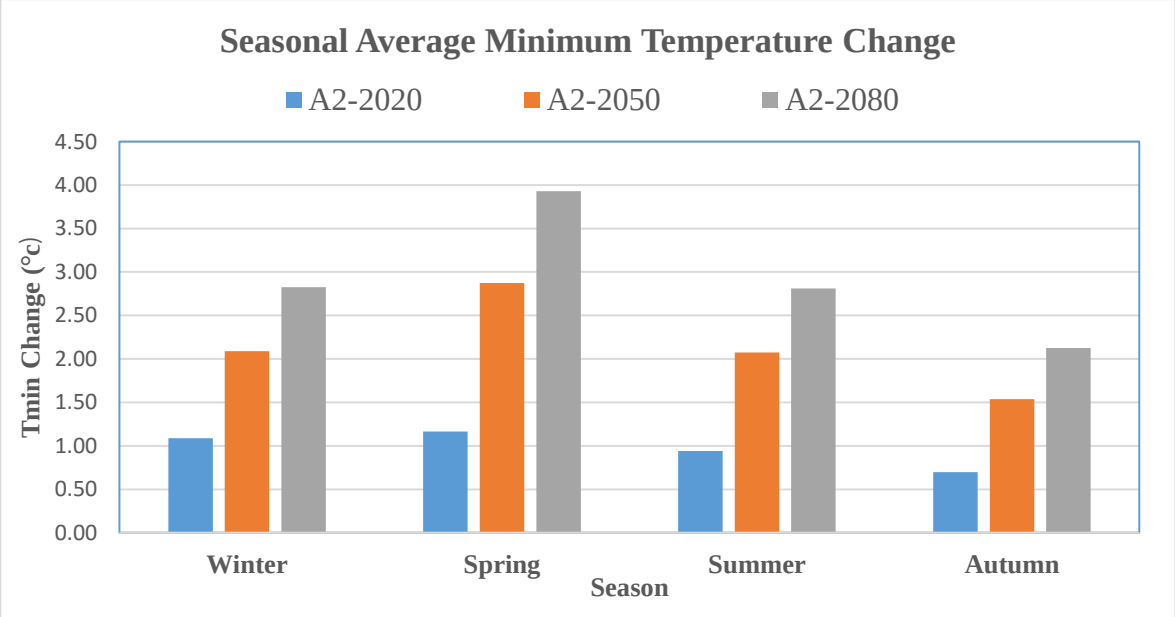

Figure 4-15:- Seasonal average absolute change in mean monthly minimum temperature change in the future HadCM3A2a emission scenarios

Absolute change from historical period it indicates the increment of minimum temperature is higher than maximum temperature (Figure 4-15 and Table 4-6). In 2080s the absolute change seasonal average mean monthly temperature lowered in autumn by 2.12 °c and higher in spring by 3.93°c for HadCM3A2 emission scenarios. Although in 2020s seasonal average absolute change in mean monthly minimum temperature changed from 0.70 °c to 1.17 °c in higher emission scenarios. The mean annual absolute change of minimum temperature changed by 0.97°c, 2.14 °c and 3.12 °c in 2020s, 2050s and 2080s of A2 scenarios.

Table 4-6:- Seasonal average absolute change in mean monthly minimum temperature change for future HadCm3A2a and B2 emission scenarios (all is in °c)

	A2-2020	**A2-2050**	**A2-2080**	**B2-2020**	**B2-2050**	**B2-2080**
Winter	1.09	2.09	2.82	1.02	1.20	2.28
Spring	1.17	2.87	3.93	1.13	2.56	3.76
Summer	0.94	2.08	2.81	0.68	1.68	2.60
Autumn	0.70	1.53	2.12	0.60	1.23	1.46
Annual	0.97	2.14	3.12	0.86	1.84	2.53

HadCM3B2a scenarios absolute change is less than HadCM3A2a scenarios. HadCM3B2 scenarios of seasonal average absolute change in mean monthly minimum temperature highly changed in spring season by 2080 and shows less change in summer of autumn of 2020s (Figure 4-16). The maximum change is observed by 3.76 °c in 2080 and the minimum observed by 0.60 °c in 2020. Annual absolute change minimum temperature increased by 0.86°c, 1.84°c, and 2.53°c in HadCM3B2a for 2020s, 2050s and 2080s. The mean monthly temperature change is available in **appendix 11** in SDSM 4.2.

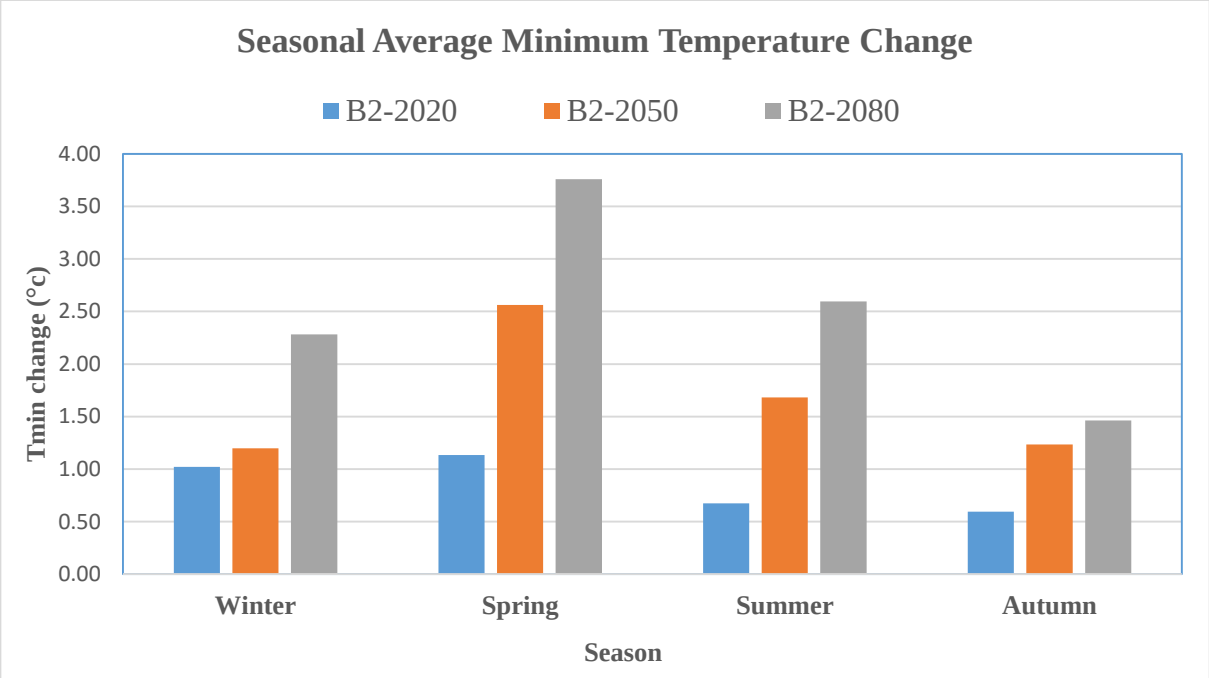

Figure 4-16:-Seasonal average absolute change in mean monthly minimum temperature change in the future HadCM3B2a emission scenarios

Future result of Precipitation

Unlike the maximum and minimum temperature the projected precipitation does not show an increase trend from near to end century. Seasonal average percentage of precipitation change shows increasing for winter and spring the rest seasons displays decreasing for HadCM3A2a and HadCM3B2a emission scenarios of all future time periods.

According to Wilby *et al.* (2004) statement success of statistical downscaling under present climate condition does not implies that the model is valid under future climate condition because of the transfer function invalidity and the weight attached to different predictors may changes. In the report he mentioned atmospheric moisture content doesn't exert some control over present day precipitation occurrence and amount, but is expected to assume greater sign in the future. Charles *et al.* (1999) concludes the test of stationary of statistical transfer schemes using comparable relationship in regional climate models, suggest that the assumption of stationarity may be robust provided that the choice of predictors is judicious (charles *et al.*, 1999).

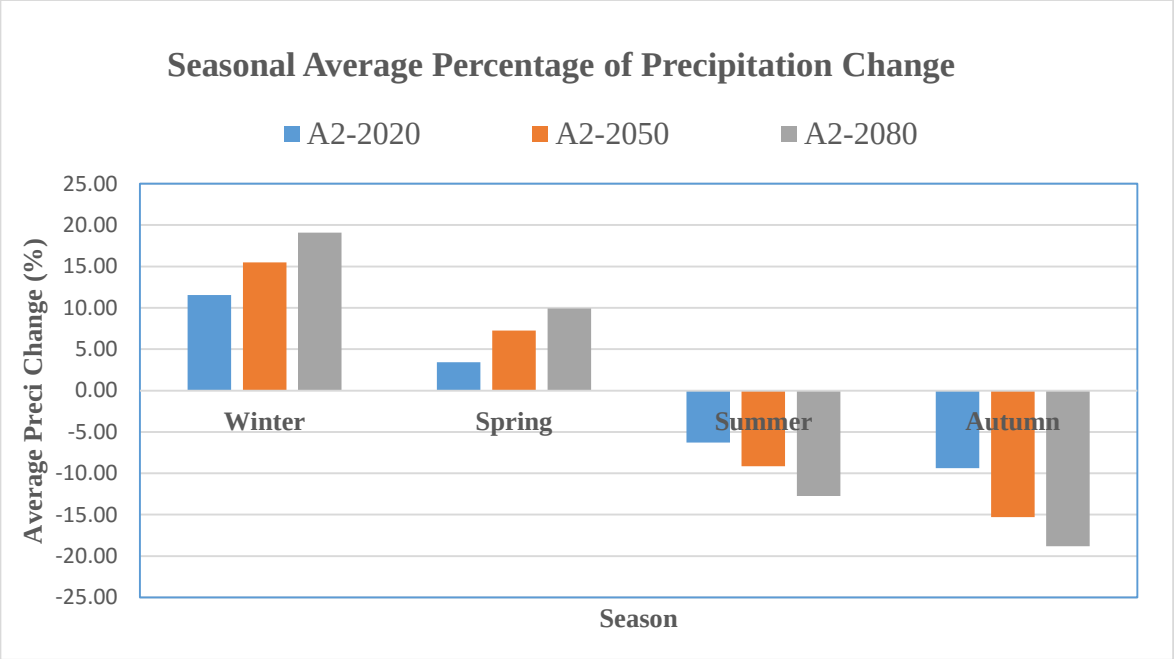

Figure 4-17:- Seasonal average percentage change of precipitation in the future generated for HadCM3A2a emission scenarios

The percentage of change increases in winter by 11.56 %, 15.48 %, and 19.11 % also decreases autumn by -9.37 %, -15.28 % and -18.82 % for HadCM3A2a emission scenarios. Annual percentage difference of future generated HadCM3A2a emission scenarios indicates declination of precipitation amount by -2.03 %, -5.05 % and -7.60 % for 2020s, 2050s and 2080s (Figure 4-17 and Table 4-7).

Table 4-7:- Seasonal average precipitation change in the future for HadCM3A2a and HadCM3B2a emission scenarios (all is in % difference)

	A2-2020	**A2-2050**	**A2-2080**	**B2-2020**	**B2-2050**	**B2-2080**
Winter	11.56	15.48	19.11	8.78	11.88	14.90
Spring	3.41	7.25	9.38	2.20	7.10	7.16
Summer	-6.28	-9.14	-12.75	-3.72	-6.90	-9.95
Autumn	-9.37	-15.28	-18.82	-7.60	-13.44	-14.10
Annual	-2.03	-5.05	-7.60	-0.99	-4.11	-5.96

(- sign) shows the percentage change is reduced comparing to baseline period

HadCM3B2a scenarios show the same increasing and decreasing seasonality trend similar to A2a scenarios except less percentage difference. Increasing percentage of precipitation occurs at winter by 8.78 %, 11.88 % and 14.90 % and decreases in autumn by -7.66 %, -13.44 % and -14.10 % for 2020s, 2050s and 2080s of B2 emission scenarios (Figure 4 -18 and Table 4-7). The annual percentage difference of precipitation decreases by 0.99 %, 4.11 % and 5.96 % from present time to future for B2a scenarios.

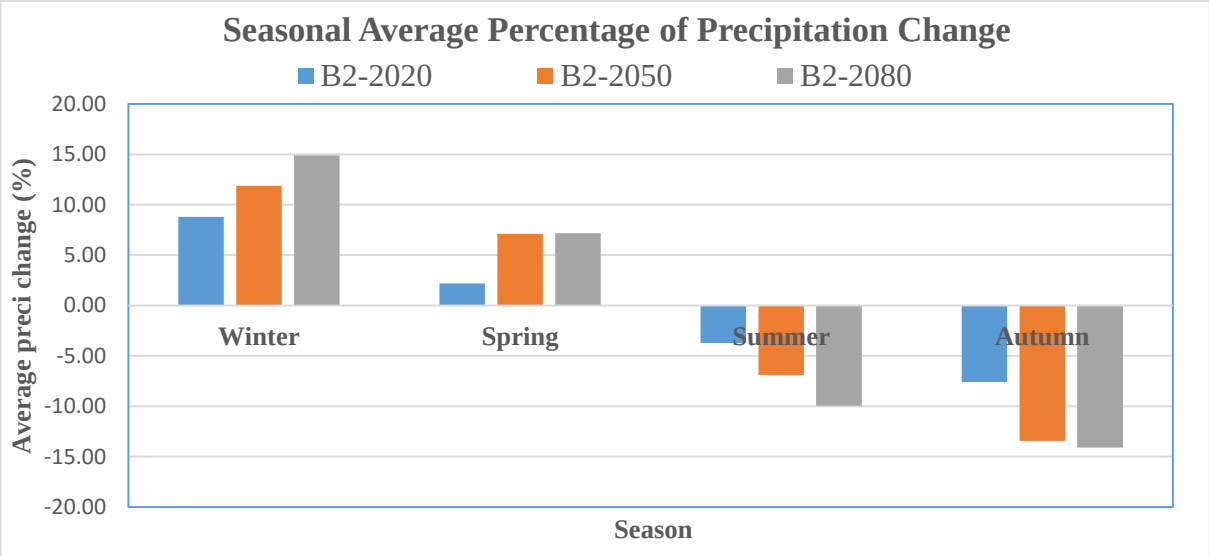

Figure 4-18:- Seasonal average percentage change of precipitation in the future generated for B2a emission scenarios

4.4 Mann Kendall trend Analysis of Future Generated Scenario

From Section 3.4.1 mean annual maximum temperature of observed period is statistical significant increasing trend or accepted H_1 (alternative hypothesis) and precipitation and minimum temperature accepted the Ho (null hypothesis). No trend mean the available data was not sufficient to conclude it was increasing or decreasing trend but it have statistical insignificant trend in that shows the mean annual of given variables in Mann-Kendall trend test analysis.

The mean annual of generated maximum and minimum temperature reject the null hypothesis (Ho) or no trend. Mean annual generated maximum and minimum temperature of both

HadCM3A2a and HadCM3B2a indicates statistical significant trend that accepted the alternative hypothesis (H_1).

Table 4-8:- Mann-Kendall test result for future generated HadCM3A2a and HadCM3B2a scenarios mean annual precipitation, maximum and minimum temperature of Gonder station.

Mann-Kendall test result					
variables	**Z_S**	**$Z_{crit,.05}$**	**Son slope**	**Test Interpretation**	**MK trend**
HadCM3A2a (1993 – 2099)					
Precipitation	-0.063	> 1.96	- 0.003	Accepted Ho	NO
Maximum temperature	3.90	> 1.96	0.029	Reject Ho	Sign (+)
Minimum temperature	2.70	> 1.96	0.0218	Reject Ho	Sign (+)
HadCM3B2a (1993 – 2099)					
Precipitation	-0.063	> 1.96	-0.002	Accepted Ho	NO
Maximum temperature	4.19	> 1.96	0.0191	Reject Ho	Sign (+)
Minimum temperature	3.39	> 1.96	0.017	Reject Ho	Sign (+)

"**No**" implies there is no statically significant trend, "**Sign**" represents the presence of statically significant trend, and **(+)** increasing trend and **(-)** decreasing trend with the values of X which is the time series.

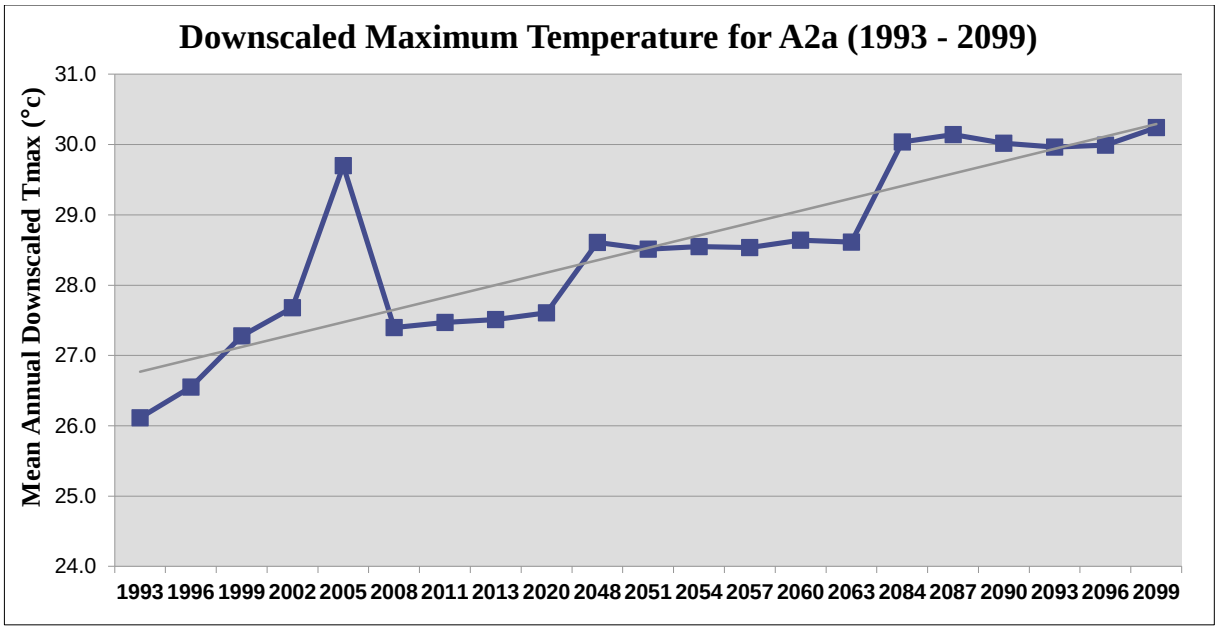

Figure 4-19: Mean annual Maximum generated temperature for HadCM3A2a scenarios in Mann- Kendall trend test shows increasing from 1993 to 2099

The Mann-Kendall trend test result of mean annual generated temperature for HadCM3A2a scenarios shows rejecting of the null hypothesis (Ho). The Z_s value is greater than $Z_{crit,.05}$. That indicated the statics is significant to conclude the generated mean annual maximum temperature increasing from 1993 to 2099.

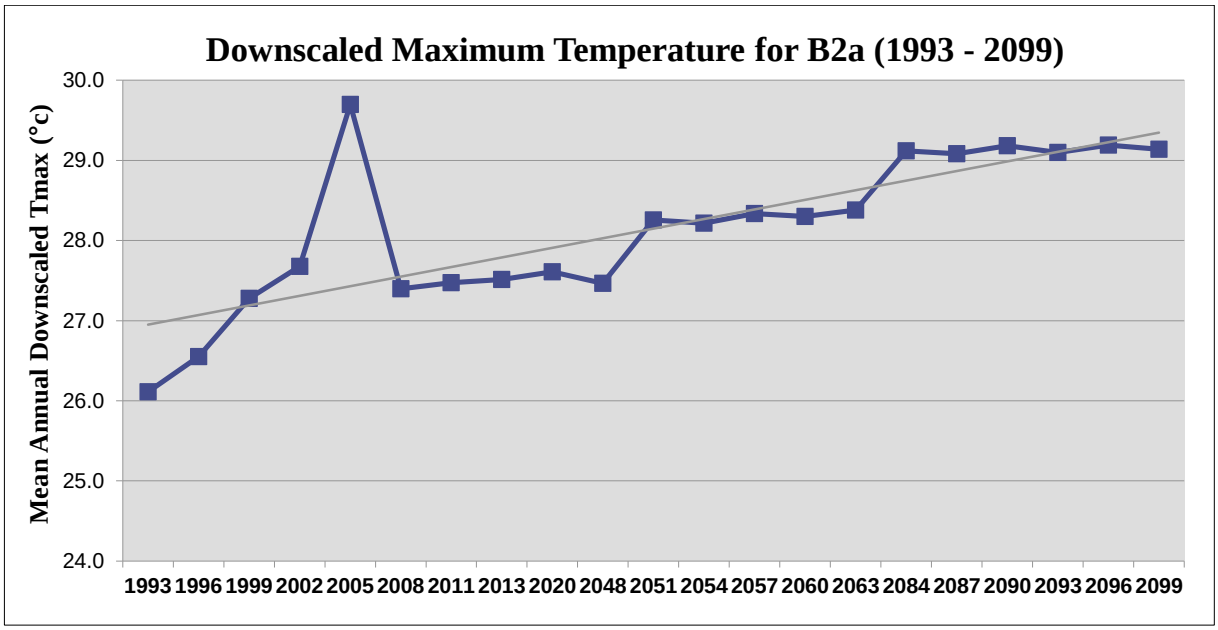

Figure 4-20: Mean annual Maximum generated temperature for HadCM3B2a scenarios in Mann-Kendall trend test shows increasing from 1993 to 2099

Similar to the mean annual maximum generated temperature of HadCM3A2a scenarios the HadCM3B2a scenarios reject the null hypothesis (Ho). The statics is significant to conclude the trend is increasing from 1993 to 2099. Similar to HadCM3A2a the Z_s value is greater than $Z_{crit,.05.}$ (Figure 4-20).

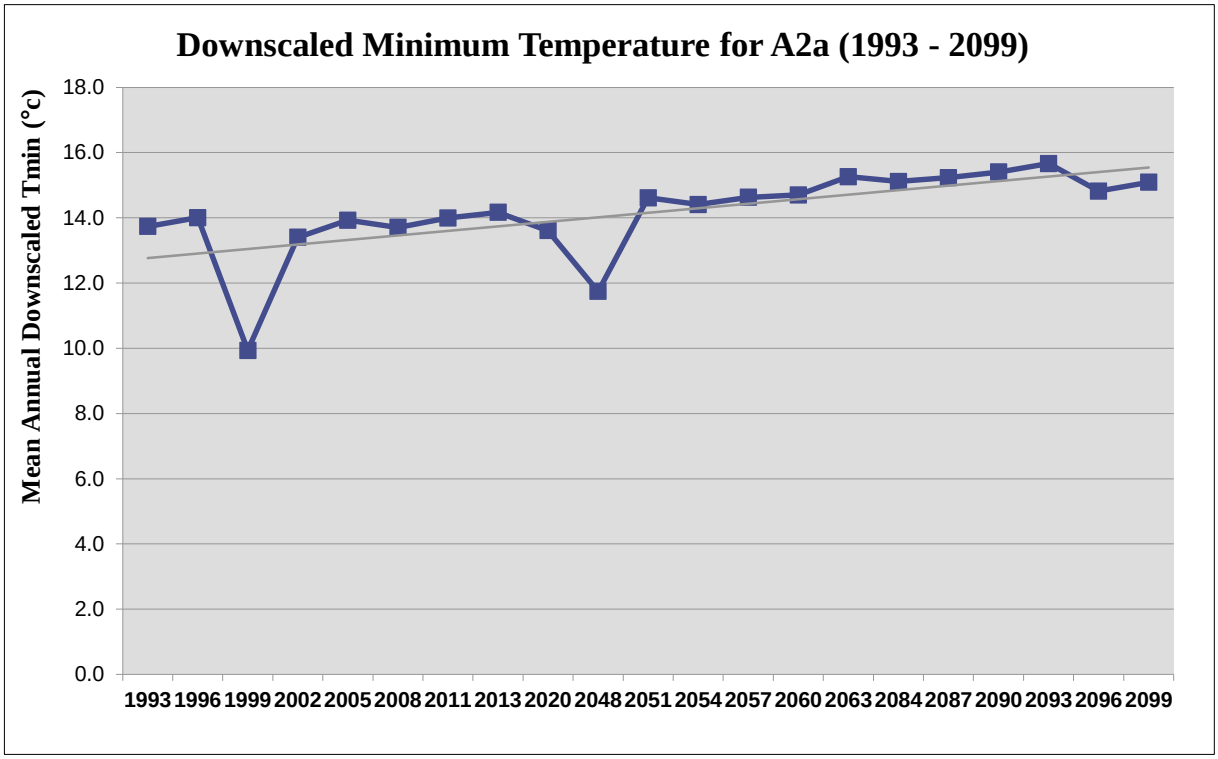

Figure 4-21:- Mean annual Minimum temperature generated for HadCM3A2a scenarios in Mann- Kendall trend shows increasing from 1993 to 2099

Like generated mean annual maximum temperature of both HadCM3 scenarios generated mean annual minimum temperature of HadCM3A2a and HadCM3B2a scenarios show increasing trend in Mann-Kendall trend test analysis. Similar to generated maximum temperature the Z_s value is greater than $Z_{crit, .05.}$ for mean annual generated minimum temperature higher emission scenarios (Figure 4-21).

Generated mean annual minimum temperature of HadCM3B2a scenarios shows increasing trend in Mann-Kendalls trend test from 1993 to 2099. Like that of mean annual generated maximum temperature and generated mean annual minimum temperature HadCM3A2a scenarios the Z_s value is greater than $Z_{crit, .05.}$ Table 4-8 shows the Z_s , $Z_{crit, .05}$ and son slope values of generated mean annual minimum temperature of HadCM3B2a scenarios.

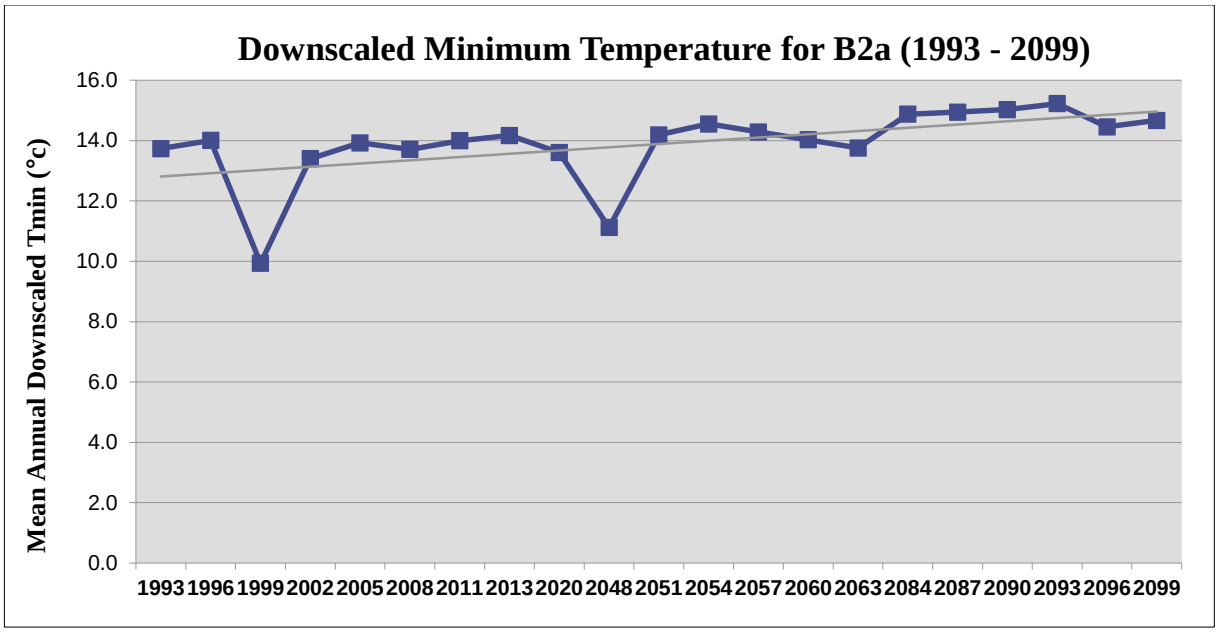

Figure 4-22:- Mean annual Minimum temperature generated for HadCM3B2a scenarios in Mann- Kendall trend shows increasing from 1993 to 2099

The generated mean annual minimum temperature HadCM3B2a scenarios shows higher declination of minimum temperature observed 1993 and 2048. The mean annual minimum temperature for B2a scenarios in 1993 was 9.93 °c comparing to the future minimum temperature it will be the lowest minimum temperature (Figure 4-22).

In case of precipitation both scenarios indicates statistical insignificant trend or accepted null hypothesis (NO trend). Figure 4-23 and 4-24 point out statistical insignificant trends that indicates the given mean annual of generated data is not sufficient data to conclude future precipitation from observed time period is increased or decreased.

The Mann-Kendall trend of generated mean annual precipitation for higher emission scenarios shows statistical insignificant trend that is not sufficient to conclude it is neither increasing nor decreasing. Figure 4-23 shows high variation of mean annual downscaled precipitation for higher emission scenarios. Because of the variation in time period the Mann-Kendall trend test unable to conclude either it increases or decreases. Unlike mean annual generated maximum and minimum temperature the Z_s value is less than $Z_{crit, .05}$ for precipitation. The amount of annual mean generated precipitation highly declined 1963 and 2093 (Figure 4-23).

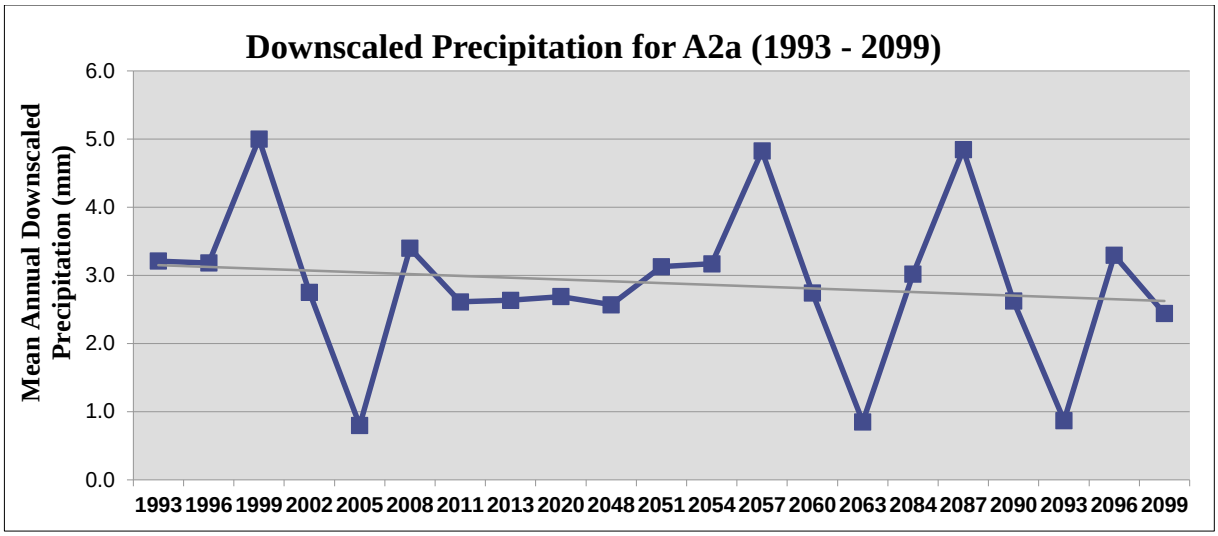

Figure 4-23:- Mean annual precipitation generated for HadCM3A2a scenarios in Mann Kendall trend shows statistical insignificant trend from 1993 to 2099

Similar to mean annual generated precipitation for HadCM3A2a scenarios the B2a scenarios shows declination high variation of mean annual precipitation (Figure 4-24). Like A2a scenarios the B2a scenario Mann-kendall trend result show statistical insignificant that show trend but unable to conclude either increasing or decreasing. The Z_s value is less than $Z_{crit, .05}$ for generated mean annual precipitation HadCM3B2a scenarios (see Table 4-8).

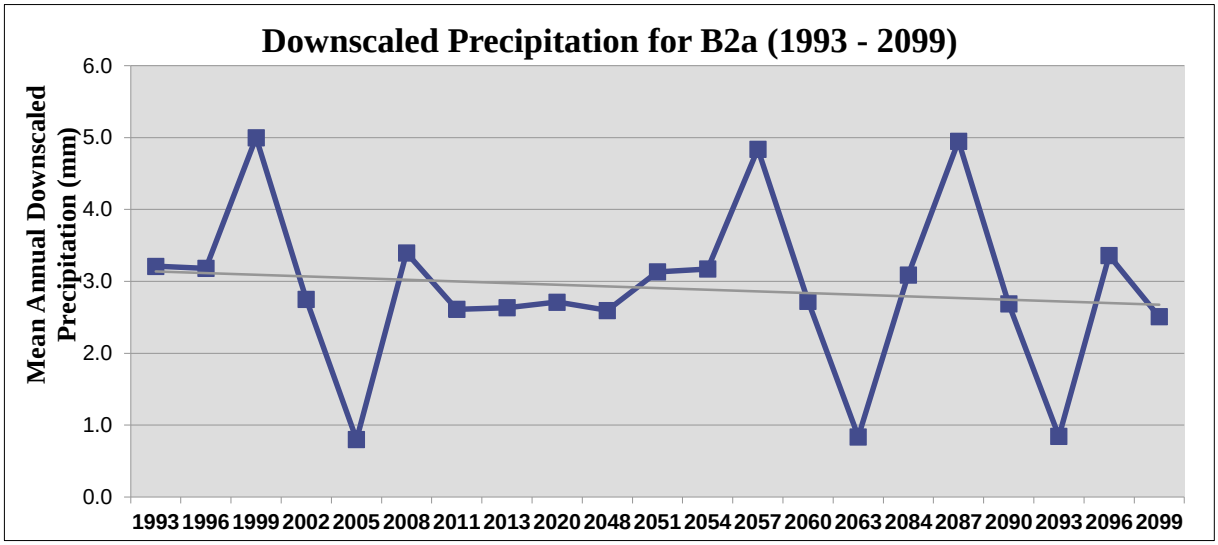

Figure 4-24:- Mean annual precipitation generated for HadCM3B2a scenarios in Mann Kendall trend shows statistical insignificant trend from 1993 to 2099

4.5 SWAT Model Result

The Megech watershed modeling was done by using a time series dataset of 21 years from 1993 to 2013 out of which nine years (1995 to 2003) were used for calibration period and five years (2002 to 2008) for validation period. The simulated flow at the outlet of the watershed sub basin 29 were compared with the observed flow. The sensitivity analysis and calibration for land use phases were done at the outlet sub basin of the Megech watershed (sub basin 29).

4.5.1 Sensitivity Analysis

The model was run for a period of nine years (from 01/01/1995 to 31/12/2003) excluding the validation period, this time period was taken for sensitivity analysis. Sensitivity analysis was conducted to determine the influence of a set of parameters had on predicting total inflow. The most sensitive parameters for flow of the watershed drawn by SWAT model (Table 4-9). The sensitive parameters identified for Megech watershed represents the important physical processes involved in the stream flow generation of the basin. These are, in particular, groundwater parameters (ALPHA_BF, REVAPMN, GWQMN, and GW_Revap), runoff parameters (CN2 and CANMX), Crop (Blai), evaporation (ESCO), channel (CH_K2) and soil (SOL_AWC and SOL_Z) parameters.

Table 4-9:- Sensitivity analysis result for stream flow in Megech Watershed

Parameters	Unit	Rank	Mean Sensitivity	Category of Sensitivity
ALPHA_BF	Days	1	1.219	Very high
ESCO		2	0.256	High
CN2	%	3	0.218	High
GWQMN	mm	4	0.201	High

SOL_AWC	mm water/ mm soil	5	0.0532	Medium
REVAPMN	mm	6	0.0525	Medium
SOL_Z	mm	7	0.0524	Medium
GW_Revap		8	0.0514	Medium
CANMX	mm	9	0.0510	Medium
Blai		10	0.0169	Small
CH_K2	mm/h	11	0.0104	Small
SOL_K	mm/h	12	0.00964	Small

The result denotes that base flow alpha factor (ALPHA_BF), soil evaporation compensation factor (ESCO), SCS_CN for moisture condition II (CN2), ground water parameters like thresh fold depth of water in the shallow aquifer required for return flow to occur (GWQMN), soil available water capacity (SOL_AWC), thresh hold depth of water in the shallow aquifer required for evaporation to occur (REVAPMN), the soil parameters inclusive of soil depth (SOL_Z), ground water evaporation coefficient (GW_Revap) and Maximum canopy Index (CANMX) are found the influencing flow parameters (having relative mean sensitivity from high to medium degree of sensitivity). Finally, had also contributing effect on stream flow and were taken as a guideline for the calibration.

4.5.2 Calibration and Validation

The calibration of stream flow was conducted depending on the sensitive parameters which were demonstrated as influential variables on the simulated water balance by the model. The parameters which were believed to have influence on the simulated flow were taken in to consideration from sensitivity analysis result. Using the most sensitive parameters, the

first 11 were used in calibration having small to high class of sensitivity. Calibration of stream flow was carried out at the outlet of sub basin 29 (Near Azezo gauging station). The Calibration for stream flow was first done for monthly averaged mean annual conditions.

Table 4-10:- Result of final calibrated flow parameters for Megech watershed

Parameters	**Default Values**	**Allowable Range To Change**	**Adjusted Parameter value**
ALPHA_BF	0.048	0 - 1	0.078
ESCO	0	0 - 1	0.1
CN2	Default *	± 25 %	+20 %
GWQMN	0	0 - 5000	300
SOL_AWC	**	± 25 %	+15 %
REVAPMN	1	0 - 500	240
SOL_Z	**	± 25 %	+ 15 %
GW_REVAP	0.02	0.02 – 0.2	0.05
CANMX	0	1 – 2	1

Default* shows the default SWAT model values ** indicates the input soil properties of the watershed (varies for each soil).

Adjustment was done till observed and simulated values were correlated well by changing the parameters in their allowable range. The SWAT default parameters values were adjusted as follows. First, the surface flow components of average annual water balance by adjusting the CN. An effort was also made to keep the curve numbers close to standard table values. Next, ALPHA_BF, ESCO , GWQMN, SOL_AWC, SOL_Z, Blai, GW_REVAP & REVAPMN were adjusted till the deviation between simulated and observed values get minimized and the performance indicators lie in the acceptable range. Accordingly the final calibrated parameters were presented for flow in Megech watershed (Table 4-10).

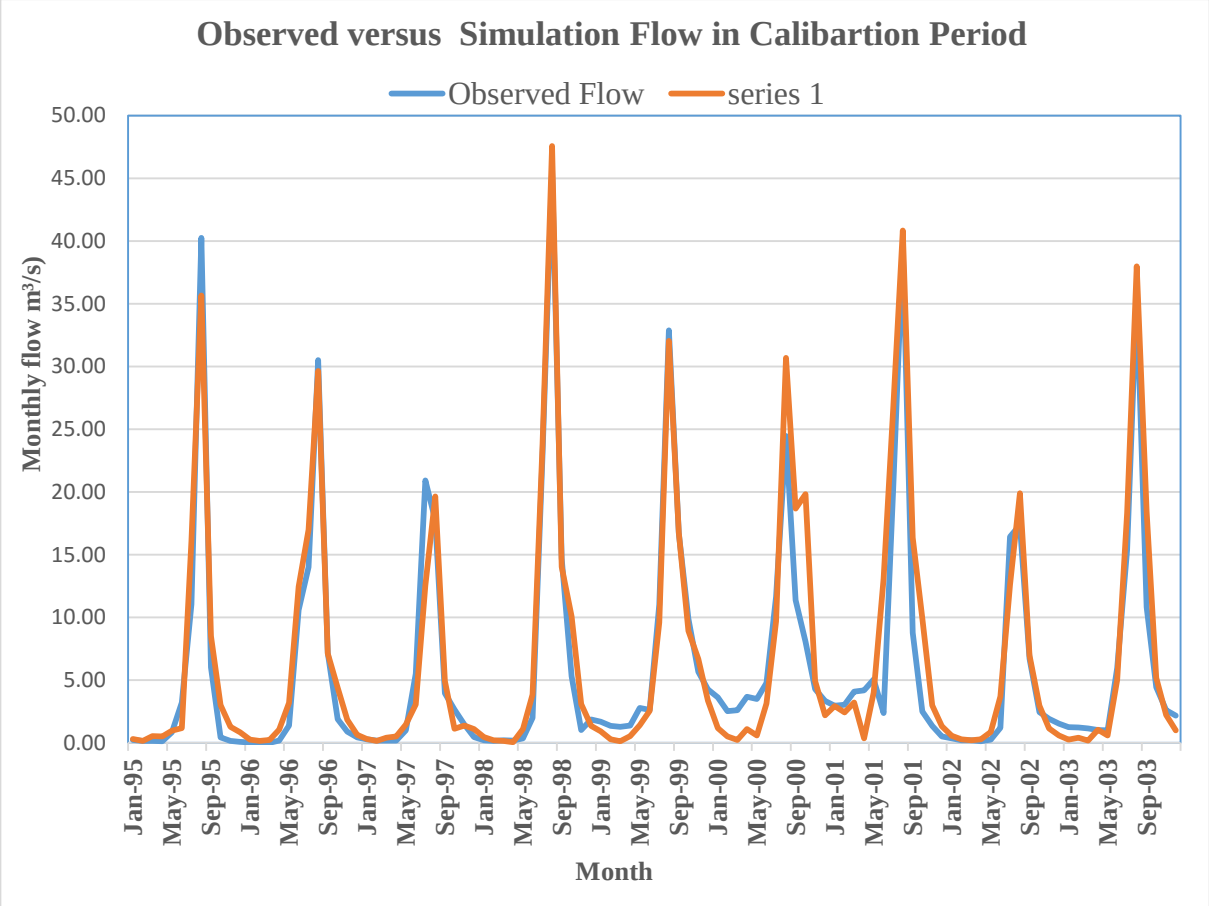

Figure 4-25:- Time series of simulated and observed monthly Megech River flow for the calibration period at Megech watershed.

Undulation of stream flow was observed during calibration & validation periods in both low and high flow seasons (see Figure 4-25 and 4-27), this fluctuation might exist due to the model low capability to capture peak rainfall event, the data quality's occurred during filling missed

data's and error during measurement records. The simulated mean annual stream flow (monthly averaged) after calibration shows a good agreement with the observed data set (Table 4-11). After mean annual stream flow calibration the monthly time step calibration was carried out by varying flow sensitive parameters iteratively within the allowable ranges until satisfactory agreement between observed and simulate stream flow was obtained.

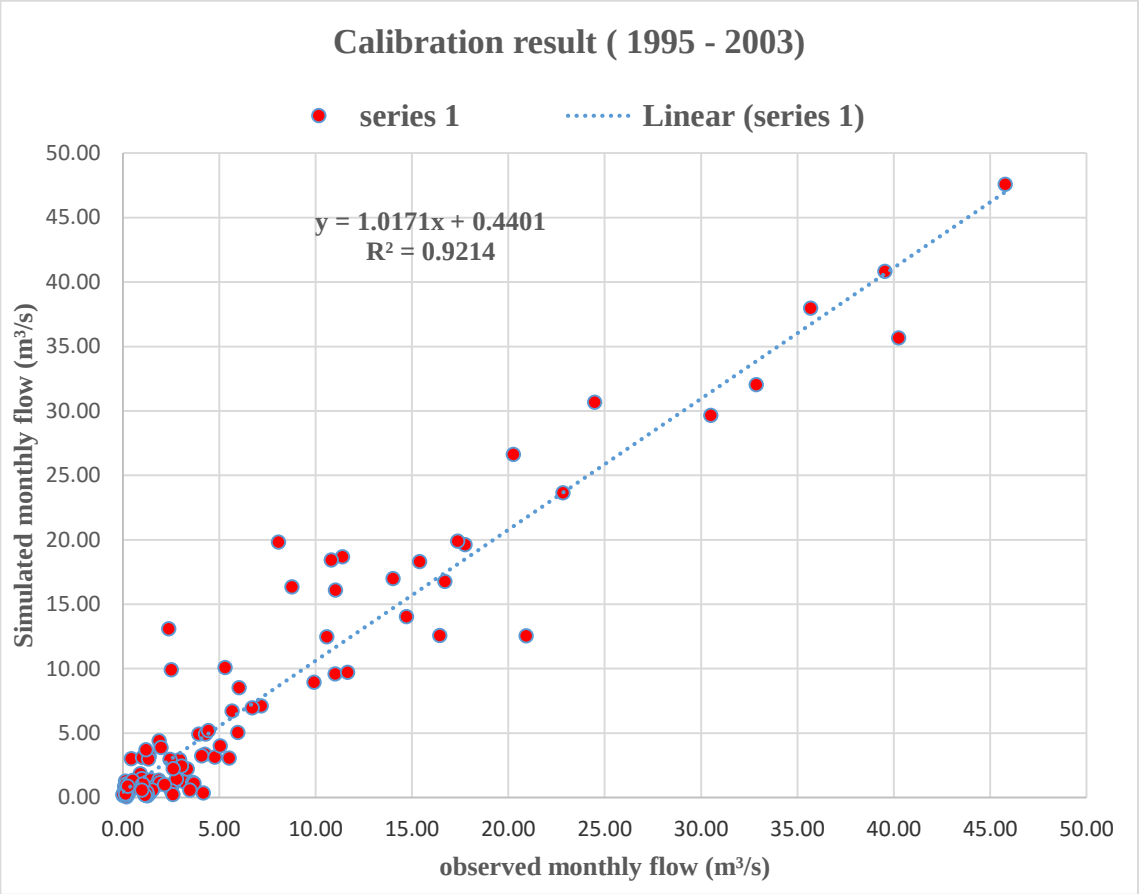

Figure 4-26 :- Scatter plot of observed versus simulated monthly Megech River flow of calibration period at Megech watershed

After stream flow is calibrated the next step was validation with independent data sets which are not used in the calibration period without changing the fitted parameters. Maximum flow observed and SWAT model result was 1998 in the calibration period. The validation was undertaken for a period of five years (01/01/2004 to 12/31/2008) is due to absence of flow data in the study area after 2008 (Figure 4-27).

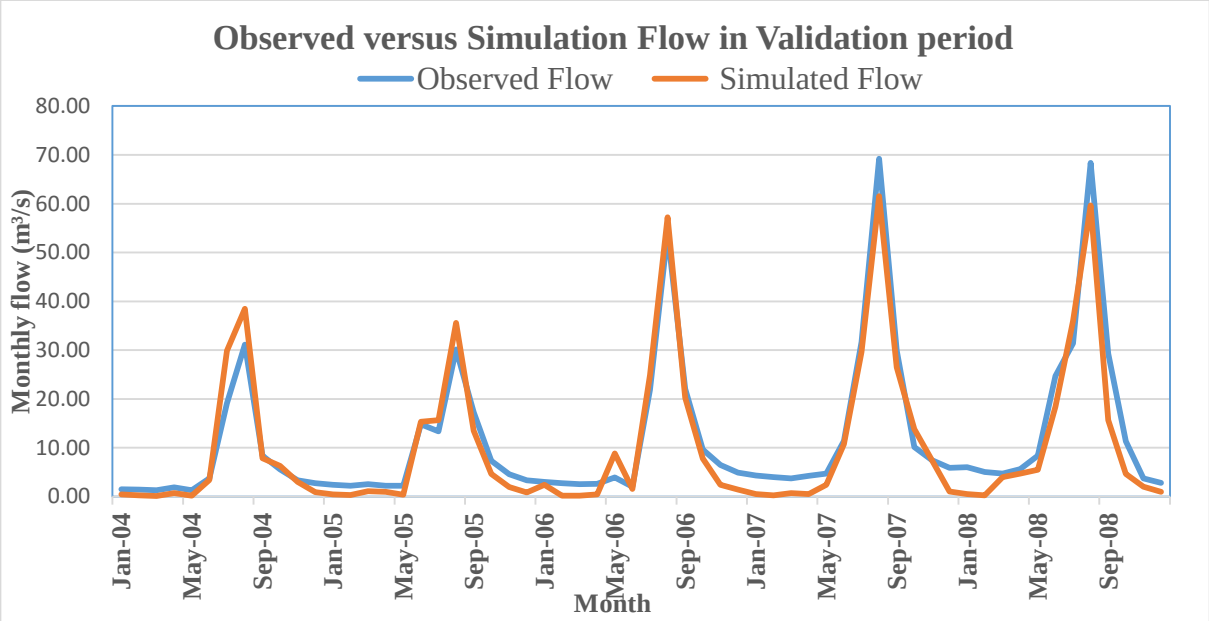

Figure 4-27:- Time series of simulated and observed monthly Megech River flow for the validation period at Megech watershed

From figure 4-27 shows the similar flow trend between the observed flow of Megech River at the Megech dam inlet and simulated result. In starting period the simulated flow slight higher than observed. The rainy months of 2004, 2005 and 2006 shows high simulated flow and the rest 2007 and 2008 show high observed flow than the SWAT results.

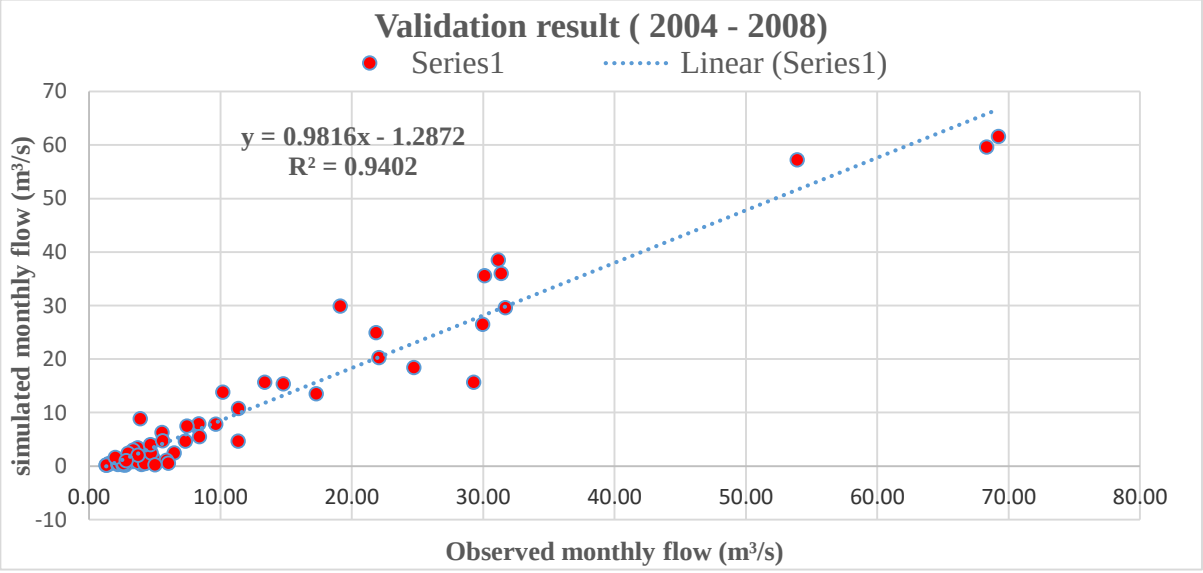

Figure 4-28:- Scatter plot of observed versus simulated monthly Megech River flow for the validation period of Megech watershed

Coefficient of determination (R^2) between observed and simulated monthly Megech flow shows good agreement (Figure 4-28). In general the observed monthly Megech flow shows high similar trend with simulated monthly flow. Quantitative measurement of performance of the SWAT model are the Nash-Sutcliffe model efficiency (NSE), the percentage of bias (PBIAS) and coefficient of determination (R^2), as discussed in Section 3.6.1 (see Equation 3.15 to 3.17). The values are listed in Table 4-11.

Table 4-11:- Statistical measures of the SWAT model performance of Megech watershed calibration- and validation period result.

Monthly time step	**Over Year mean Monthly stream flow(m^3/s)**		**PBIAS**	**NSE**	**R^2**
	Observed	**Simulated**			
Calibration(1995-2002)	6.3	6.8	-8.7	0.90	0.92
Validation (2003-2008)	11.73	10.69	9.88	0.92	0.94

4.6 Observed land use change on Megech watershed

From land use map of Ministry of Agriculture and Natural resource the Megech watershed have visible land use changes during compared time from 1984 to 2008. Land use/ land cover map of 1984, 1986, 2006, 2008 and 2009 year are available for Megech watershed. But all the maps were not have the same scale and season of map preparation. From above land use phases of different years the first 1984 LULC and 2008 LULC were selected based on their correspondence in scale, spatial resolution and season of map preparation. Both have same scale with 1:250,000 and their season of map preparation were in dry season.

2008 LULC shows change of percentage area coverage land use/land cover comparing to historical reference period of 1984 LULC. 2008 LULC indicates increasing of area coverage

for cultivated, urban and shrub land by 6.26 %, 0.95 % and 0.32%. The rest grass land, plantation and bare land declined by 5.9 %, 0.95 % and 0.62%.

Table 4-12:- Comparison land use change between the 1984 LULC and 2008 LULC for 24 years in Megech watershed area

		Area (ha)		**Area coverage (%)**	
Land use	SWAT code	1984 LULC	2008 LULC	1984 LULC	2008 LULC
Cultivated land	AGRC	22914.38	25358.37	58.08	64.34
Plantation	FRSE	843.57	469.09	2.14	1.19
Grass land	PAST	5400.43	3074.70	13.70	7.80
Shrub land	RNGB	7990.27	8116.41	20.27	20.59
Bare land	URLD	1407.27	1162.87	3.57	2.95
Urban	URHD	863.28	1237.76	2.19	3.14

Megech watershed is vulnerable to land use/ land cover change for compared 24 years. The areal coverage of cultivated land maximally increased by 6.26 % and declined in grass land by 5.9 % for the past 24 years (Figure 4-12). This study used 2008 land use/ land cover and soil property data to generate the impact of climate change on the flow. It considers the climatic variability's change due to human activity mean increasing of carbon dioxide. Those climatic variables (temperature and precipitation) change cause effect on land use changes and have a potential to change the soil properties. Expansion of large scale irrigation, afforestation by community farmers, construction of Megech dam and other activities will held in this watershed from present to far period. Those activities leads to land use/land cover change on the watershed area. In this study SWAT model calculates actual evapotranspiration, soil moisture and ground water recharge with assumption of the future period will stay the same land cover as 2008 land use/ land cover.

4.7 Simulation of Future Megech River Flow

One of the objective of this study was to show the impacts of climate change on the water resource of Megech watershed. Regional calibrated and validated model of SWAT was utilized to quantify the effect of climate change on the flow of Megech based on manipulated climate parameters precipitation and temperature. Then output of SDSM 4.2, as discussed in Section 4.3 used as input in SWAT hydrological model i.e. precipitation, minimum and maximum temperature were used to simulate the future flow of Megech River.

Comparing the reference of corrected mean monthly flow of Megech River (1995 – 2008) to future flow decreased in both HadCM3A2a and HadCM3B2a scenarios. SWAT model result indicates percentage change of mean monthly flow and annual mean flow in both scenarios. For both scenarios seasonal average flow increases in percentage for winter and spring and decreased in summer and autumn (Table 4-13).

Table 4-13:- Seasonal average stream flow change in the future for HadCM3A2a and HadCM3B2 emission scenarios **(% difference)**

Season	HadCM3A2			HadCM3B2		
	A2-2020	**A2-2050**	**A2-2080**	**B2-2020**	**B2-2050**	**B2-2080**
Winter	3.50	10.52	12.76	2.68	11.12	11.74
Spring	0.30	4.27	2.99	0.39	2.22	2.28
Summer	- 12.31	- 25.95	- 36.14	- 10.79	- 22.83	- 32.89
Autumn	- 12.26	- 26.57	- 29.88	- 10.44	- 22.10	- 25.38
Annual	- 5.19	- 9.43	- 12.57	- 4.54	- 7.90	- 11.06

(- sign) shows the percentage change is reduced comparing to basely stream flow period

SWAT model simulation result using HadCM3A2a scenarios inputs indicated annual declination of flow by - 5.19 %, - 9.43 %, -12.57 % in 2020s, 2050s and 2080s. HadCM3A2a scenarios result of SWAT model average seasonal percentage change of flow increased by 3.50

%, 10.52 %, 12.76 % in winter seasons and the declined by - 12.31 %, - 25.95 %, - 36.14 % in summer seasons for 2020s, 2050s and 2080s (see Figure 4-29 and Table 4-13). Although the scenario indicates the percentage change of seasonal average flow declined by -12.26 %, - 26.57 % and - 29.88 % in autumn from near to end of the century. Less increment in percentage change of seasonal average flow observed form 2020s to 2080s in spring seasons by 0.30 %, 4.27 % and 2.99 %.

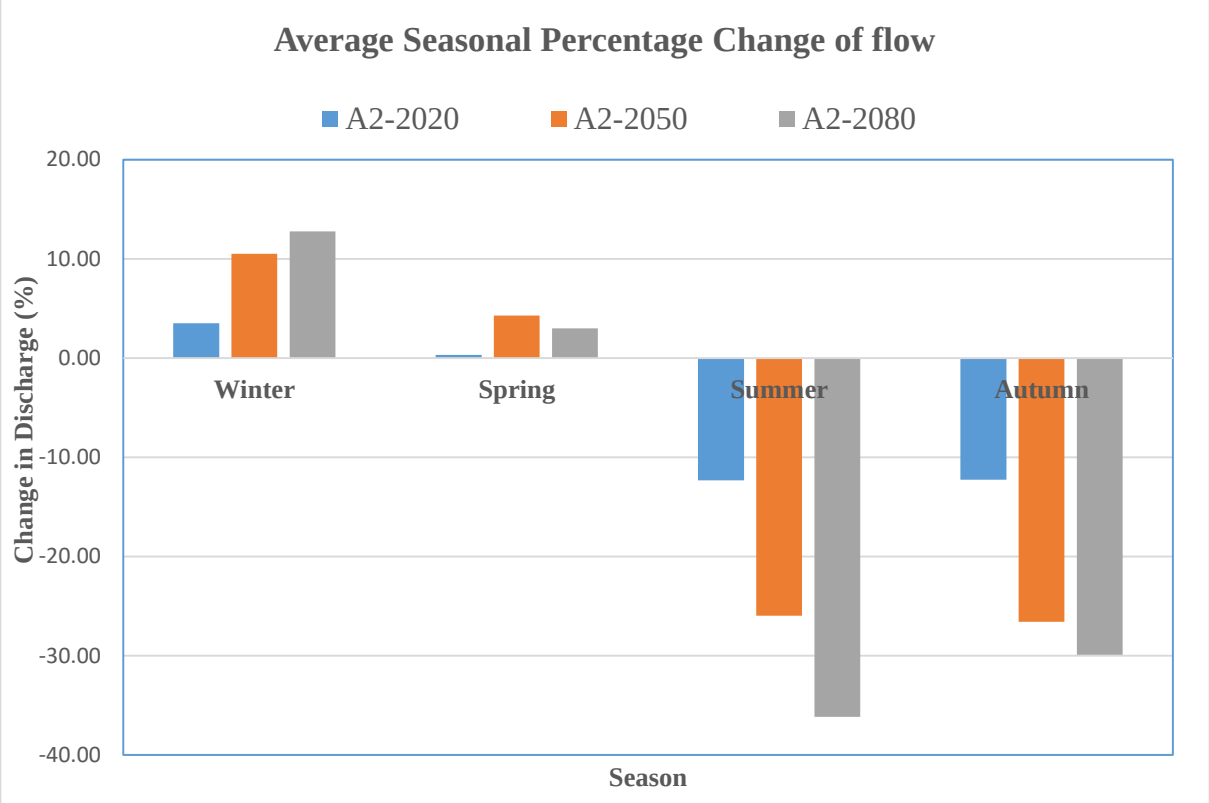

Figure 4-29:- Seasonal average percentage change of Megech River flow in the time horizons of HadCM3A2a emission scenarios in Megech watershed

The monthly flow shows declination from December to April for 2020s, 2050s and 2080s. Higher declination observed in maximum flowing month August by - 19.71 %, - 33.30 % and - 40.63 %. The rest months from May to November decline in monthly Megech River flow for 2020s (2011- 2040), 2050s (2041-2070) and 2080s (2071- 2099). This scenarios SWAT output is similar trend of increasing and decreasing with HadCM3A2a scenarios SWAT result except differ in amount (Figure 4-30).

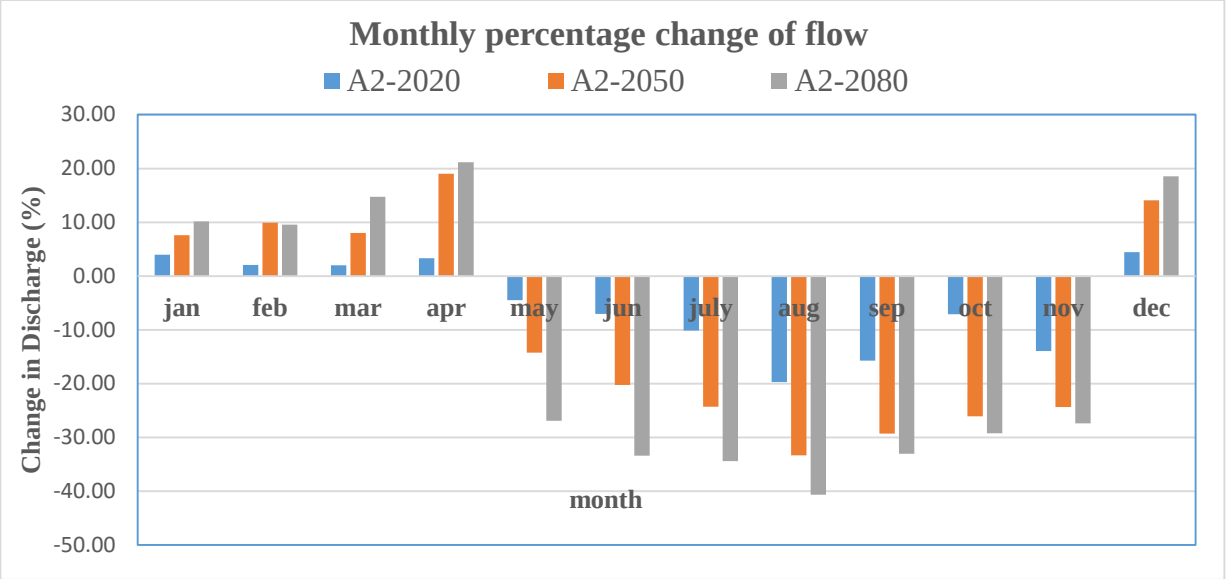

Figure 4-30:- Monthly percentage change of Megech River flow HadCM3A2a scenarios comparing to the observed period in the Megech River flow.

HadCM3B2a scenarios consider medium- low emission than A2a scenarios. Based on SWAT result maximum increment of flow observed in winter seasons by 2.68 %, 11.12 % and 11.74 % and declined in autumn -10.79 %, -22.83 % & - 32.89 % for 2020s, 2050s & 2080s. Similarly less percentage of flow change observed in spring by 0.39 %, 2.22 %, 2.28 % and decreased in autumn by -10.44 %, -22.10 %, -25.38 % from near to end of century (Figure 4-31).

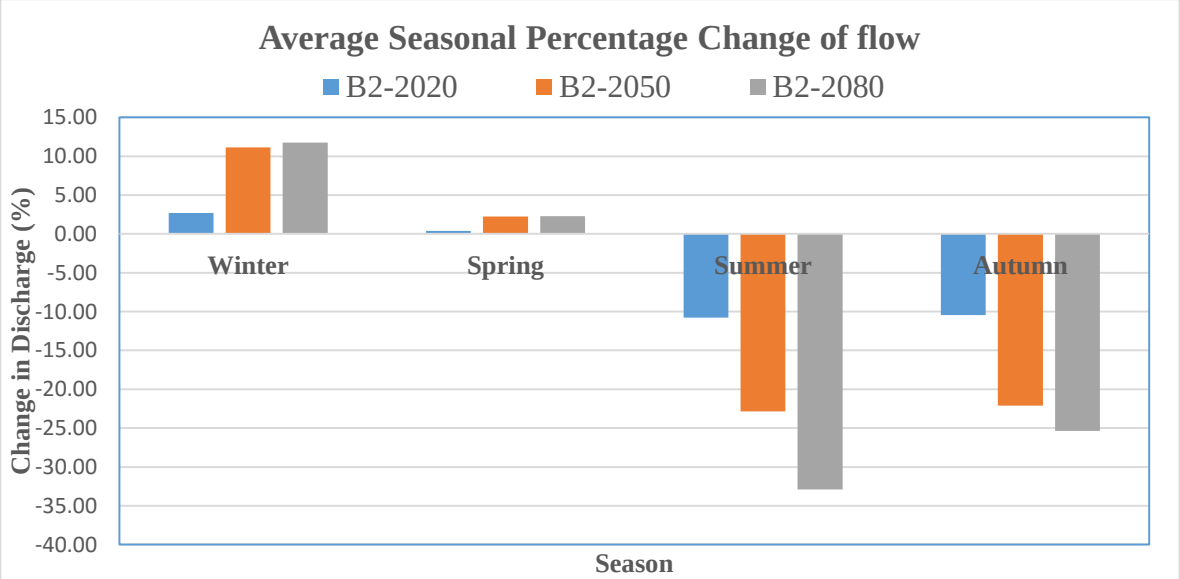

Figure 4-31:- Seasonal average percentage change Megech River flow at in the time horizons of HadCM3B2a emission scenarios in Megech watershed.

Similar to HadCM3A2a scenarios B2a scenarios monthly percentage change of Megech River flow indicates the maximum declination of flow observed in August by - 15.89 %, - 28.56 %, - 36.29 % form all time periods . The flow of Megech River increased from December to April like A2a scenarios. Although the rest months declines from near to end of the century (see Figure 4-32).

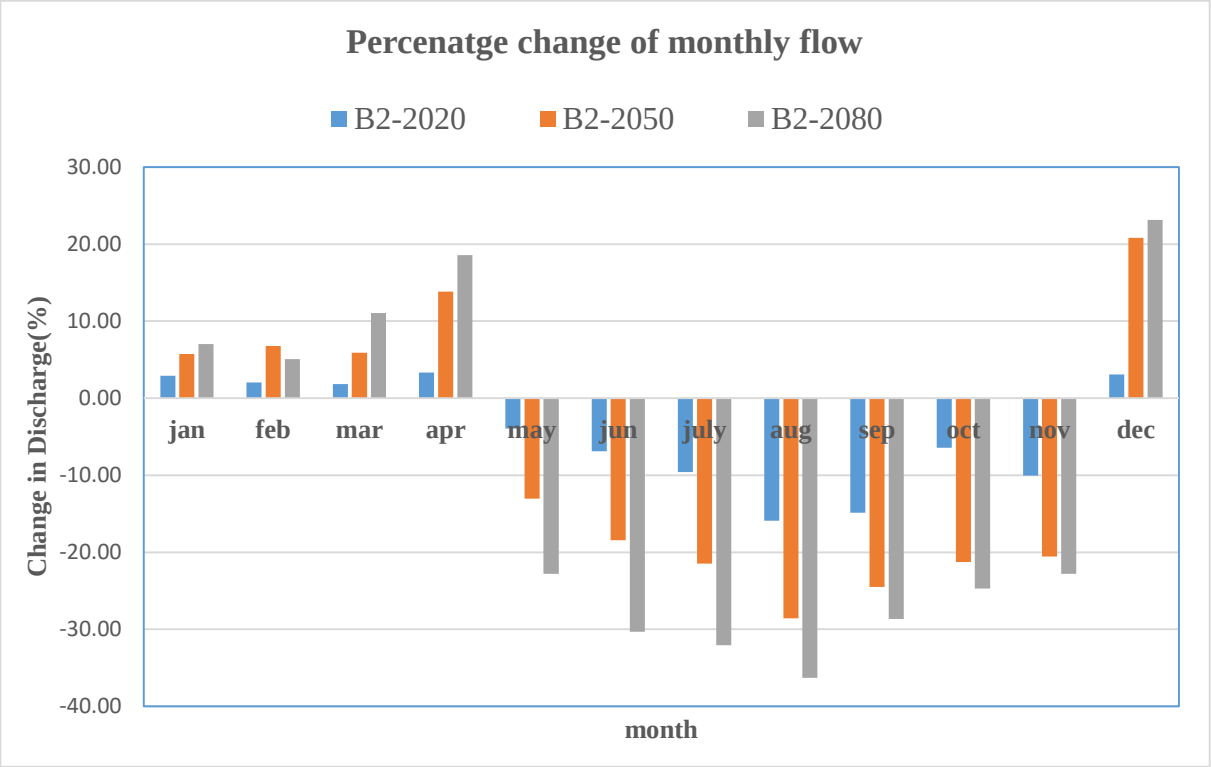

Figure 4-32:- Percentage change between the baseline and HadCM3 scenarios period of average monthly Megech River flow for B2a scenarios.

In comparing with the 20th century reference situation, the future Megech River flow decreased in both SRES scenarios. This mainly due to a decrease of future precipitation and increase of future temperature. The impact of climate change on the hydrology of Megech watershed based on downscales UK Hadley center for climate prediction and research (HadCM3) of A2a and B2a scenarios shows result. SWAT model indicates the flow is declined in both scenarios. The declination is higher in HadCM3A2a scenarios because of it consider medium higher scenario with more production of carbon dioxide concentration than HadCM3B2a scenarios.

Section 4.6 discussed Megech watershed land use/ land cover changes due to climate change for past 24 years. This indicates there will be impact of climate change on the land use/land

cover on the future time. Based on the result of SDSM 4.2 Megech climatic variables like maximum and minimum temperature will increase in the watershed on the future period and precipitation will reduce in next coming years. Although SWAT model indicates the mean monthly flow of Megech River reduces in future period it may cause by change in climatic variable and land use/ land cover form near to end of the century. The change of mean Megech River flow is detail discussed as flow.

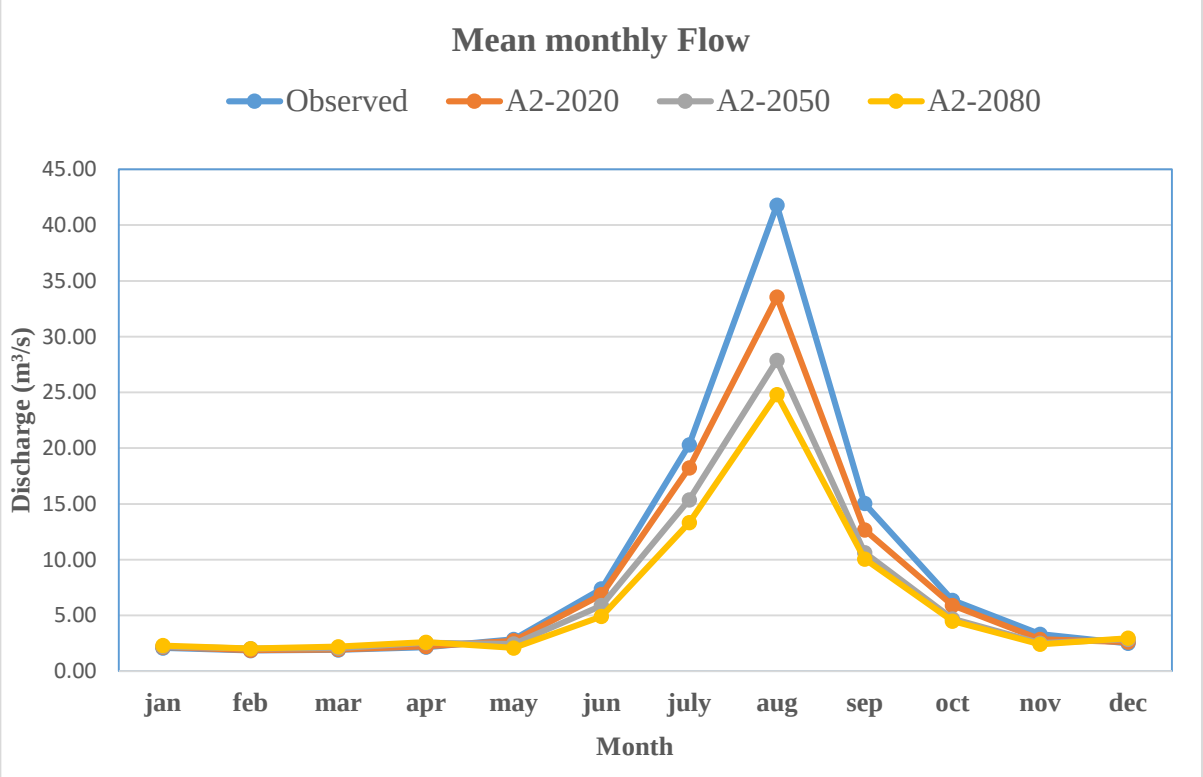

Figure 4-33:- Mean monthly Megech River flow using SWAT model under downscaled GCM-generated HadCM3A2a scenarios compared with observed period .

Mean monthly future SWAT simulated flow of Megech River using HadCM3A2a and HadCM3B2a scenarios in compared with mean monthly observed baseline period (1993- 2008) (Figure 4-33 and Figure 4-34). In general the winter seasons of Megech watershed shows increasing in temperature and maximum increment in precipitation comparing to the other seasons. The flow of Megech flow maximally increased in this seasons for both A2a and B2a scenarios. In December the mean monthly flow changed to 2.61 m^3/s, 2.85 m^3/s, 2.97 m^3/s and 2.58 m^3/s, 3.02 m^3/s, 3.08 m^3/s for 2020s, 2050s and 2080s of A2a and B2a scenarios. The

second seasons spring have similar to the winter except less increment in precipitation and higher in temperature. March and April shows less increment of mean monthly flow. Monthly flow declined in May 2.73 m³/s, 2.45 m³/s, 2.09 m³/s and 2.74 m³/s, 2.48 m³/s, 2.28 m³/s for A2a and B2a scenarios from near to future period. Summer seasons indicates higher increment in temperature and decreasing in precipitation.

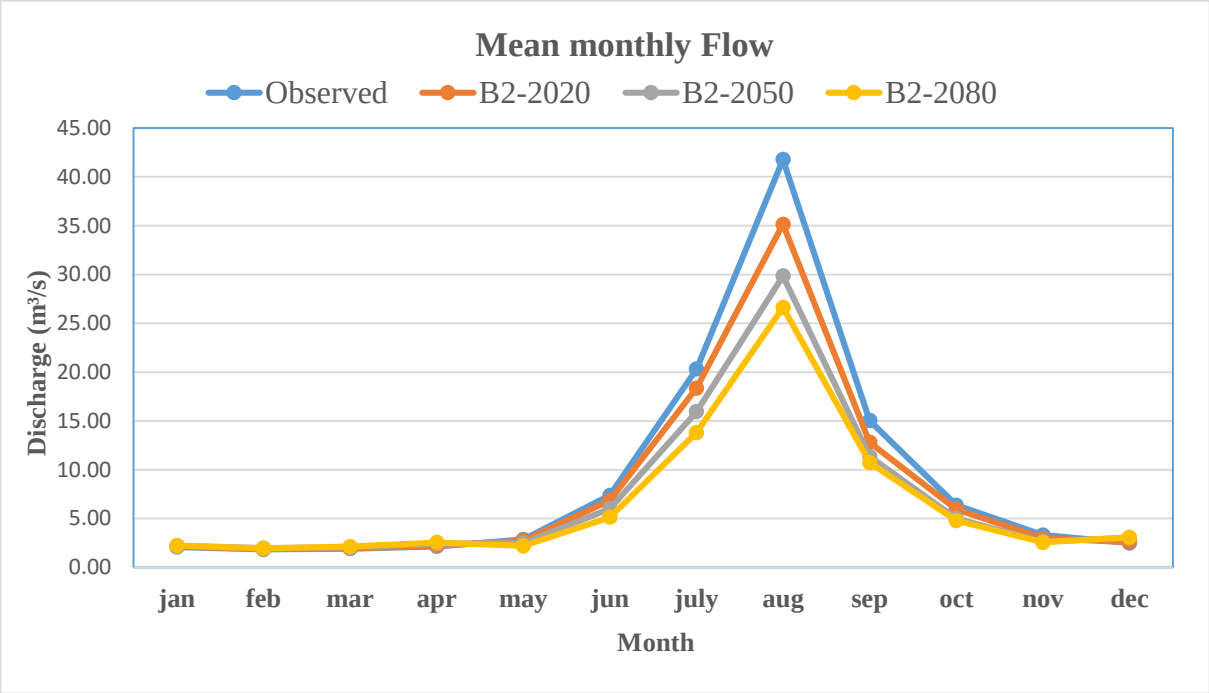

Figure 4-34:- Mean monthly Megech River flow using SWAT model under downscaled GCM-generated HadCM3B2a scenarios compared with observed period.

Both months June and July show declination of mean monthly flow. August the peak flow month for Megech highly reduced and changed to 33.54 m³/s, 27.87 m³/s, 24.81 m³/s and 35.14 m³/s, 29.85 m³/s, 26.62 m³/s for A2a and B2a scenarios of 2020s, 2050s and 2080s. In 2080s the peak flow reduced by half for both scenarios. Lastly, autumn season shows the less temperature change comparing to all seasons. In this season the declination of precipitation is very higher comparing to other for both scenarios. Although the mean monthly flow of Megech declined for autumn seasons from near to far time periods. Based on SWAT result mean monthly flow of Megech highly reduced in mid and end of the century for both HadCM3A2a and B2a scenarios. For Detail please see **Appendix 19**

CHAPTE R FIVE

5 CONCLUSION AND RECOMMENDATION

5.1 CONCLUSION

The climate projection shows that SDSM is significantly good statistical tool to reproduce mean and variance of observed maximum and minimum temperature in Megech watershed. The mean and variance of observed baseline period and SDSM generated HadCM3A2a and HadCM3B2a scenarios values are very close to each other and shows very less absolute model error. Whereas for precipitation, the model shows slight difficulty to fit with mean and variance of the observed data using the adjustment parameters event threshold, bias correction and variance inflation to capture the full range of observed precipitation data.

The SDSM result indicated Megech watershed is vulnerable to climate change. The model indicated that both minimum and maximum temperature shows an increasing trend in all future horizons for HadCM3A2a and HadCM3B2a scenarios. The annual average temperature increased from 0.61 ⁰c to 2.94 ⁰c and 0.52 ⁰c to 2.03 ⁰c for medium-higher emission and medium-lower emission from the near to end of the century. Although annual average minimum temperature increased from 0.97 ⁰c to 3.12 ⁰c and 0.86 ⁰c to 2.53 ⁰c for A2a and B2a scenarios of the same time period. In Megech watershed the average annual minimum temperature highly change in comparing with maximum temperature and both temperatures of all months shows increasing. In addition the medium-higher emission (A2a) scenarios temperature change is higher than medium-lower emission (B2a) scenarios.

Downscaled precipitation of Megech watershed indicates less annual average precipitation change from - 2.03 % to - 7.60 % and - 0.99 % to - 5.96 % from near to end of century for A2a and B2a scenarios. This watershed will face declination of precipitation in two wet seasons (summer & autumn) and increment of precipitation in the rest two dry seasons (winter and spring) for both scenarios of the same time periods.

Trend analysis is important for charcterizing the change behaviour of input parameter (i.e for precipitation, maximum and minimum temperature) for a watershed with respect to time. The time series of observed and future generated SDSM outputs of both scenarios were conducted

using Mann-Kendall statistical test method. Maximum temperature shows statistical significantly increasing trend in observed and future period of SDSM outputs in HadCM3A2a and HadCM3B2a senarios. Minimum temperature trend indicates statistically insignificant trend for observed data that neither indicates increasing and decreasing but SDSM generated output of HadCM3A2a and HadCM3B2a senarios shows statistical significantly increasing trend for all future periods. Statistically insignificant trend not sufficient to conclude it increased or decreased observed in precipitation for baseline observed data and SDSM future generated HadCM3A2a and HadCM3B2a senarios.

The government prepared huge investment plan to develop the water resource of Tana sub-basins (WWDSE, 2008). Megech watershed is under construction of water conveyance and storage structure for hydropower and irrigation developments, increasing population density, expansion of large scale projects and farmers agricultural land by causing land and environmental degradation. This activities will lead the watershed to increase the carbon dioxide (higher emission). The HadCM3A2a scenarios consider higher emission, rapid technological usage and population growth than HadCM3B2a scenarios. By considering the above mentioned ongoing activities and newly future planned projects Megech watershed will have more similar future climatic variability changes (precipitation, maximum and minimum temperature) to HadCM3A2a scenarios emission than that of HadCM3B2a emission scenarios.

Based on the result of commonly applies performance measurements namely coefficient of determination (R^2), Nash-Sutcliffe model efficiency (NSE) and percent of bias (PBIAS), the SWAT model is satisfactory for simulation river discharge in Megech watershed in baseline period (1993-2008). Even though the performance parameter values indicates that the model is good to simulate this watershed. The model under estimates some high flows and over estimates of the base flows. Next calibration SWAT model is applied to simulate future river discharge using result of downscaled future climate prediction of HadCM3A2a and B2a emission scenarios (precipitation, maximum and minimum temperature), soil and land use/land cover data (same land use/land cover of baseline period) to study effect of climate change in future period. Using of the same soil and land cover data of present time for future simulation increase uncertainty on the hydrological model. The soil and land cover data have to update from time

to time to accurately quantify the effect of climate change on the hydrology of Megech watershed for the future time.

The SWAT model result shows declination of flow of Megech due to climate change from near to end of the century. The predicted flow of Megech using SDSM downscaled output shows annual percentile declines in - 5.19 %, - 19.71 %, - 12.57 % and - 4.54 %,- 7.90 %,- 11.06 % for HadCM3A2a and HadCM3B2a scenarios of 2020s, 2050s and 2080s. Thus, the stream flow reduction is large for 2080s than 2050s, large for SRES scenarios A2a than B2a. The main climate features of Megech watershed for 2050s and 2080s future time period are declination of precipitation along with a warmer temperature, both conjunction, may leads to reduction of future flow of Megech. This is mainly due to limited water availability from lower precipitation falling and temperature driven increment of evapotranspiration in future period of Megech watershed.

5.2 RECOMMENDATION

- The SWAT model has its own limitation in evaluating the impact of land use dynamics on stream flow of watershed. The numbers of hydraulic response unit within the watershed vary due to the land use dynamics which latter affect the model outputs because, SWAT model generates runoff for the whole watershed from each HRU through flow. Therefore, to get a better evaluation of land use dynamics impact on stream flow of the watershed the future researchers are recommended to use another hydrological model
- IPCC (2007) prior to this findings, it had been thought that climate models are imperfect but AOGCM provides highly crediable quantitative estimation of future climate change, particularly at continenatal, large scale and have high confidence on temeprature that for precipitation. Because of this climatic model have to be modified to increase the confidenality in estimating of precipitation.
- The study is based on single station, GCM (HadCM3) and two emission scenarios. However, it often recommended to apply different GCMs and emission scenarios so as to make comparison b/n different models as well as to explore a wide range of climate change scenarios that would result in different hydrological impacts. Hence this study can be extended in the future using more than one weather station and GCMs, emission scenarios and hydrological models that considers land use/ land cover changes.
- As Richard Jones *et al.* (2004) point out to investigate regional climate the length of observed year collected from stations have to be at least 10 years to give reasonalbe idea of the mean climate change, if 20 – 30 years available it's better to get statistical significant change in extreme precipitation. This study was conducted by 20 years of meteorological data it better to conduct by 30 years data to get 75% of variance of the true signal as recommended in the report.
- SWAT model is physcal based model, doesn't consider land use/ land cover change and response of soil parameters that influence the soil propertiy of the watershed. This study negelected the changes on land use and soil properity. It was quantifying only the changes caused by climatic variables (tempearture and rainfall) on the hydrology of the Megech watershed. So this study strongly recommended it is better to study the

combined effect of climate change and land use/land cover on the hydrology of the study area.

- The result of this study specifically gives information not only the projectes going on the present time also for policy makers, water resouce management bodies and interseted stakeholders to make effective and economical viable plans for sustainable future development in the Megech watershed.
- This case study indicate there is impact of climate on the stream of the river and water resource utilization in basin shall be planned in due consideration to such fluctuation in stream flow, rainfall and temperature.

6 .REFERENCE

Abouabdillah , Ons O, Anna M and Antonio L. (2010). modeling the impact of climate change in mediterranean catchement. *Fresenius Environmental Bulletin*, 1-14.

Fadil , Hassen R , Abdelhadi K, Youness K and Omar A (2011, september 22). *Hydrologic Modeling of the Bouregreg Watershed (Morocco) Using GIS and SWAT Model.* Hassan II Univertsit, Geosciences Laboratory, Faculty of Sciences-Ain Chock, . Casablanca, Morocco: Hassania School of Public Works.

Agizew. (2010). *Hydrological and Suspended Sediment Modeling in the Lake Tana basin.* university Joseph-Fourier-Grenoble 1. Retrieved from http:// tel.archives-ouvertes.fr/tel-00539152

Anthony & William. (2012). *Global Climate Models and their Limitations.* international panel on climate change (IPCC).

Beven. (1985). *distributed model in hydrological forcasting.* (m. a. burt, Ed.) manchihester, uk.

Beven. (2000). *Distributed models In Hydrological Forecasting.* (M. &. Anderson, Ed.) Chichester, UK.

Charles (1999). Validation of downscaled condition (case study on south western, Australia). *climate research 12*, 1-14.

Cherie. (2013). Downscaling and Modeling the Effects of Climate Change on Hydrology and Water Resources in the Upper Blue Nile River Basin, Ethiopia. Germany: Department of Civil Engineering,University of Kassel .

Chow. (1964). *Hand Book Of Applied Hydrology.* Ny, USA: MC Grew-Hill Book Company

Daniel , Janey V,Camp, Eugene J. LeBoeuf, Jessica R. Penrod, James P. Dobbins. (2011). "Watershed modeling and its applications: A state-of-the-art review," . *The Open journal vol. 5*, 26--50.

David B , Curt C , William G, Issac H, Kenneth K, Ronald M, Robin T and Minghua Z. (2008). Climate Models: An Assessment of Strengths and Limitations. Retrieved from http://digitalcommons.unl.edu/usdoepub

David G. Groves, D Yates and C Tebaldi (2008). developing and applying uncertain global climate change projections for regional water managemnet planning. *water resource reserch*, 2.

Robert L. Wilby and Christian W. Dawson. (2007). *SDSM 4.2- A decision support tool for assessment of rgional climate change impact user manual.* UK: science Department, Enviromental Agency of England and wales.

Elshamy, M . E., I . A. Seierstad, Sorteberg .(2009). impact of climate change on the Blue Nile flow using bias corrected GCM senarios. *Hydrology earth system, 13*, 551-565.

Emelie (2013). ethiopian enviromental and climate chanage police brief. In A. Ebom, *ethiopian enviromental and climate chanage police* (pp. 1- 6). USA: Goteborge University .

Gebresenbet. (2015 , April 15). Modeling of Cascade Dams and Reservoirs Operation for Optimal Water Use:Application to Omo Gibe River Basin, Ethiopia. Kassel, Germany: Faculty of Civil & Environmental Engineering of the University of Kassel.

Getnet. (2009, September). Modelling the Flows of the White Nile BasinWhite Nile Basin uuuusing SWAT. *INTERUNIVERSITY PROGRAM E IN WATER RESOURCES ENGINERING*.

Gupta, H . V ., S . Sorooshian, P. O. Yapo (1999). *Status of automatic calibration for hydrologic models: Comparison with multi-level expert calibration* (Vols. Journal of Hydrologic Engineering,).

Helsel and Hirsch. (2002). *statistical method in water resource.* book 4, chapter A3: U.S. Gelogical survey techniques of water resource investigiation.

Hubbard . (1994). Spatail varability of daily weather variables in the high plains of the USA. In *Agric forest metero.*

IPCC. (2000). *Ipcc Special Report Emissions scenarios.* (O. D. Nebojs˘a Nakic´enovic´, Ed.) Intergovernmental Panel on Climate Change.

IPCC. (2013). *Climate Change 20013:The Scientific Basis.* United Kingdom: Cambridge University press.

IPCC. (2013). *Climate Change 20013:The Scientific Basis. The Physical Science Basis; Contribution of Working Group I to the Fifth Assessment Report of the* Intergovernmental Panel on Climate Change; United Kingdom: Cambridge University press

IPCC. (2007). *An Assesement of the intergovernmental pannel on climate change.* spain: Intergovernmental panal on climate change(IPCC).

International Water Management Insititute. (2009). *Flexible Water Storage Option and Adaptation to Climate Change.* Ethiopia: international water management institute.

Karmeshu. (2012). *rend Detection in Annual Temperature & Precipitation using the Mann Kendall Test – A Case Study to Assess Climate Change on Select States in the Northeastern United States.* University of Pennsylvania , Department of Earth & Environmental Science,.

Kumar (2006, February 10). Specail Section Climate Change. *High-resolution Climate Change Scenarios for the 21st century*. India: India Insitute of Tropical Metrology.

Cunderlik. (2003). *Hydrologic Model Selection For CFCAS Project: Assesment of water Resource Risk and Vulnerability to changing climate condition.* CFCAS Project team.

Merid, F. (2002). *National Nile Basin Water Quality Monitoring Baseline Report for Ethiopia.* addis ababa: Nile Basine Initiative (Transboundary Envromental action Project).

Moriasi, D. N., J. G. Arnold, M. W. Van Liew, R. L. Bingner, R. D. Harmel, T. L. Veith (2007). *Model evaluation guidelines for systematic Quantification of accuracy in watershed simulations* (Vol. 50(3)). Transaction of ASABE.

Nash, J Ea and Sutcliffe, JV. (1970). *River flow forecasting through conceptual models, Part I - A* (Vol. Journal of hydrology).

Neitsch, S. L, J. G. Arnold, J. R. Kiniry, J. R. Williams . (2000). *soil and water Assesment tool user manual* . TEXAS : GRASSLAND, SOIL AND WATER RESEARCH LABORATORY ○ AGRICULTURAL RESEARCH SERVICE .

Karl, T. (2009). *Global climate change impact in the united state.* New York, U.S.A: Cambridege University Press.

Richard Jones, D. A., R. A. Wood, S. Bony (2004). *Generating High Resolution Climate Change Scenarios Using precis.* (R. Taylor, Ed.) Hadley Centre for Climate Prediction and Research, UK: Met Office Hadley Centre.

Sahin, S. (2010). *Homogeneity analysis of Turkish meteorological data set.* Istanbul, Turkey: Wiley InterScience. doi:DOI: 10.1002/hyp.7534

Shimelis G, David R, Assefa M. Melesse, Bijan D (2011). climate chanage impact on agricultural water resouce availabilty in the north highland of ethiopia. *chapter 12*. Miami, USA: Florida International University.

Simon N. Gosling, Rachell W, Nigel W. Arnell, Peter G, Jhon C, Dan B, Jason A. lowe, Paul V, Jesse R and Stephen M (2011). A review of recent developments in climate change science. Part II: The global-scale impacts of climate change. *Progress in Physical Geography*, 6.

Steffen. (2004). Global Change and Earth System; A Planet Under Pressure. In P. D. A. Sanderson, *A Planet Under Pressure* (pp. 11-14). Stocholm: Sewden.

Carter, M . L. Parry, H . Harasawa, S . Nishioka (1994). IPCC technical guidelines for assessing climatic change impact and adaptation. *center for Global enviromental reserch*, 8-9.

Carter, M. Hulmeand and M. Lal (1999). *Guideline on the use of scenario data for Climate Impact and Adaptation Assessment.* helsink: Task Group on Scenarios for Climate Impact Assement Intergovernmental Panal on Climate Change.

Tazebe beyene, Dennis P . Lettenmaier and Pavel K (2009). *Hydrologic Impact of Climate Change on Nile River Basin: Implications of the 2007 IPCC Climate scenarios.* seattle: department of civil and enivromental enginerring ,University of Washington.

Tronci N ,Molteni F, Bozzini M (1986). A Comparison of Local approximation on method for the analysis of metrological data . In *Archives for Meterology, Biophysics and Bioclimatology series B vol 36.*

UNEP. (1998). *Handbook on Methods for Climate Change Impact Assessment and Adaptation Strategies.* (I. B. Jan F. Feenstra, Ed.) Amsterdam, Netherland: United Nations Environment Programme.

Water Works Design & Supervision Enterprise (WWDSE), (2007) "Megech Dam feasibility Design Report, Addis Abeba, Ethiopia.

Water Works Design & Supervision Enterprise (WWDSE) in association, (2008). Hydrology of Megech Dam, Final Design Report.Addis Abeba, Ethiopia.

White, Kati L and Chaubey, Indrajeet (2005). *Kati L and Chaubey, Indrajeet, "Sensitivity analysis, calibration, and validations for a multisite and multivariable swat mode.*

Wilby & Dawson. (2000). *sdsm — a decision support tool for the assessment of regional climate change impacts.* Saskatchewan, Canada : Canadian Climate Impacts Scenarios (CCIS) Project, c/o Environment Canada — Prairie and Northern Region.

Wilby & Dawson. (2002). *A decision support for the assesment of region climate change impacts* . saskatchewan,canada: candian climate impacts scenrios(CCIS) project.

Wilby R. L., Christian W. Dawson (2004). *Guidelines for using of climate scenarios developed for Stastical Downscaling Model* . UK: task group on data and scenarios for impact and climate analysis (TGICA) .

Wilby & Dawson. (2007). *Statistical Downsacling Model(SDSM 4.2) a decision support tool for the assesment of regional climate chnage impacts , user manual.* loughbourough university: Department of computer science,oughbourough university ,uk.

Wilby R.L &. Wigley, T.M.L (2000). *SDSM- A decision support tool for assessement of regional climate change impacts.* albert street, saskatchewan: candian climate impact senarios(CCIS) project.

APPENDIX

Appendix 1: Long term Monthly Maximum temperature in and around Megech watershed (1993 -2013)

	Gonder	Ambagiorgis	Gorgora	Maksegnit	Aykel	mean
Jan	28.14777266	19.31290323	29.69646697	28.8235023	25.03133641	26.20239631
Feb	29.81231029	20.2762226	31.13153457	30.4010118	26.78701518	27.68161889
Mar	30.26866359	21.24546851	31.59831029	31.16159754	27.43333333	28.34147465
Apr	30.39444444	21.4768254	32.14984127	31.2368254	27.63460317	28.57850794
May	29.2499232	20.73102919	31.54669739	30.16420891	25.77296467	27.49296467
Jun	25.82603175	18.99666667	28.60746032	27.07555556	22.53492063	24.60812698
July	23.19416283	17.03963134	26.20921659	24.37895545	20.1577573	22.1959447
Aug	23.32242704	17.206298	25.71075269	24.54577573	20.24731183	22.20651306
Sep	25.37190476	18.55190476	27.2468254	26.7315873	21.79793651	23.94003175
Oct	26.73732719	18.43195084	28.24454685	28.15115207	22.80875576	24.87474654
Nov	27.5147619	18.37444444	29.09206349	28.1431746	24.0831746	25.44152381
Dec	27.70261137	18.61228879	29.39923195	27.9952381	24.4390169	25.62967742
Annul	27.27636245	19.1779661	29.20435463	28.21697523	24.0405867	25.58324902

Appendix 2: Long term Monthly Minimum temperature in and around Megech watershed (1993 -2013)

	Gonder	Ambagiorgis	Gorgora	Maksegnit	Aykel	mean
Jan	11.4115	6.9522	12.0766513	10.93087558	2.599231951	8.794101382
Feb	12.8949409	8.194097808	13.09595278	12.98634064	8.354637437	11.10519393
Mar	13.9903225	8.791551459	13.34254992	14.6390169	8.851612903	11.92301075
Apr	15.0001587	9.495555556	14.15269841	15.6468254	9.681904762	12.79542857
May	14.6927803	9.646236559	13.80875576	15.29892473	3.511981567	11.39173579
Jun	13.6965079	9.359365079	13.0947619	14.4847619	4.676825397	11.06244444
July	13.0717357	8.755145929	13.79508449	14.23978495	6.811520737	11.33465438
Aug	13.0279569	8.66344086	13.39201229	14.08156682	6.810752688	11.19514593
Sep	12.4495238	8.627777778	13.54111111	13.55206349	7.254444444	11.08498413
Oct	12.0818740	7.967127496	13.19139785	12.81474654	7.557603687	10.72254992
Nov	11.7801587	6.670793651	12.28666667	12.14507937	4.582857143	9.493111111
Dec	11.4158218	5.91797235	11.95729647	11.10199693	1.711674347	8.420952381
annual	12.9569491	8.250769231	13.1435854	13.49225554	6.010560626	10.77082399

Appendix 3: Long term Mean Monthly Rainfall in and around Megech watershed (1993 - 2013)

	Gonder	Ambagiorgis	Gorgora	Maksegnit	Aykel	Makesnit
Jan	3.4	2.8	0.9	4.9	0.0	2.2
Feb	2.5	3.4	3.1	1.4	0.9	1.0
Mar	14.4	16.2	15.1	11.7	13.3	16.2
Apr	49.6	36.3	45.5	31.3	28.1	32.7
May	164.8	88.8	57.9	62.4	89.3	68.6
Jun	256.3	157.5	130.2	185.2	193.1	153.1
July	372.8	289.0	314.4	254.6	303.6	321.5
Aug	348.1	271.5	274.3	249.2	254.5	318.1
Sep	218.8	115.9	60.9	129.1	139.3	98.8
Oct	140.0	71.1	42.7	71.6	80.6	46.7
Nov	23.2	19.3	18.9	14.5	16.2	23.0
Dec	4.7	8.3	4.6	3.6	2.8	4.8
annul	3.4	2.8	0.9	4.9	0.0	2.2

Appendix 4: Measured Mean Monthly Stream flow (m^3/s) at Megech Near Azezo gauging station (1993 – 2008)

	jan	feb	mar	apr	may	jun	jul	aug	sep	oct	nov	dec
1993	0.31	0.25	0.25	0.29	0.80	3.44	8.92	24.22	13.86	4.40	1.24	0.30
1994	0.32	0.15	0.09	0.09	0.39	2.53	11.71	39.96	12.52	1.53	0.88	0.47
1995	0.25	0.17	0.16	0.15	0.93	3.50	12.02	43.84	6.57	0.47	0.16	0.09
1996	0.03	0.01	0.01	0.19	1.49	11.53	15.27	33.23	7.82	2.06	0.99	0.48
1997	0.30	0.20	0.19	0.19	1.08	6.01	22.80	19.33	4.30	2.88	1.59	0.51
1998	0.21	0.17	0.22	0.20	0.38	2.16	24.88	**49.87**	16.02	5.78	1.11	2.04
1999	1.77	1.45	1.39	1.50	3.03	2.85	11.99	35.81	18.19	10.79	6.17	4.63
2000	3.80	2.68	2.83	4.01	3.79	5.20	12.71	26.66	12.41	8.79	4.66	3.65
2001	3.09	3.25	4.45	4.55	5.51	2.58	22.06	43.07	9.56	2.74	1.46	0.56
2002	0.37	0.22	0.22	0.14	0.28	1.31	17.91	18.92	7.32	2.66	2.09	1.66
2003	1.32	1.31	1.25	1.12	1.08	6.50	16.76	38.88	11.78	4.84	2.84	2.35
2004	1.59	1.52	1.41	2.09	1.42	4.03	20.81	33.92	9.10	6.05	3.66	2.96
2005	2.54	2.34	2.76	2.39	2.44	16.10	14.57	32.81	18.83	8.00	5.01	3.63
2006	3.12	2.93	2.81	2.86	4.24	2.18	23.81	58.73	24.04	10.51	7.06	5.31
2007	4.51	4.27	4.05	4.62	5.13	**12.39**	34.51	75.40	32.63	11.09	8.12	6.41
2008	6.34	5.34	5.10	6.10	9.16	26.94	34.17	74.44	31.88	12.37	**4.07**	**3.06**

NB: Bold is missed values and filled

Appendix 5: Corrected mean flow of Megech river flow due to construction of Megech Dam (inflow of Megech dam)

	Jan	feb	mar	apr	may	jun	jul	aug	Sep	Oct	nov	dec
1993	0.28	0.23	0.23	0.27	0.74	3.16	8.19	22.24	12.72	4.03	1.13	0.28
1994	0.30	0.14	0.09	0.08	0.35	2.32	10.75	36.68	11.49	1.41	0.81	0.43
1995	0.23	0.16	0.14	0.13	0.85	3.21	11.03	40.25	6.03	0.43	0.14	0.08
1996	0.03	0.01	0.01	0.18	1.37	10.58	14.01	30.51	7.18	1.89	0.90	0.44
1997	0.27	0.18	0.18	0.18	0.99	5.52	20.93	17.75	3.94	2.65	1.46	0.47
1998	0.19	0.15	0.20	0.18	0.35	1.99	22.84	**45.78**	14.71	5.30	1.02	1.87
1999	1.63	1.33	1.27	1.38	2.78	2.62	11.01	32.87	16.70	9.91	5.66	4.25
2000	3.48	2.46	2.60	3.68	3.48	4.77	11.66	24.48	11.39	8.07	4.28	3.35
2001	2.84	2.98	4.08	4.17	5.06	2.37	20.25	39.53	8.78	2.51	1.34	0.51
2002	0.34	0.20	0.20	0.13	0.26	1.20	16.44	17.37	6.72	2.44	1.92	1.52
2003	1.21	1.20	1.15	1.03	0.99	5.96	15.39	35.69	10.82	4.45	2.61	2.16
2004	1.46	1.39	1.29	1.92	1.31	3.70	19.11	31.14	8.35	5.55	3.36	2.72
2005	2.33	2.15	2.53	2.19	2.24	14.78	13.38	30.12	17.29	7.34	4.60	3.33
2006	2.87	2.69	2.58	2.62	3.89	2.00	21.86	53.91	22.07	9.64	6.48	4.88
2007	4.14	3.92	3.72	4.24	4.71	**11.38**	31.68	69.22	29.96	10.18	7.45	5.88
2008	5.82	4.90	4.68	5.60	8.41	24.73	31.37	68.33	29.27	11.35	**3.73**	**2.81**

NB: Bold is missed values and filled

Appendix 8: Mean Monthly increment of Maximum Temperature from the observed period (1993-2013) in 2020(2011 – 2040) and 2050(2041 – 2070) and 2080(2071 – 2099) for A2a emission scenarios

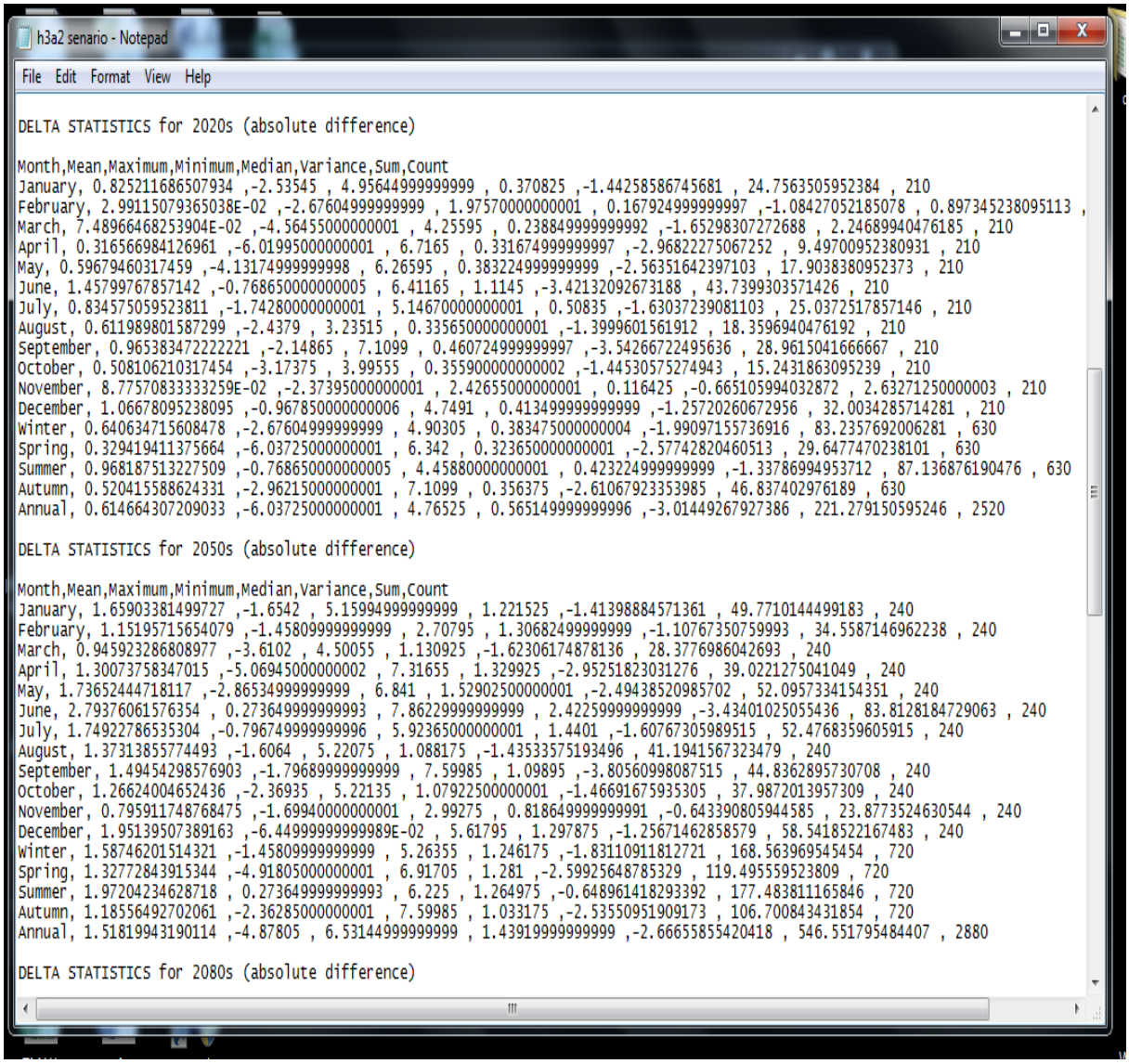

h3a2 senario - Notepad

File Edit Format View Help

DELTA STATISTICS for 2020s (absolute difference)

Month,Mean,Maximum,Minimum,Median,Variance,Sum,Count
January, 0.825211686507934 ,-2.53545 , 4.95644999999999 , 0.370825 ,-1.44258586745681 , 24.7563505952384 , 210
February, 2.99115079365038E-02 ,-2.67604999999999 , 1.97570000000001 , 0.167924999999997 ,-1.08427052185078 , 0.897345238095113 ,
March, 7.48966468253904E-02 ,-4.56455000000001 , 4.25595 , 0.238849999999992 ,-1.65298307272688 , 2.24689940476185 , 210
April, 0.316566984126961 ,-6.01995000000001 , 6.7165 , 0.331674999999997 ,-2.96822275067252 , 9.49700952380931 , 210
May, 0.59679460317459 ,-4.13174999999998 , 6.26595 , 0.383224999999999 ,-2.56351642397103 , 17.9038380952373 , 210
June, 1.45799767857142 ,-0.768650000000005 , 6.41165 , 1.1145 ,-3.42132092673188 , 43.7399303571426 , 210
July, 0.834575059523811 ,-1.74280000000001 , 5.14670000000001 , 0.50835 ,-1.63037239081103 , 25.0372517857146 , 210
August, 0.611989801587299 ,-2.4379 , 3.23515 , 0.335650000000001 ,-1.3999601561912 , 18.3596940476192 , 210
September, 0.965383472222221 ,-2.14865 , 7.1099 , 0.460724999999997 ,-3.54266722495636 , 28.9615041666667 , 210
October, 0.508106210317454 ,-3.17375 , 3.99555 , 0.355900000000002 ,-1.44530575274943 , 15.2431863095239 , 210
November, 8.77570833333259E-02 ,-2.37395000000001 , 2.42655000000001 , 0.116425 ,-0.665105994032872 , 2.63271250000003 , 210
December, 1.06678095238095 ,-0.967850000000006 , 4.7491 , 0.413499999999999 ,-1.25720260672956 , 32.0034285714281 , 210
Winter, 0.640634715608478 ,-2.67604999999999 , 4.90305 , 0.383475000000004 ,-1.99097155736916 , 83.2357692006281 , 630
Spring, 0.329419411375664 ,-6.03725000000001 , 6.342 , 0.323650000000001 ,-2.57742820460513 , 29.6477470238101 , 630
Summer, 0.968187513227509 ,-0.768650000000005 , 4.45880000000001 , 0.423224999999999 ,-1.33786994953712 , 87.136876190476 , 630
Autumn, 0.520415588624331 ,-2.96215000000001 , 7.1099 , 0.356375 ,-2.61067923353985 , 46.837402976189 , 630
Annual, 0.614664307209033 ,-6.03725000000001 , 4.76525 , 0.565149999999996 ,-3.01449267927386 , 221.279150595246 , 2520

DELTA STATISTICS for 2050s (absolute difference)

Month,Mean,Maximum,Minimum,Median,Variance,Sum,Count
January, 1.65903381499727 ,-1.6542 , 5.15994999999999 , 1.221525 ,-1.41398884571361 , 49.7710144499183 , 240
February, 1.15195715654079 ,-1.45809999999999 , 2.70795 , 1.30682499999999 ,-1.10767350759993 , 34.5587146962238 , 240
March, 0.945923286808977 ,-3.6102 , 4.50055 , 1.130925 ,-1.62306174878136 , 28.3776986042693 , 240
April, 1.30073758347015 ,-5.06945000000002 , 7.31655 , 1.329925 ,-2.95251823031276 , 39.0221275041049 , 240
May, 1.73652444718117 ,-2.86534999999999 , 6.841 , 1.52902500000001 ,-2.49438520985702 , 52.0957334154351 , 240
June, 2.79376061576354 , 0.273649999999993 , 7.86229999999999 , 2.42259999999999 ,-3.43401025055436 , 83.8128184729063 , 240
July, 1.74922786535304 ,-0.796749999999996 , 5.92365000000001 , 1.4401 ,-1.60767305989515 , 52.4768359605915 , 240
August, 1.37313855774493 ,-1.6064 , 5.22075 , 1.088175 ,-1.43533575193496 , 41.1941567323479 , 240
September, 1.49454298576903 ,-1.79689999999999 , 7.59985 , 1.09895 ,-3.80560998087515 , 44.8362895730708 , 240
October, 1.26624004652436 ,-2.36935 , 5.22135 , 1.07922500000001 ,-1.46691675935305 , 37.9872013957309 , 240
November, 0.795911748768475 ,-1.69940000000001 , 2.99275 , 0.818649999999991 ,-0.643390805944585 , 23.8773524630544 , 240
December, 1.95139507389163 ,-6.449999999999989E-02 , 5.61795 , 1.297875 ,-1.25671462858579 , 58.5418522167483 , 240
Winter, 1.58746201514321 ,-1.45809999999999 , 5.26355 , 1.246175 ,-1.83110911812721 , 168.563969545454 , 720
Spring, 1.32772843915344 ,-4.91805000000001 , 6.91705 , 1.281 ,-2.59925648785329 , 119.495559523809 , 720
Summer, 1.97204234628718 , 0.273649999999993 , 6.225 , 1.264975 ,-0.648961418293392 , 177.483811165846 , 720
Autumn, 1.18556492702061 ,-2.36285000000001 , 7.59985 , 1.033175 ,-2.53550951909173 , 106.700843431854 , 720
Annual, 1.51819943190114 ,-4.87805 , 6.53144999999999 , 1.43919999999999 ,-2.66655855420418 , 546.551795484407 , 2880

DELTA STATISTICS for 2080s (absolute difference)

Appendix 9: Mean Monthly increment of Maximum Temperature from the observed period (1993-2013) in 2020(2011 – 2040) and 2050(2041 – 2070) and 2080(2071 – 2099) for B2a emission scenarios

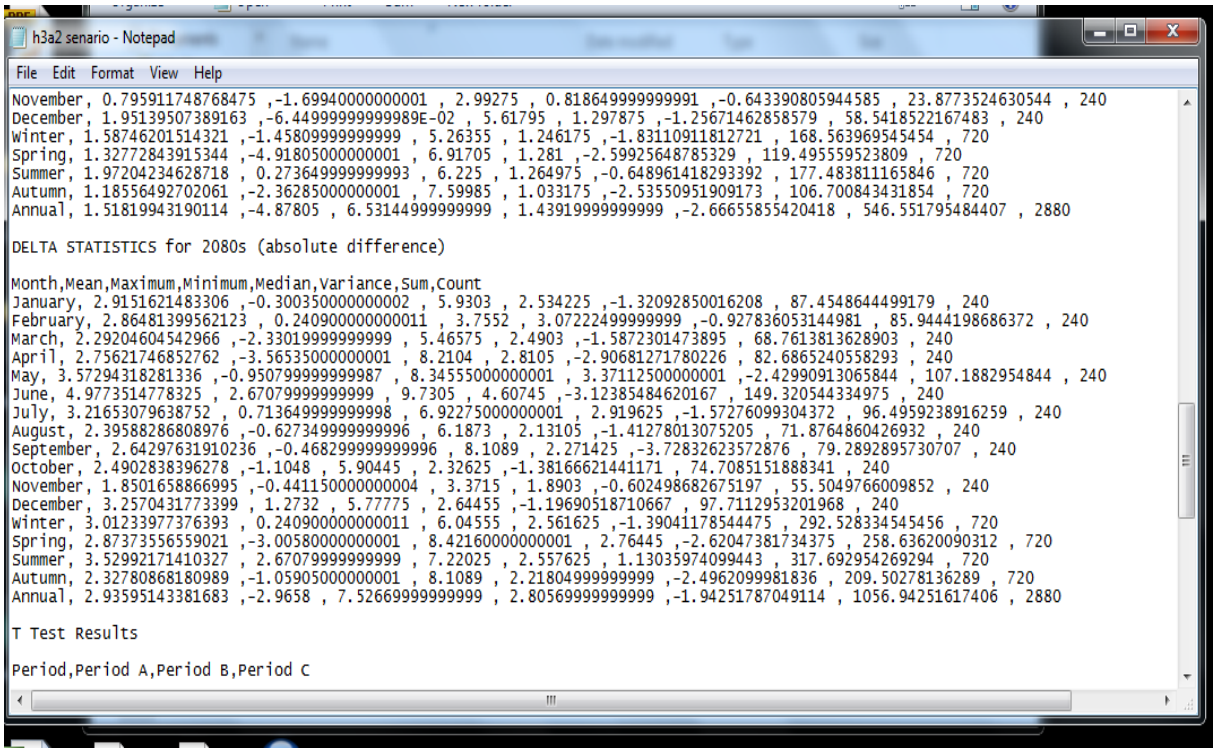

h3a2 senario - Notepad

File Edit Format View Help

```
November, 0.795911748768475 ,-1.69940000000001 , 2.99275 , 0.818649999999991 ,-0.643390805944585 , 23.8773524630544 , 240
December, 1.95139507389163 ,-6.449999999999989E-02 , 5.61795 , 1.297875 ,-1.25671462858579 , 58.5418522167483 , 240
Winter, 1.58746201514321 ,-1.45809999999999 , 5.26355 , 1.246175 ,-1.83110911812721 , 168.563969545454 , 720
Spring, 1.32772843915344 ,-4.91805000000001 , 6.91705 , 1.281 ,-2.59925648785329 , 119.495559523809 , 720
Summer, 1.97204234628718 , 0.273649999999993 , 6.225 , 1.264975 ,-0.648961418293392 , 177.483811165846 , 720
Autumn, 1.18556492702061 ,-2.36285000000001 , 7.59985 , 1.033175 ,-2.53550951909173 , 106.700843431854 , 720
Annual, 1.51819943190114 ,-4.87805 , 6.53144999999999 , 1.43919999999999 ,-2.66655855420418 , 546.551795484407 , 2880

DELTA STATISTICS for 2080s (absolute difference)

Month,Mean,Maximum,Minimum,Median,Variance,Sum,Count
January, 2.9151621483306 ,-0.300350000000002 , 5.9303 , 2.534225 ,-1.32092850016208 , 87.4548644499179 , 240
February, 2.86481399562123 , 0.240900000000011 , 3.7552 , 3.07222499999999 ,-0.927836053144981 , 85.9444198686372 , 240
March, 2.29204604542966 ,-2.33019999999999 , 5.46575 , 2.4903 ,-1.5872301473895 , 68.7613813628903 , 240
April, 2.75621746852762 ,-3.56535000000001 , 8.2104 , 2.8105 ,-2.90681271780226 , 82.6865240558293 , 240
May, 3.57294318281336 ,-0.950799999999987 , 8.34555000000001 , 3.37112500000001 ,-2.42990913065844 , 107.1882954844 , 240
June, 4.9773514778325 , 2.67079999999999 , 9.7305 , 4.60745 ,-3.12385484620167 , 149.320544334975 , 240
July, 3.21653079638752 , 0.713649999999998 , 6.92275000000001 , 2.919625 ,-1.57276099304372 , 96.4959238916259 , 240
August, 2.39588286808976 ,-0.627349999999996 , 6.1873 , 2.13105 ,-1.41278013075205 , 71.8764860426932 , 240
September, 2.64297631910236 ,-0.468299999999996 , 8.1089 , 2.271425 ,-3.72832623572876 , 79.2892895730707 , 240
October, 2.4902838396278 ,-1.1048 , 5.90445 , 2.32625 ,-1.38166621441171 , 74.7085151888341 , 240
November, 1.8501658866995 ,-0.441150000000004 , 3.3715 , 1.8903 ,-0.602498682675197 , 55.5049766009852 , 240
December, 3.25704317733399 , 1.2732 , 5.77775 , 2.64455 ,-1.19690518710667 , 97.7112953201968 , 240
Winter, 3.01233977376393 , 0.240900000000011 , 6.04555 , 2.561625 ,-1.39041178544475 , 292.528334545456 , 720
Spring, 2.87373556559021 ,-3.00580000000001 , 8.42160000000001 , 2.76445 ,-2.62047381734375 , 258.63620090312 , 720
Summer, 3.52992171410327 , 2.67079999999999 , 7.22025 , 2.557625 , 1.13035974099443 , 317.692954269294 , 720
Autumn, 2.32780868180989 ,-1.05905000000001 , 8.1089 , 2.21804999999999 ,-2.4962099981836 , 209.50278136289 , 720
Annual, 2.93595143381683 ,-2.9658 , 7.52669999999999 , 2.80569999999999 ,-1.94251787049114 , 1056.94251617406 , 2880

T Test Results

Period,Period A,Period B,Period C
```

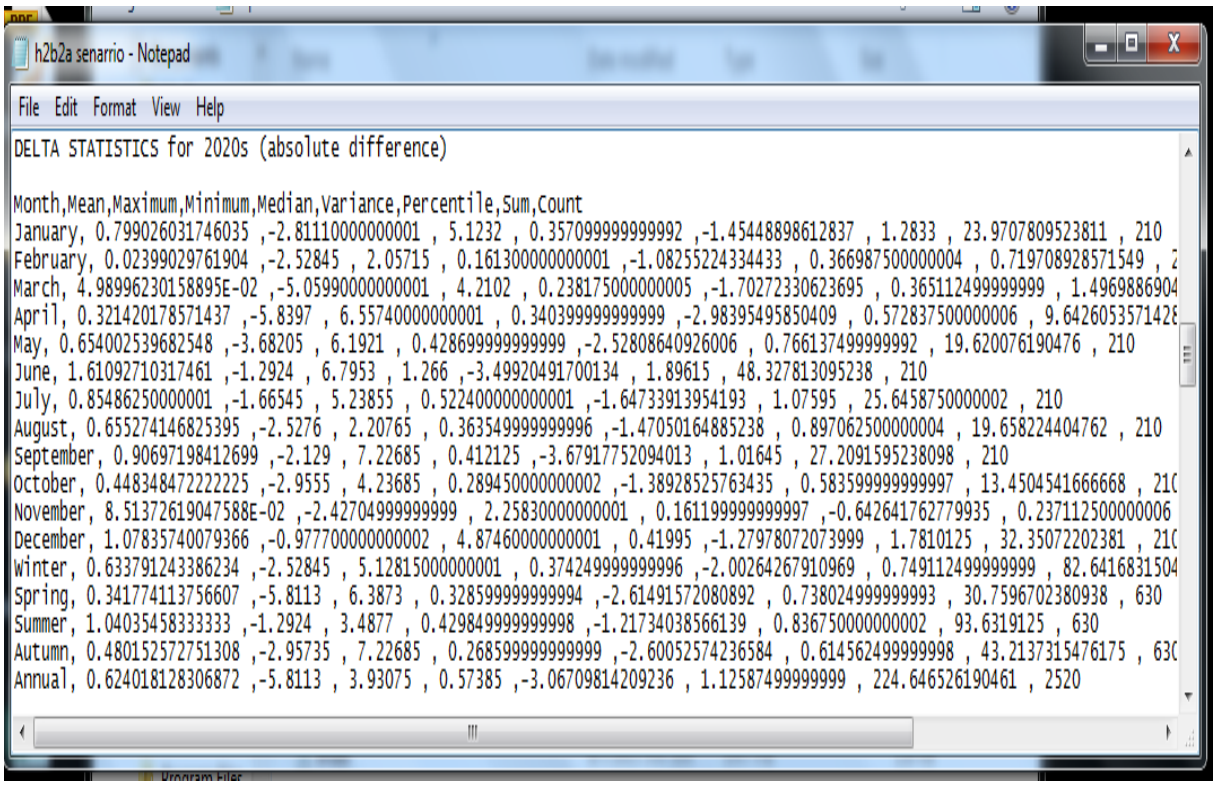

h2b2a senarrio - Notepad

File Edit Format View Help

```
DELTA STATISTICS for 2020s (absolute difference)

Month,Mean,Maximum,Minimum,Median,Variance,Percentile,Sum,Count
January, 0.799026031746035 ,-2.81110000000001 , 5.1232 , 0.357099999999992 ,-1.45448898612837 , 1.2833 , 23.9707809523811 , 210
February, 0.02399029761904 ,-2.52845 , 2.05715 , 0.161300000000001 ,-1.08255224334433 , 0.366987500000004 , 0.719708928571549 , 2
March, 4.98996230158895E-02 ,-5.05990000000001 , 4.2102 , 0.238175000000005 ,-1.70272330623695 , 0.365112499999999 , 1.4969886904
April, 0.321420178571437 ,-5.8397 , 6.55740000000001 , 0.340399999999999 ,-2.98395495850409 , 0.572837500000006 , 9.6426053571428
May, 0.654002539682548 ,-3.68205 , 6.1921 , 0.428699999999999 ,-2.52808640926006 , 0.766137499999992 , 19.620076190476 , 210
June, 1.61092710317461 ,-1.2924 , 6.7953 , 1.266 ,-3.49920491700134 , 1.89615 , 48.327813095238 , 210
July, 0.85486250000001 ,-1.66545 , 5.23855 , 0.522400000000001 ,-1.64733913954193 , 1.07595 , 25.6458750000002 , 210
August, 0.655274146825395 ,-2.5276 , 2.20765 , 0.363549999999996 ,-1.47050164885238 , 0.897062500000004 , 19.658224404762 , 210
September, 0.90697198412699 ,-2.129 , 7.22685 , 0.412125 ,-3.67917752094013 , 1.01645 , 27.2091595238098 , 210
October, 0.448348472222225 ,-2.9555 , 4.23685 , 0.289450000000002 ,-1.38928525763435 , 0.583599999999997 , 13.4504541666668 , 210
November, 8.51372619047588E-02 ,-2.42704999999999 , 2.25830000000001 , 0.161199999999997 ,-0.642641762779935 , 0.237112500000006
December, 1.07835740079366 ,-0.977700000000002 , 4.87460000000001 , 0.41995 ,-1.27978072073999 , 1.7810125 , 32.35072202381 , 210
Winter, 0.633791243386234 ,-2.52845 , 5.12815000000001 , 0.374249999999996 ,-2.00264267910969 , 0.749112499999999 , 82.6416831504
Spring, 0.341774113756607 ,-5.8113 , 6.3873 , 0.328599999999994 ,-2.61491572080892 , 0.738024999999993 , 30.7596702380938 , 630
Summer, 1.04035458333333 ,-1.2924 , 3.4877 , 0.429849999999998 ,-1.21734038566139 , 0.836750000000002 , 93.6319125 , 630
Autumn, 0.480152572751308 ,-2.95735 , 7.22685 , 0.268599999999999 ,-2.60052574236584 , 0.614562499999998 , 43.2137315476175 , 630
Annual, 0.624018128306872 ,-5.8113 , 3.93075 , 0.57385 ,-3.06709814209236 , 1.12587499999999 , 224.646526190461 , 2520
```

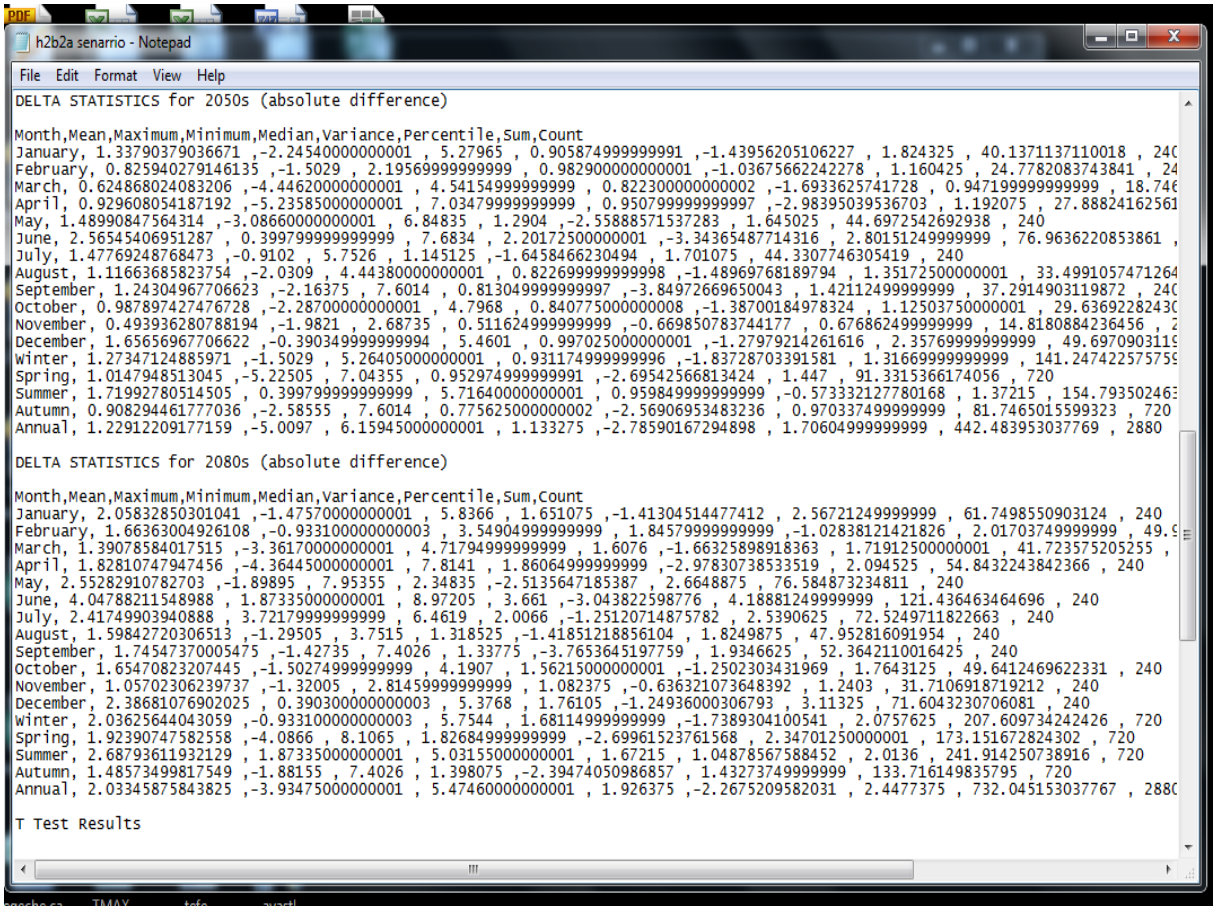

Appendix 10: Mean Monthly increment of Minimum Temperature from the observed period (1993-2013) in 2020(2011 – 2040) and 2050(2041 – 2070) and 2080(2071 – 2099) for A2a emission scenarios

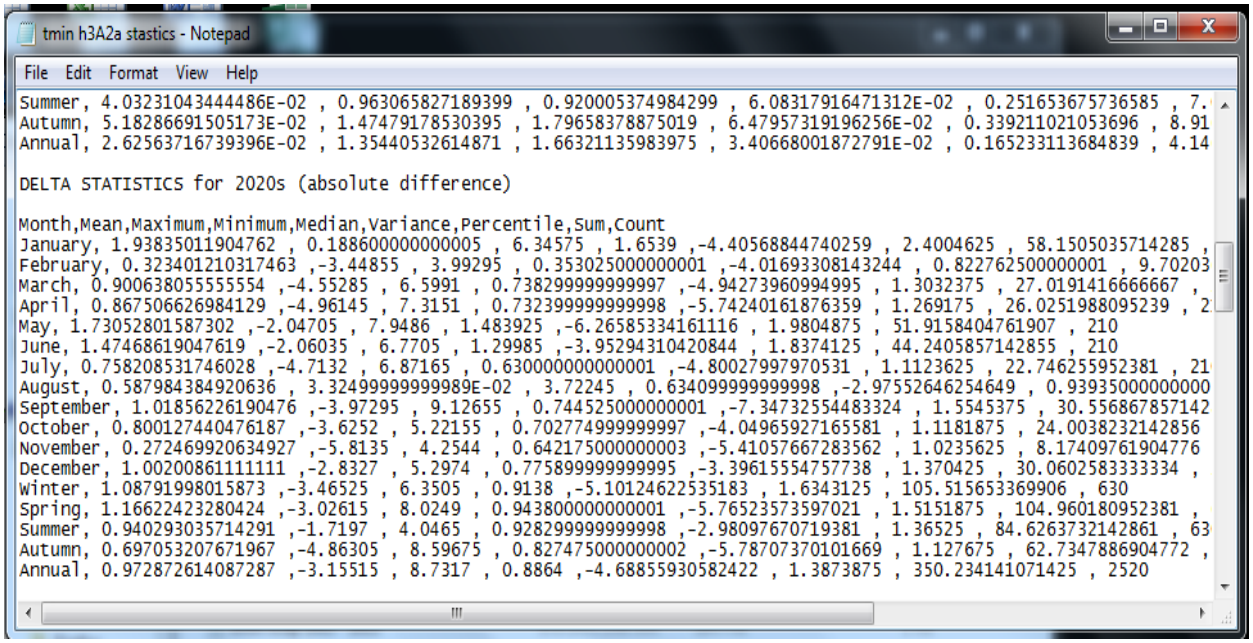

Appendix 11: Mean Monthly increment of Minimum Temperature from the observed period (1993-2013) in 2020(2011 – 2040) and 2050(2041 – 2070) and 2080(2071 – 2099) for HadCM3B2a emission scenarios

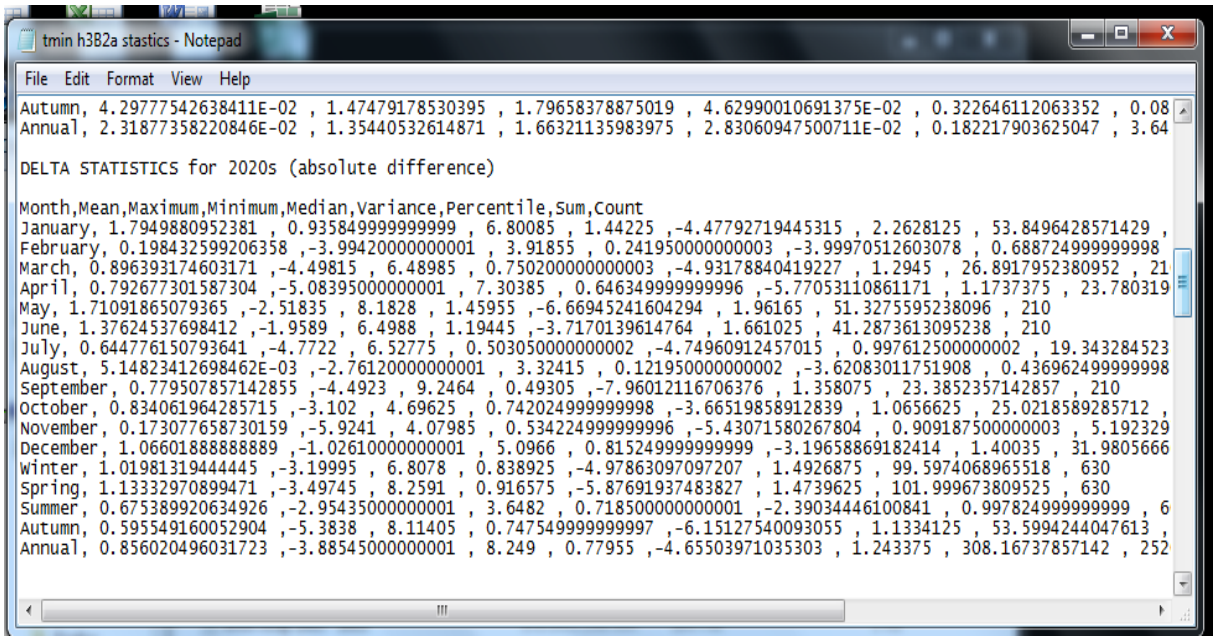

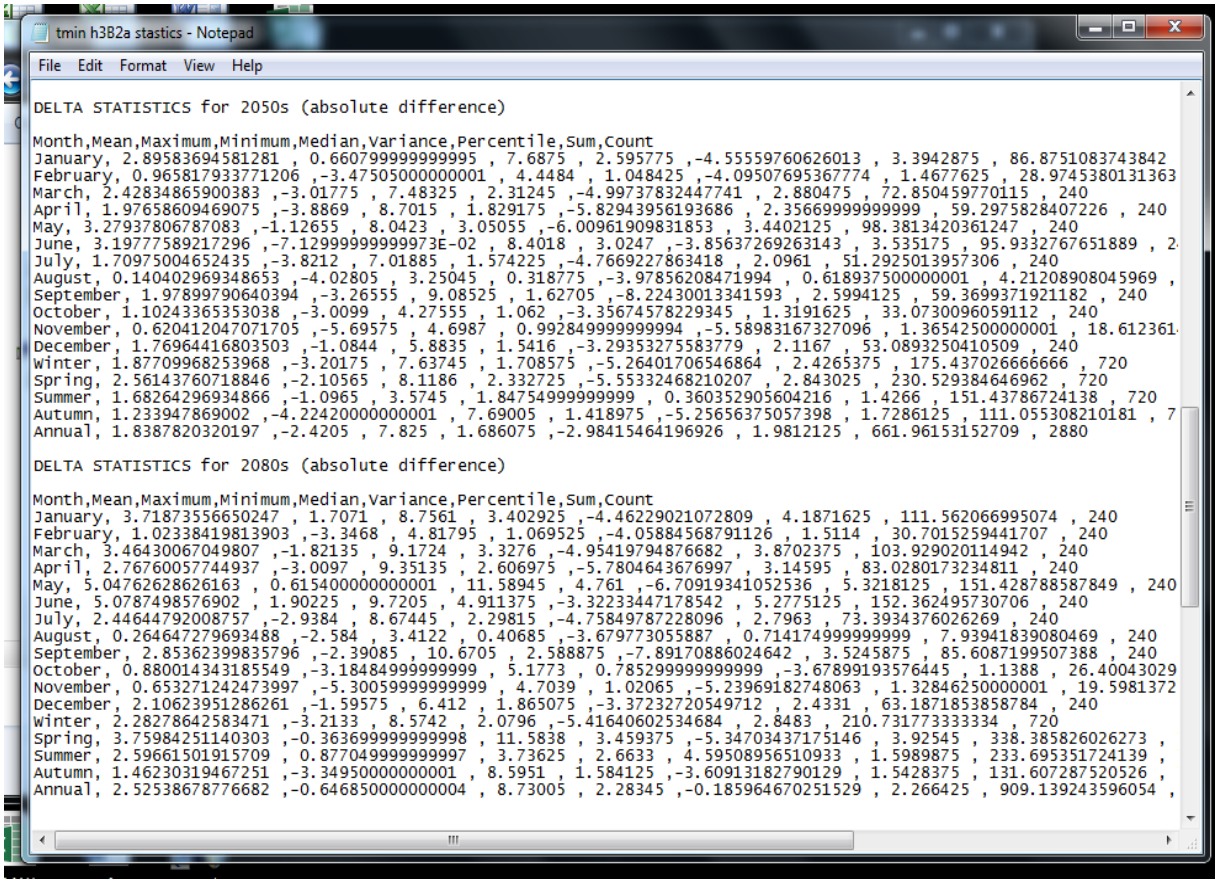
tmin h382a stastics - Notepad
File Edit Format View Help
DELTA STATISTICS for 2050s (absolute difference)
Month,Mean,Maximum,Minimum,Median,Variance,Percentile,Sum,Count
January, 2.89583694581281 , 0.660799999999995 , 7.6875 , 2.595775 ,-4.55559760626013 , 3.3942875 , 86.8751083743842
February, 0.965817933771206 ,-3.47505000000001 , 4.4484 , 1.048425 ,-4.09507695367774 , 1.4677625 , 28.9745380131363
March, 2.42834865900383 ,-3.01775 , 7.48325 , 2.31245 ,-4.99737832447741 , 2.880475 , 72.850459770115 , 240
April, 1.97658609469075 ,-3.8869 , 8.7015 , 1.829175 ,-5.82943956193686 , 2.356699999999999 , 59.2975828407226 , 240
May, 3.27937806787083 ,-1.12655 , 8.0423 , 3.05055 ,-6.00961909831853 , 3.4402125 , 98.3813420361247 , 240
June, 3.19777589217296 ,-7.12999999999973E-02 , 8.4018 , 3.0247 ,-3.85637269263143 , 3.535175 , 95.9332767651889 , 2
July, 1.70975004652435 ,-3.8212 , 7.01885 , 1.574225 ,-4.7669227863418 , 2.0961 , 51.2925013957306 , 240
August, 0.140402969348653 ,-4.02805 , 3.25045 , 0.318775 ,-3.97856208471994 , 0.618937500000001 , 4.21208908045969 ,
September, 1.97899790640394 ,-3.26555 , 9.08525 , 1.62705 ,-8.22430013341593 , 2.5994125 , 59.3699371921182 , 240
October, 1.10243365353038 ,-3.0099 , 4.27555 , 1.062 ,-3.35674578229345 , 1.3191625 , 33.0730096059112 , 240
November, 0.620412047071705 ,-5.69575 , 4.6987 , 0.992849999999994 ,-5.58983167327096 , 1.36542500000001 , 18.612361
December, 1.76964416803503 ,-1.0844 , 5.8835 , 1.5416 ,-3.29353275583779 , 2.1167 , 53.0893250410509 , 240
Winter, 1.87709968253968 ,-3.20175 , 7.63745 , 1.708575 ,-5.26401706546864 , 2.4265375 , 175.437026666666 , 720
Spring, 2.56143760718846 ,-2.10565 , 8.1186 , 2.332725 ,-5.55332468210207 , 2.843025 , 230.529384646962 , 720
Summer, 1.68264296934866 ,-1.0965 , 3.5745 , 1.84754999999999 , 0.360352905604216 , 1.4266 , 151.43786724138 , 720
Autumn, 1.233947869002 ,-4.22420000000001 , 7.69005 , 1.418975 ,-5.25656375057398 , 1.7286125 , 111.055308210181 , 7
Annual, 1.8387820320197 ,-2.4205 , 7.825 , 1.686075 ,-2.98415464196926 , 1.9812125 , 661.96153152709 , 2880
DELTA STATISTICS for 2080s (absolute difference)
Month,Mean,Maximum,Minimum,Median,Variance,Percentile,Sum,Count
January, 3.71873556650247 , 1.7071 , 8.7561 , 3.402925 ,-4.46229021072809 , 4.1871625 , 111.562066995074 , 240
February, 1.02338419813903 ,-3.3468 , 4.81795 , 1.069525 ,-4.05884568791126 , 1.5114 , 30.7015259441707 , 240
March, 3.46430067049807 ,-1.82135 , 9.1724 , 3.3276 ,-4.95419794876682 , 3.8702375 , 103.929020114942 , 240
April, 2.76760057744937 ,-3.0097 , 9.35135 , 2.606975 ,-5.7804643676997 , 3.14595 , 83.0280173234811 , 240
May, 5.04762628626163 , 0.615400000000001 , 11.58945 , 4.761 ,-6.70919341052536 , 5.3218125 , 151.428788587849 , 240
June, 5.0787498576902 , 1.90225 , 9.7205 , 4.911375 ,-3.32233447178542 , 5.2775125 , 152.362495730706 , 240
July, 2.44644792008757 ,-2.9384 , 8.67445 , 2.29815 ,-4.75849787228096 , 2.7963 , 73.3934376026269 , 240
August, 0.264647279693488 ,-2.584 , 3.4122 , 0.40685 ,-3.679773055887 , 0.714174999999999 , 7.93941839080469 , 240
September, 2.85362399835796 ,-2.39085 , 10.6705 , 2.588875 ,-7.89170886024642 , 3.5245875 , 85.6087199507388 , 240
October, 0.880014343185549 ,-3.18484999999999 , 5.1773 , 0.785299999999999 ,-3.67899193576445 , 1.1388 , 26.40043029
November, 0.653271242473997 ,-5.30059999999999 , 4.7039 , 1.02065 ,-5.23969182748063 , 1.32846250000001 , 19.5981372
December, 2.10623951286261 ,-1.59575 , 6.412 , 1.865075 ,-3.37232720549712 , 2.4331 , 63.1871853858784 , 240
Winter, 2.28278642583471 ,-3.2133 , 8.5742 , 2.0796 ,-5.41640602534684 , 2.8483 , 210.731773333334 , 720
Spring, 3.75984251140303 ,-0.363699999999998 , 11.5838 , 3.459375 ,-5.34703437175146 , 3.92545 , 338.385826026273 ,
Summer, 2.59661501915709 , 0.877049999999997 , 3.73625 , 2.6633 , 4.59508956510933 , 1.5989875 , 233.695351724139 ,
Autumn, 1.46230319467251 ,-3.34950000000001 , 8.5951 , 1.584125 ,-3.60913182790129 , 1.5428375 , 131.607287520526 ,
Annual, 2.52538678776682 ,-0.646850000000004 , 8.73005 , 2.28345 ,-0.185964670251529 , 2.266425 , 909.139243596054 ,

Appendix 12: Definition of weather generator parameters

parameter	Definition
TMPMX	Average or Mean maximum air temperature for month(0°C)
TMPMN	Average or Mean minimum air temperature for month(0°c)
TMPSTMX	Standard deviation for daily maximum temperature for month (0°c)
TMPSTDMN	Standard deviation for daily maximum temperature for month(0°c)
PCPMM	Average or Mean total monthly precipitation (mm H_2o)
PCPSTD	Standard Deviation for daily precipitation in month (mm H_2o)
PCPSKW	Coefficient For daily Precipitation in month
PR_W(1)	Probability of a wet following a dry day in the month
PR_W(2)	Probability of a wet following a wet day in the month
PCPD	Average number of days of precipitation in month
SOLARAV	Average daily solar radiation for month (MJ/m^2/day)
RAINHHMX	Average maximum half hour rainfall(mm)

Appendix 13: Definition of soil parameters

Code	Description
SNAM	Soil Name
NLAYERS	No of layers
HYDGRP	Soil Hydrologic Group(A,B,C,D)
SOL_ZMX	Maximum Rooting Depth of the soil profile
TEXTURE	Soil texture
SOL_Z	Depth from soil surface to bottom layer
SOL_BD	Moist bulk density for soil

SOL_AWC	Available Water Capacity Of soil Layer
SOL_K	saturated Hydraulic conductivity
SOL_CBN	Organic Carbon Content
CLAY	Clay Content
SILT	Silt Content
SAND	Sand Content
ROCK	Rock Fragment Content
SOL_ALB	Moist Soil Albedo

Appendix 14: Weather generator Statistics for Gonder station

code	Jan	Feb	Mar	Apr	May	Jun	Jul	Aug	Sep	Oct	Nov	Dec
TMPMX	28.2	29.8	30.3	30.4	29.2	25.7	23.2	23.4	25.5	26.8	27.5	27.7
TMPMN	11.4	12.9	13.9	15.0	14.7	13.7	13.1	13.0	12.5	12.1	11.8	11.4
TMPSTMX	1.35	1.48	1.99	2.03	2.36	2.04	1.57	1.53	1.51	1.36	1.18	0.96
TMPSTDMN	2.40	2.76	3.07	3.12	3.50	2.65	2.62	2.49	2.53	2.55	2.58	2.26
PCPMM	3.65	3.11	14.2	31.67	88.3	191.1	329.8	318.8	116.4	88.16	21.21	8.50
PCPSTD	1.15	0.87	2.46	3.41	6.67	10.5	11.7	11.4	6.97	7.93	3.12	2.06
PCPSKW	12.6	10.7	11.7	5.77	3.87	3.02	2.10	2.02	2.84	4.45	6.82	11.5
PR_W(1)	0.02	0.03	0.09	0.16	0.28	0.59	0.91	0.84	0.42	0.25	0.09	0.04
PR_W(2)	0.25	0.20	0.31	0.49	0.58	0.73	0.92	0.90	0.59	0.46	0.36	0.32
PCPD	0.76	0.95	3.52	6.86	12.3	20.4	28.3	27.7	15.7	10.1	3.81	1.62
SOLARAV	20.3	21.5	21.2	21.3	20.3	16.4	16.0	17.2	19.8	19.7	19.2	19.3
RAINHHMX	10.2	9.76	10.6	11.2	13.6	16.2	16.9	16.7	16.5	14.6	12.5	10.7

Appendix 15: Weather generator Statistics for Ayekel station

Code	Jan	Feb	Mar	Apr	May	Jun	Jul	Aug	Sep	Oct	Nov	Dec
TMPMX	25.03	26.7	27.4	27.63	25.8	22.54	20.16	20.25	21.80	22.81	24.08	24.4
TMPMN	11.27	13.2	13.5	14.40	12.9	12.06	11.53	11.53	11.97	12.27	11.65	11.1
TMPSTMX	1.43	1.64	1.82	2.05	2.57	2.11	2.00	1.85	1.74	1.58	1.24	1.15
TMPSTDMN	4.70	4.67	5.11	4.99	5.66	3.82	2.96	2.95	2.97	3.21	4.27	4.70
PCPMM	1.97	1.74	12.1	36.6	99.6	208.2	289.8	265.2	159.7	87.06	18.94	4.50
PCPSTD	0.83	0.52	2.1	5.12	6.76	9.78	10.66	10.19	8.80	6.94	3.99	2.39
PCPSKW	18.9	11.3	7.51	7.87	3.10	2.14	1.76	2.27	3.20	4.33	9.92	23.2
PR_W(1)	0.01	0.02	0.06	0.11	0.26	0.64	0.80	0.85	0.60	0.28	0.05	0.02
PR_W(2)	0.33	0.20	0.46	0.53	0.65	0.76	0.92	0.92	0.75	0.61	0.33	0.24
PCPD	0.43	0.71	2.81	5.43	12.8	21.62	28.10	28.43	21.52	13.48	2.29	0.81
SOLARAV	20.0	21.3	21.3	20.92	20.2	16.53	15.35	16.14	18.43	19.34	19.03	19.0
RAINHHMX	2.54	2.81	2.89	2.79	2.69	2.65	2.25	2.15	2.08	1.99	2.10	2.29

Appendix 16: the mean annual precipitation, maximum and minimum temperature of observed data used for Mann-Kendall test

year	Total mean annual precipitation (mm)	Total mean annual max temperature (°c)	Total mean annual min temperature (°c)
1993	3.2	26.1	13.7
1994	2.7	27.0	14.2

1995	2.7	27.3	14.4
1996	3.2	26.5	14.0
1997	3.1	27.0	12.0
1998	4.2	27.4	7.1
1999	5.0	27.3	9.9
2000	4.8	27.0	9.0
2001	5.1	26.6	13.1
2002	2.8	27.7	13.4
2003	2.9	28.0	14.2
2004	3.2	27.5	13.9
2005	0.8	29.7	13.9
2006	3.4	27.1	13.4
2007	3.2	27.2	13.1
2008	3.4	27.4	13.7
2009	2.7	28.0	12.6
2010	2.9	27.5	13.9
2011	2.6	27.5	14.0
2012	3.1	27.8	14.1
2013	2.6	27.5	14.2

Appendix 17: mean monthly percentage change of stream flow for HadCM3A2a and HadCM3B2a scenarios (% change)

month	**A2-2020**	**A2-2050**	**A2-2080**	**B2-2020**	**B2-2050**	**B2-2080**
Jan	3.97	7.61	10.17	2.91	5.75	7.04

Feb	2.09	9.89	9.54	2.04	6.77	5.05
Mar	2.03	8.04	14.57	1.84	5.89	11.04
Apr	3.34	19.01	21.16	3.31	13.84	18.58
May	-4.46	-14.24	-26.93	-3.95	-13.06	-22.78
Jun	-7.06	-20.26	-33.39	-6.88	-18.45	-30.32
July	-10.15	-24.29	-34.41	-9.58	-21.49	-32.06
Aug	-19.72	-33.30	-40.63	-15.90	-28.56	-36.29
Sep	-15.75	-29.30	-33.05	-14.85	-24.50	-28.64
Oct	-7.11	-26.07	-29.25	-6.42	-21.25	-24.72
Nov	-13.92	-24.35	-27.35	-10.05	-20.55	-22.80
Dec	4.45	14.06	18.56	3.08	20.83	23.13
Annual	-5.19	-9.43	-12.57	-4.54	-7.90	-11.06

Appendix 18: mean monthly Megech stream flow for HadCM3A2a and HadCM3B2a scenarios (M^3/S)

Month	**Observed**	**A2-2020**	**A2-2050**	**A2-2080**	**B2-2050**	**B2-2020**	**B2-2080**
Jan	2.09	2.17	2.21	2.30	2.15	2.21	2.24
Feb	1.85	1.89	2.03	2.02	1.88	1.97	1.94
Mar	1.92	1.96	2.07	2.20	1.95	2.03	2.13
Apr	2.15	2.22	2.56	2.61	2.22	2.45	2.55
May	2.86	2.73	2.45	2.09	2.74	2.48	2.20
Jun	7.38	6.86	5.88	4.91	6.87	6.02	5.14
July	20.38	18.24	15.37	13.32	18.36	15.94	13.80
Aug	41.78	33.54	27.87	24.81	35.14	29.85	26.62

Sep	15.03	12.66	10.63	10.06	12.80	11.35	10.73
Oct	6.36	5.91	4.70	4.50	5.95	5.01	4.79
Nov	3.32	2.86	2.51	2.41	2.98	2.64	2.56
Dec	2.50	2.61	2.85	2.97	2.58	3.02	3.08